UNIVERSITÀ DEGLI STUDI DI TORINO

DOTTORATO IN SCIENZE AGRARIE, FORESTALI ED AGROALIMENTARI

CICLO: XXXI

Physiological, chemical and anatomical responses to abiotic stresses and strigolactone deficiency in Poplar spp.

Maryam Ashofteh Beiragi

Supervisor:
Prof. Francesca Secchi

Coordinator of Cycle:
Prof. Aldo Ferrero

2020

“You Don’t Have To Be Great To Start, But You Have To Start To Be Great.” – Zig Ziglar

Table of Contents

Acknowledgements

Firstly, I would like to thank my supervisor Professor Francesca Secchi for her excellent mentoring during my studies. Francesca, I am deeply grateful for your time, ideas, support and constant guidance. I also would like to thank Dr. Chiara Pagliarani who gives me her kind support and always being willing to help and discuss ideas. I will remember the wonderful time we spend in the lab.This work would not have been possible without your help. Throughout my PhD I was sitting in the same office and I saw many people come and go. I thank all my colleagues and friends who were close to me during my stay in University of Turin, especially Dr Olga Kedrina, Dr Mojde Sedaghat, Cristina Morabito, Dr Manuela Ferrero, Dr Marco Maghenzani, Dr Rossella Brianoand and Dr Wajeeha Saeed. I would like to thank all my lab members and friends, Dr Giulia Russo, Dr Francesco Gresta, Dr Christian Constán, Dr Chiara Agliassa, Dr Daniela Minerdi, Davide Patono and Alessio Caracci for their help and support. I would express my gratitude to all my colleagues and Professors from the department of plant physiology and molecular biology for pleasant environment and any kind of their help especially Prof. Andrea Schubert, Prof. Claudio Lovisolo, Prof. Francesca Cardinale and Dr. Ivan Visentin. I would like to thank Prof. Vit Gloser and Dr. Radek Jupa for their help and support, they taught me the knowledge of anatomy in Czech Republic. Words are not enough to express the gratitude that you deserve for all that you have done for me. I would like to thank my dear friends Dr. Nima Zabihi, Dr. Sara Keramati and Eng. Khashayar Varposhti who give me support during my Ph.D study.

Finally, I wish to thank my mother, my father, my sister Toktam and my brothers: Ali, Mohammad, Morteza and my sister-in-law, Mahdiyeh for their understanding, support and love during the past years.

List of abbreviations

A	Photosynthetic rate
ABA	Abscisic acid
CTR	Control plants
E	Transpiration rate
EC	Electrical conductivity
g_s	Stomatal conductance
HT	High temperature
PLC	Percentage loss of hydraulic conductivity
K_{sx}	Specific conductivity
K_{ht}	Theoretical hydraulic conductivity
NSC	Non structural carbohydrate
RLER	Relative leaf expansion rate
REC	re-watered/recovery plant from stress
SLs	Strigolactones
SS	Severe drought stress
Ψ_{leaf}	Leaf water potential
Ψ_{stem}	Stem water potential

Abstract

Continuous global warming imposes environmental stresses such as high temperature and drought, which can threaten plant growth and productivity. These stresses, as exogenous factors, can trigger alterations in physiological, anatomical and chemical features of plants. In addition endogenous factors, such as phytohormones, can affect the response of plants to a wide range of environmental conditions such as strigolactones (SLs), recently recognized class of plant hormones that serve as main players in stress physiology. Other phytohormones, such as Abscisic acid (ABA), Ethylene, Jasmonic acid and Salicylic acid (SA), cooperatively regulate adaptive physiological, molecular, or anatomical responses to environmental changes. Up until now, there is no information linking xylem anatomy and SLs in woody plants. Woody plants, as poplars, are major trees species that are widely used in the wood industry. Poplars are fast-growing trees with high biomass and large population; thus, they play a main role in forestry production, afforestation, and environmental conservation.

This thesis describes the obtained results related to: i) the study of physiological and chemical responses of poplars during severe drought stress and recovery. The hypothesis of this research is that, if the response of xylem parenchyma cells to severe stress is a coordinated biological process resulting in priming xylem for hydraulic recovery, then concurrent changes in xylem pH and sugar concentration have to be observed. ii) investigation of heat stress on poplar functions. In order to gain a better understanding of the effects of prolonged intense heat waves, a study based on the following hypothesis was conducted: prolonged heat waves would lead to limitations in g_s, photosynthesis, and water potential, along

with alterations in the levels of non-structural carbohydrates and apoplastic pH. iii) study of structural changes of xylem components and hydraulic conductivity in transgenic-SLs deficient poplar plants. I hypothesized that SL deficiency will lead to great vulnerability to embolism formation in SL deficient transgenic plants, and higher vulnerability can be determined by wider vessels, higher vessel density, and/or longer vessels.

The results obtained here show that:

(I) Water stress induced meaningful decreases of stem water potential and leaf gas exchanges in parallel with drop in xylem sap pH, increase in starch degradation rate, accumulation of non-structural carbohydrates content (NSC), and ABA in sap. After rehydration, plants showed symptoms of stress relief in stomatal conductance, photosynthesis, Ψ_{stem}, NSC, and ABA content, even if pH remained in acidic range and did not return to prestress condition. Totally, drought resulted in an alteration of carbohydrate contents and starch degradation. After re-watering, sugars washed away and pH changed in apoplast. During drought and recovery, a complex network of coordinated physiological and biochemical signals is activated at the relations between xylem and parenchyma cells that primes xylem for hydraulic recovery.

(II) High temperature reduced eco-physiological traits, lower Ψ_{leaf} associated with an impairment of stomatal conductance, photosynthesis, transpiration rate, and chlorophyll fluorescence was observed. Furthermore, high temperature affected total NSC content; in stem, NSC content dropped while NSC concentration increased in xylem sap upon stress. The increased sugar concentration was accompanied by decreased xylem sap pH. Overall, these results propose that heat stress induced a water stress which had synergistic impacts on the gas exchange and reduced transpiration rates. Additionally, a drop in xylem sap pH, which is a typical

symptom of drought in poplars, was also observed. Data from this study confirmed the presence of drought concomitant with heat stress.
(III) Xylem analysis of SLs deficiency transgenic lines, along with hydraulic conductivity measurement, revealed that absence of SL resulted in an increase in vessel diameter, higher proportion of xylem vessel, less proportion of bark area, lower intervessel lateral contact in stem, and a greater vessel density in roots. Transgenic lines had higher maximum specific hydraulic conductivity and showed more vulnerability to xylem embolism, with 50% percent loss of conductance occurring 0.32 MPa for T22-5 and 0.24 MPa for T14-4 earlier than in wild-type plants. Transgenic plants also displayed symptoms of a reduced capacity to control percent loss of conductance through stomatal conductance in response to drought, because they had a much narrower vulnerability safety margin. Altogether, SLs deficiency altered xylem anatomical features in transgenic lines in parallel with the stem hydraulic conductivity. The data disclosed that the SLs deficient poplars are more vulnerable to cavitation formation or embolism spread than wild type plant.

Keyword: ABA, apoplastic pH, drought, heat, hydraulic conductivity, leaf gas exchange, non-structural carbohydrates, PLC, Poplar, strigolactones deficiency, vessel development, water potential, xylem.

CHAPTER I

General Introduction

1.1 Introduction

Ongoing climate change is leading to enhancement in climate extremes which result in adverse environmental conditions (drought, heat, cold, salinity, etc.), resulting in huge effects on plant growth, development and survival (Niu *et al,* 2014). As stated in the IPCC (2014) report, the food production and quality are being reduced by abiotic stresses, consequently leading to a big concern of future risk in many areas of the world. Plant morphological, physiological, biochemical, and molecular traits can be severely affected by abiotic stresses (Szymańska *et al,* 2017; Koolhaas *et al,* 2011). Heat and drought are two main stresses negatively affecting growth and productivity of the annual and perennial plants (Mencuccini *et al,* 2015; Fahad *et al,* 2017). In general, drought stress arises with low humidity of the air and soil, along with high temperature, which can negatively impact plant growth and development (Lipiec *et al,* 2013). Drought stress induces several plant physiological changes such as water potential reduction, loss of turgor, stomatal closure, and decrement of CO_2 flow into the leaf, which consequently leads to a decline in photosynthesis rate and CO_2 assimilation (Grant, 2012; Prasad *et al,* 2008; Chaves *et al,* 2003). Typically, drought is associated with elevated temperature and heat waves, which can trigger a high rate of evaporative demand under elevated temperature (Anderegg *et al,* 2016). Hence, the occurrence of simultaneous drought and heat stress can induce high mortality rate of crops and trees (Allen *et al,* 2010; Savi *et al,* 2015). Elevated temperature is one of the main consequences of worldwide climate change. As predicted by the IPCC, ongoing warming will be enhanced 2.4-6.4°C by the year 2100 (IPCC, 2007). Such global warming is projected to increase temperature, inferior cold and frosted days, enhance heat waves continuity, and alter patterns of precipitation around

the world (Frich *et al,* 2002; Chmura *et al,* 2011; Anderegg *et al,* 2016). Heat waves are usually defined as a period of at least five constant days each with temperature higher than 35^{o}C or three consecutive days with temperature higher than 40^{o}C, compared to average number of days with a normal temperature (Fischer and Schär, 2010; Frich *et al,* 2002, IPCC, 2007). Heat stress can be induced by prolonged heat waves in plants; indeed, heat-stressed plants often display serious alterations in morphological traits, such as growth inhibition, leaf burn, bud deformation, leaves and fruits discoloration, reduced dry matter production, and total yields of trees (Wahid, 2007; Prasad *et al,* 2008; Chmura *et al,* 2011; Fahad *et al,* 2017).

1.2. Drought and Heat Impact on physiological processes

Drought is one of the main environmental stresses, which may occur at different stages of plant life cycles with various intensities (Nardini *et al,* 2013; Anderegg *et al,* 2015). Experimental studies have provided evidence that two firmly inter-related physiological mechanisms are associated with mortality of trees by drought: xylem embolism (Anderegg *et al,* 2016; Schumann *et al,* 2019; Choat *et al,* 2018) and carbohydrate depletion (Triflò *et al,* 2017; Dietrich *et al,* 2018). The water column disruption in the xylem conduit is induced by the formation of gaseous bubbles (hypothesis of air-seeding; Tyree and Zimmermann, 2002), which results in the interruption of water transport in conduit and makes the conduit hydraulically inactive, while also progressively reducing stem water transport capacity (Nardini *et al,* 2013; Secchi and Zwieniecki, 2012; Mayr *et al,* 2014; Choat *et al,* 2018). The hypothesis of air-seeding states that cavitation happens when air penetrates into a functional conduit through inter-conduit pits, and if these

bubbles gradually expand beyond the conduit then the gas-filled conduit becomes inactive, which can initiate the formation of embolism (Christman *et al,* 2009, 2012). Such conditions can be seen during high transpiration rates and limited water supply in soil, when the pressure gradient and tension become simultaneously greater in conduits (McDowell *et al,* 2008; Choat *et al,* 2012). Embolism accumulation is inferred to impair water supply to the foliage and eventually lead to tissue desiccation and plant death (Nardini *et al,* 2011; Cochard *et al,* 2013; Secchi and Zwieniecki, 2011). The percentage loss of conductivity (PLC) is low under well water conditions and xylem water potential has a less negative value (near zero) and rises, generally following a sigmoidal function, when xylem water potential turns more negative (Peguero-Pina *et al,* 2014; Creek *et al,* 2018). By stomatal regulation, plants are able to reduce the risk of facing hydraulic dysfunction under water stress (Blackman *et al,* 2009; Hochberg *et al,* 2017). It has been proven that stomatal closure occurs before reaching the threshold xylem water potential at which substantial cavitation is pioneered, despite the negative impacts of stomatal closure (Martinez-Vilalta and Garcia-Forner, 2017). This stomatal closure has the disadvantage of reducing CO_2 uptake and photosynthetic rate, which can result in depletion of carbohydrate pools and then eventually lead to a shortage of carbohydrate metabolites in different tissues, as well as carbon starvation (Klein, 2014; Anderegg *et al,* 2016; Nardini *et al,* 2018). Carbon starvation can occur when the storage of carbon is insufficient and it can’t maintain turgor and cellular metabolism, causing a negative carbon imbalance and also reducing the production of useful secondary metabolites in plants against pathogens (Anderegg *et al,* 2016). During severe stress conditions, the sugar transport failure in phloem and the incapability for cells to consume existent carbohydrates owing to dehydration can occur, causing

tree mortality (Sala *et al,* 2012; Martorell *et al,* 2014; Triflò *et al,* 2019). Phloem transport failure could arise due to enhanced phloem sap viscosity or phloem turgor collapse (Sevanto, 2014). As the demand of carbohydrates increases to preserve plant metabolisms, plants may need reserve mobilizations; this mechanism, in turn, could promote carbon starvation because it would determine the inability to utilize carbohydrates and/or reallocate them to starving tissues (Sala *et al,* 2010; Sevanto, 2014, Savi *et al,* 2019). As a consequence, drought can diminish carbon mobilization, alter allocation of carbon and change action of phloem (Adams *et al,* 2017; Hartmann *et al,* 2013; Nardini *et al,* 2016). Post-drought recovery of plants has been shown to rely on the recovery of hydraulic function with elongation of the drought severity that plants incurred (Brodribb and Cochard, 2009; Martorell *et al,* 2014; Knipfer *et al,* 2015; Creek *et al,* 2018). Recent studies suggest that during drought recovery, a restoration of xylem functionality may occur in several plant species, even with the lower amount of water in the xylem (Zwieniecki and Holbrook, 2009; Brodersen *et al,* 2010; Nardini *et al,* 2011; Secchi and Zwieniecki, 2011). Different experimental evidences suggest that water can be stored in parenchyma cells and can be derived from parenchyma to the embolize conduits during decreasing water potential (Tyree and Zimmermann, 2002; Secchi *et al,* 2017). Subsequently, in the presence of living xylem cells such as parenchyma cells, living fibres could be crucial in the recovery process and embolism removal (Pagliarani *et al,* 2019). Parenchyma cells act as storages of water (Salleo *et al,* 2004; Nardini *et al,* 2011; Secchi *et al,* 2017), non-structural carbohydrates (NSC), mineral nutrients, mediate their retranslocation within xylem (Brodersen and McElrone 2013; Rosner *et al,* 2018; Trifilò *et al,* 2019), and radially connect xylem with adjacent tissues (e.g., pith, cambium, phloem) (Plavcová *et al,* 2016; Kiorapostolou *et al,* 2019). In addition, they may mediate refilling of

embolized conduits (Brodersen *et al,* 2010; Nardini *et al,* 2011) or regulate ionic composition of xylem sap, and thereby actively modulate xylem hydraulic properties (Zwieniecki *et al,* 2004; Nardini *et al,* 2011).

Photosynthesis produces non-structural carbohydrates (NSC). NSCs provide substrates for growth and metabolism and can play an important role in plant tolerance to diverse conditions (Hartmann and Trumbore, 2016; Grant, 2012; Quentin *et al,* 2015). NSCs basically contain starch and free sugars such as sucrose, glucose, and fructose. Under well water condition, low concentrations of various NSCs have been detected in the xylem sap (Nakamura *et al,* 2008; Krishnan *et al,* 2011). Moreover, concentrations of NSCs fluctuate on a daily and seasonal basis, owed to their utilization within certain physiological processes, such as support of growth and production of leaves (Hoch *et al,* 2003; Landhausser and Lieffers, 2012), repair of embolised conduits (Brodersen and McElrone, 2013; Trifilò *et al,* 2019), tolerance to low or high temperatures (Kasuga *et al,* 2007; Bita and Gerats, 2013), and defense against pathogens (Goodsman *et al,* 2013; Lahr and Krokene 2013). According to current active embolism removal models, during water stress, starch in wood parenchyma cells is hydrolyzed to soluble sugars, which are transported along with ions to the apoplast (Secchi and Zwieniecki, 2012). Accumulation of osmotica decreases the apoplastic water potential, allowing aquaporin-mediated water entry into the empty vessels upon relief from water stress. Once vessels have been refilled and become functional, sugars and ions are washed away with the transpiration stream (Zwieniecki and Holbrook, 2009; Secchi and Zwieniecki, 2012; Brodersen and McElrone, 2013; Secchi and Zwieniecki, 2016). These models are consistent with observations of NSC accumulation dynamics in parenchyma cells of drought-stressed plants.

Depending on the species, xylem hydraulic limitation or chemical signaling can be involved in the stomatal regulations (McAdam and Brodribb, 2015). It can be noted that other components like ABA precursors and cytokinins have a main role in changes of mineral composition or pH of the xylem sap (Wilkinson and Davies, 2008). During drought, ABA of xylem sap has been enhanced concomitant with changes in water status and stomatal conductance diminution (Dodd *et al,* 2006). Therefore, the increase of ABA in sap can influence stomatal behavior (Hartung *et al,* 1998). In drought conditions, abscisic acid hormone (ABA) mediates stomatal closure, which is responsible for the reduction of stomatal conductance and transpiration (Cornic and Fresneau, 2002; Chaves, 1991; Kamanga *et al,* 2018; McAdam *et al*, 2016). The role of apoplastic pH in the ion channel's activity in the plasma membrane of guard cells has been demonstrated by Roelfsema and Hedrich (2002). Sharp and Davies (2009) showed that significant xylem sap pH changes were detected mostly in herbaceous, rather than in other plants, when exposed to water stress. In fact, alkalization or acidification is one of the first chemical changes observed in the xylem sap of drought-exposed plants (Bahrun *et al,* 2002, Sharp and Davies, 2009, Sobeih *et al,* 2004).

Extreme heat can cause great shifts in plant vegetation, productivity, and the dynamic of species communities (Smith, 2011; Ciais *et al,* 2005; Wang *et al,* 2016). Decreases in relative growth rate under elevated temperature, due to decrement in assimilation, has been proven in several crops (Hasanuzzaman *et al,* 2013). Likewise, high temperature can lead to malfunction of physiological processes in all plants, including enhancement of photorespiration and reduction of photosynthetic efficiency, plant life cycle, and plant productivity (Bita and Gerats, 2013; Wang *et al,* 2014).

Many specific changes to the primary processes of photosynthesis that could enhance carbon assimilation of canopy and production through step changes contain the modification of the catalytic properties of Rubisco (Parry *et al,* 2013; Murchie *et al,* 2009; Ort *et al,* 2015). Under physiologically relevant conditions, biochemical models have shown that CO_2 fixation rates are limited by the carboxylation of ribulose-1,5-bisphosphate (RuBP) (Farquhar *et al,* 1980; von Caemmerer, 2000; Hermida-Carrera *et al,* 2016). RuBP carboxylation is restricted by the regeneration of RuBP or by the activity of the carboxylating enzyme, RuBP carboxylase/oxygenase (Rubisco). The limitations inflicted by Rubisco result from its notorious catalytic inefficiencies, including slow catalysis and defective discrimination among CO_2 and O_2 (Whitney *et al,* 2011; Galmés *et al,* 2016). Because of these inefficiencies, plants have to accumulate high amounts of Rubisco, and lose substantial amounts of previously fixed CO_2 and NH_3 in the process of photorespiration (Keys, 1986). These inefficiencies limit not only the rate of CO_2 fixation but also the capacity of plants for an optimal usage of resources, principally water and nitrogen (Long *et al,* 2006; Galmés *et al,* 2014; Hermida-Carrera *et al,* 2016). Rubisco kinetic parameters have characterized in vitro at 25°C for nearly 250 species of higher plants, of which only approximately 8% are crop plant species (Bird *et al,* 1982; Prins *et al,* 2016; Ishikawa *et al,* 2009). These studies discovered the presence of substantial variability in the main Rubisco kinetic parameters among C_3 species (Bird *et al,* 1982; Bota *et al,* 2002; Ishikawa *et al,* 2009) and across C_3 and C_4 species (Sage, 2002; Kubien *et al,* 2008; Perdomo *et al,* 2015). Many studies suggest that the key factor shaping the specialization in Rubisco kinetics among higher plants is the availability of CO_2 at the active sites of the enzyme in the chloroplastic stroma (Delgado *et al,* 1995; Young and Hopkinson, 2017; Galmés *et al,*

2016). With the actual Rubisco kinetic constants, it is possible to quantify the limitation that mesophyll conductance constrains on photosynthesis at each temperature (Bernacchi *et al,* 2002). Additionally, Rubisco kinetic traits optimization in the CO_2 prevailing which has necessarily to handle with the trade-off between Rubisco affinity for CO_2 and enzyme turnover rate (Badger and Andrews, 1987; Galmés *et al,* 2016; Hermida-Carrera *et al,* 2016). Through periods of stress for plant growth, NSC can preserve metabolic functions, and, after disturbances that contain a loss of tissue, NSC can mobilize from several sources such as stems, leaves, and roots to likely sinks to maintain metabolism and/or start compensatory growth (Chapin *et al,* 1990; Dietze *et al,* 2014). NSCs concentrations may include 5-40 % of the dry matter of a plant, depending on plant functional forms and environmental situations (Würth *et al,* 2005). As NSCs are involved in repair and damage prevention, they may increase in response to heat stress and have been associated with heat stress tolerance (Couée *et al,* 2006; Sevanto and Dickman, 2015; Marias *et al,* 2017). Accumulation of nonstructural carbohydrates was suggested as a strategy for counteracting the heat stress (Teskey *et al,* 2015; Marias *et al,* 2017). In addition, by increasing temperature, unusual warmer winter can influence the nonstructural carbohydrates pool; this happens because of the respiration consumption during winter and also the increasing rate of carbon depletion with a mild heat stress in the spring (Allen *et al,* 2010). To date, research on plants' physiological response to high temperature has been mostly performed on herbaceous species (Hurkman *et al,* 1998; Kim *et al,* 2010; Guilioni *et al,* 2003; Fahad *et al,* 2017); however, little is known about the effects of high temperature events on woody plants (Li *et al,* 2014). Bauweraerts *et al,* (2014), conducted a research study on evergreen conifer (*Pinus taeda* L.) and a deciduous broadleaf (*Quercus rubra* L.),

demonstrating that extreme heat waves (+12^{o}C) had a negative impact on the growth species. In a study of four co-occurring temperate tree species, heat waves induced a huge damage on the photosynthesis and PSII system, while stomatal conductance remained functional and had not been affected by heat (Guha *et al,* 2018). Another research study, conducted on *Coffea arabica* L. (Eritrean Mokka) trees, provided evidence that physiological traits were negatively affected by heat stress; particularly, the authors found impairments in net photosynthesis, stomatal conductance, and nonstructural carbohydrate amounts (Marias *et al,* 2017). Heat may induce a negative impact on chlorophyll biosynthesis or increase degradation; consequently, elevated temperature may have impaired effects on enzymes which are involved in the chlorophyll biosynthesis pathway (Mathur *et al,* 2014). Prasad *et al* (2008) emphasized that the modulation of mitochondrial respiration subjected to heat and drought stress is a common response. Some studies have shown that leaf respiration is influenced by high temperature when the temperature increases more than 35-40 °C (Loreto *et al,* 2001; Rennenberg *et al,* 2006). Generally, extreme high temperatures could result in permanent injury to the photosynthetic proteins, particularly key PSII protein D1 and the disruption of thylakoid membranes, causing a quick reduction in maximum quantum efficiency (Zhang and Sharkey, 2009; Rungrat *et al,* 2016). The impact of high temperature could be aggravated when transpiration cooling is limited as a result of high humidity, which diminishes the vapour pressure difference, or when low soil-water content decreases stomatal aperture (Rungrat *et al,* 2016). Last but not least, thylakoid membrane function is disturbed by drought and heat stress. Heat and drought stress decline CO_2 uptake through the adjustment of stomatal or internal resistance to CO_2 diffusion which both can impel oxygenase activity; this results in increased photorespiration rate and

reduced photosynthesis rate (Prasad *et al,* 2008). Typically, when heat stress is accompanied by an increase in soil temperature, the condition is more deleterious to plants; the reason is the greater evapotranspiration demand in plants and soil simultaneously (Rennenberg *et al,* 2006; Lipiec *et al,* 2013).

1.3. Plant hormones

The most studied plant hormones are: auxin (IAA), abscisic acid (ABA), cytokinins (CKs), ethylene (ET), salicylic acid (SA), gibberellins (GAs), brassinosteroids (BRs), jasmonates (Jas) and strigolactones (SLs). The last ones which have been recently discovered are involved in the shoot architecture (Sedaghat *et al,* 2017; Gomez-Roldan *et al,* 2008). Hormonal signals have an important role in physiological responses to different stresses.

1.3.1. Abscisic Acid and environmental stresses

Abscisic acid (ABA) is a plant hormone which inducts a signaling cascade of responses in guard cell membrane channels and transporters that trigger a decline in guard cell turgor, thus closing stomata and reducing water loss (Brodribb and McAdam, 2011, 2013; Munemasa *et al,* 2015). In many studies, ABA has been shown to modulate stomatal closure under drought and also induce thermotolerance under heat stress (Larkindale *et al,* 2005; Tombesi *et al,* 2015; Zhang and Davies, 1989; Martínez-Vilalta and Garcia-Forner, 2017). ABA is a sesquiterpenoid belonging to the class of isoprenoids. The molecular structure of ABA includes one asymmetric carbon atom, which is vital for its biological activity (Cutler *et al,* 2010). Abiotic stress, such as drought, cold and/or heat, can initiate the ABA

production through induction of ABA biosynthetic genes or trigger various gene expressions for specific biochemical responses (Shinozaki and Yamaguchi-Shinozaki, 2007). The ABA synthesis was previously considered to produce mainly in the roots, prior to transport in the xylem sap to the leaves as a signal of soil drying (Davies and Zhang, 1991). New studies have recently indicated that the whole plant dynamics of ABA are more complex, with the leaves and stems playing a main role in synthesis and catabolism of ABA (Manzi *et al*, 2015; McAdam and Brodribb, 2015; Mitchell *et al*, 2016; Zhang *et al*, 2018). Recently, Zhang and colleagues (2018) found that leaves had the most significant increases in ABA levels in response to a decrease in cell volume while roots did not display changes in ABA levels after reduction in cell volume. Interestingly, they detected that floral tissue was able to synthesize ABA in response to sustained water deficit (Zhang *et al,* 2018). It has been proven that by an interaction of chemical and hydraulic signals, plants are able to respond to water shortage (Comstock, 2002; Tombesi *et al,* 2015). Initial studies used split-root systems to disclose that ABA acts as a chemical signal of soil drying which synthesized in the root and transported to the shoot, acting independently of hydraulic signals in inducing stomatal closure (Zhang *et al,* 1987; Davies and Zhang, 1991). While in poplar (*Populus nigra* L.), it has been shown that stomatal conductance rates and foliar ABA concentration remained unchanged when half of the root-zone dried (Marino *et al,* 2017). Similar patterns of stomata behavior and ABA content were detected in leaves of olive (*Olea europaea* var. Chetoui) exposed to partial root-zone drying in the split-root tests (Dbara *et al,* 2016). The stomatal aperture regulation through ABA function is crucial for plants to regulate diurnal gas exchange and drive stomatal responses to leaf-to-air vapor pressure deficit (VPD) (Buckley, 2016; McAdam and Brodribb, 2015). Mcadam and Brodribb (2016)

suggested that leaf turgor changes during a VPD transition caused the observed rapid ABA biosynthesis during these transitions and thus triggered the signal for stomatal responses to VPD. Drought responses of grapevine (*Vitis vinifera* L.) proposed that early stomatal closure was induced by hydraulic signals, which were accompanied by an elevation in foliar ABA content that also maintained stomatal closure after leaf water potentials had returned to pre-stress levels (Correia *et al*, 1995; Tombesi *et al*, 2015). In other woody plants, it has been shown that ABA did not act as a fast root-to-shoot signal of soil drying to persuade stomatal closure, but was preceded by a hydraulic signal (Christmann *et al*, 2007). Moreover, xylem sap pH variations have been suggested to signal soil drying by shifting the partition of ABA between the leaf apoplast and symplast (Wilkinson and Davies, 1997). It has been found that the conductance of mesophyll (g_m) to CO_2 is linked to the free-ABA concentration in the leaf, and in fact, ABA likely induces more rapid changes in mesophyll conductance in comparison to stomatal conductance (Sorrentino *et al*, 2016). Some studies have described that the ABA has a main role in the regulation of aquaporins under drought stress (Lipiec *et al,* 2013; Beaudette *et al,* 2007; Parent *et al,* 2009). It is possible that reduction in aquaporins activity which are involved in the transport of CO_2 among the mesophyll would be connected to ABA induction (Jang *et al*, 2004; Perez-Martin *et al*, 2014). In addition, ABA has a role in leaf hydraulic conductance (K_{leaf}) decline through decreased biochemical activity of aquaporins involved in the regulation of the permeability of transport tissues to the water movement (Pantin *et al*, 2013). Besides the roles mentioned above, ABA can also have many impacts on the metabolism of sugar and the partitioning of carbohydrates, and while inducing an increase in the activities of β-amylase and vacuolar invertase, resulting in higher starch degradation and the release of hexoses in the

cytosol (Kempa *et al*, 2008; Pelleschi *et al*, 1999). It has been reported that high concentration of ABA induces Ca^{2+} enhancement in cytosol, which is accompanied by a noticeable activity of anion channel localization in the plasma membrane, successively resulting in potassium efflux, depolarization of guard cells, reduction of turgor and guard cells volume, high generation of H_2O_2, and eventually stomata closure (Zhang *et al,* 2006; Ashraf and Harris, 2013). It has been reported that ABA is involved in the heat stress tolerance (Ding *et al,* 2010; Bita and Gerats, 2013). The high temperature impacts were reduced by the use of ABA treatment in some plants, as plant survival was enhanced after a direct heat exposure. In this regard, some ABA signaling mutants belonging to protein phosphatase *abi1* and *abi2* also display a decreased tolerance to heat stress (Larkindale *et al,* 2005; Larkindale and Knight, 2002). A reduced effect in tissue damage by MDA (Malondialdehyde) and H_2O_2 was observed in the ABA interaction with salicylic acid and JA in plants which were exposed to short term heat stress (Bandurska and Stroiński, 2005; Escandón *et al,* 2016). Heat shock proteins (HSPs) are known as thermotolerance proteins, which are induced by high temperatures (Wahid *et al,* 2007). Pareek *et al* (1998) demonstrated that ABA has been involved to enhance expression of some heat shock proteins such as HSPs 70.

1.3.2. Strigolactones impacts on the plant physiology

Strigolactones (SLs) are a small class of carotenoid-derived compounds and rhizosphere signaling molecules classified as a new class of phytohormones that regulate several different processes in plants (Ruyter-Spira *et al,* 2013). SLs are produced in the root and move upward via the xylem to the stem, where they inhibit lateral bud development (Kohlen *et al,* 2011). More recently, a noticeable relationship between P contents in shoot

tissues and SL exudation was found in various plants; the finding showed that N deficiency decreased P levels in shoots, the phenomenon that leads to the enhancement of SL exudation (Sedaghat *et al,* 2017; Czarnecki *et al,* 2014). Furthermore, SLs are implicated in the regulation of plant morphology and development and were shown to positively stimulate stem secondary growth, internode length, leaf senescence, suppress lateral root formation, and adventitious rooting while promote root hair elongation and primary root growth (Agusti *et al,* 2011; de Saint Germain *et al,* 2013; Mishra *et al,* 2017). The optimal integration between plant hormonal pathway, such as SL, ABA, and CK, is determinative of plant survival at the environmental stress events (Ha *et al,* 2014; Mishra *et al,* 2017; Cardinale *et al,* 2018). Besides such hormonal functions, SLs play a beneficial role in the symbiotic relationship between plants and arbuscular mycorrhizal fungi by stimulating chemical compound production for root development (Akiyama *et al,* 2005; Xie, 2016). Also, it was revealed that root exposure to SLs leads to the accumulation of secondary metabolites, such as flavonols or antioxidants, and these data proposed pleiotropic effects of SLs that stimulate root development (Marzec and Melzer, 2018). Beside natural SLs, multiple synthetic analogs were characterized, such as GR24, GR7, or Nijmegen-1 (Akiyama *et al,* 2010; Zwanenburg and Mwakaboko, 2011; Mishra *et al,* 2017). However, concentration of natural SLs in plants is very low and the substances are highly unstable, especially in humid environments due to hydrolysis (Yoneyama *et al,* 2009; Xie, 2016; Cardinale *et al,* 2018). The instability is proposed to be important for signaling in the rhizosphere, where concentration gradients play a role (Parniske, 2008). SLs have been shown to inhibit bud outgrowth (Guan *et al,* 2012). Auxin, cytokinin, and SL derivatives can control axillary meristem outgrowth and induce alterations in plant shape and architecture (Dun *et al,*

2012; Beveridge *et al,* 2009; Guan *et al,* 2012). It has been reported that some branching mutants showed bushy phenotypes and dwarf appearance in numerous plant species, such as *more axillary growth* (*max*) in Arabidopsis, *decreased apical dominance* (*dad*) in petunia (*Petunia hybrida* L.), *ramosus* (*rms*) in pea (*Pisum sativum* L.) and *high tillering and dwarf* (*htd*) in rice (*Oryza sativa* L.); later investigations revealed that SLs were responsible (Guan *et al,* 2012; Foster *et al,* 2018; Cardinale *et al,* 2018). SL molecules are derived from carotenoid cleavage genes which are mediated by *Carotenoid Cleavage Dioxygenase* genes (*CCD7* and *CCD8*). In the model plant Arabidopsis, *MORE AXILLARY GROWTH* genes include *MAX1*, *MAX2*, *MAX3*, and *MAX4*, all of which are members of strigolactone pathway genes. It has been shown that *MAX2* gene is involved in SL signaling, while the other three genes are involved in SL biosynthesis (Booker *et al,* 2004; Stirnberg *et al,* 2002; Czarnecki *et al,* 2014). *MAX1* is a member of the cytochrome P450 family, and its orthologues and paralogues are involved in the last steps of SL biosynthesis from carlactone (Booker *et al*, 2004; Seto *et al*, 2014). *MAX2* is known to be encoded in F-box leucine-rich protein (ubiquitin E3 ligase), and this gene is essential in strigolactone-dependent suppression of axillary bud outgrowth (Stirnberg *et al,* 2002; Nelson *et al*, 2011; Yoshimura *et al,* 2018). Loss-of-function mutations in each of these four *MAX* genes could result in increased shoot branching (Booker *et al,* 2004; Stirnberg *et al,* 2002; Czarnecki *et al,* 2014). *MAX3* and *MAX4* are orthologous genes, encoding *CCD7* and *CCD8* respectively (Booker *et al,* 2004; Sorefan *et al,* 2003; Foster *et al,* 2018). It has been indicated that in willow trees (salix spp.), such as (*Salix viminalis* and *S. aurita*) (Ward *et al,* 2013) and (*S. viminalis* x (*S. viminalis* x *S. schwerinii*)) (Salmon *et al,* 2014), *MAX4* allelic exists and may correlate with differences in branching patterns and coppicing. Czarnecki *et al,* (2014) reported that

expression of poplar (*P. trichocarpa*) *MAX* orthologs was shown to largely complement the increased branching phenotype of the corresponding *Arabidopsis* mutants. Similarly, in kiwifruit (*Actinidia chinensis* L.), *MAX3 and MAX4* orthologs (*AcCCD7* and *AcCCD8*) were also revealed to complement the corresponding *Arabidopsis* mutant phenotypes. In addition, an RNAi-mediated knockdown of *AcCCD8* was shown to increase branching, demonstrating the importance of SLs in woody perennials (Ledger *et al,* 2010). Meanwhile, in poplars, the *CCD8* genes knockdown have resulted in an increased number of branches and shorter phenotypes (Czarnecki *et al,* 2014; Muhr *et al,* 2016). Moreover, Muhr and colleges (2016) generated transgenic *MAX4* lines using *amiRNA* method and demonstrated the significance of SL role for branching control in trees. The identification of the *BRANCHED1* (*BRC1*) gene showed that this gene was a repressor of bud outgrowth (Rameau *et al,* 2015) and belonged to the *TB1 CYCLOIDEA PCF* (*TCP*) type transcription factor (Aguilar-Martínez *et al,* 2007). The TCP transcription factors control lateral organ and meristems development (Martín-Trillo and Cubas, 2010). Thus, they could adjust many growth-related processes, for instance leaf development or shoot branching (Doebley *et al,* 1997; Palatnik *et al,* 2003). Also, it was shown that the convergence of SLs and cytokinins can encode transcription factor of *BRC1* positively (Aguilar-Martínez *et al,* 2007; Braun *et al,* 2012; Dun *et al,* 2012; Brewer *et al,* 2013; Rameau *et al,* 2015). *BRC1* loss-of-function mutants were shown to have remarkably increased bud outgrowth, causing higher branch numbers (Czarnecki *et al,* 2014; Rameau *et al,* 2015). Accordingly, *BRC1* overexpression orthologs reduced the amount of bud outgrowth in rice and wheat (Lewis *et al,* 2008; Takeda *et al,* 2003). Thus, *BRC1* is known to be a negative regulator of bud outgrowth (Rameau *et al,* 2015; Muhr *et al,* 2016). A number of research studies on trees have shown SL

branching controls in willow, poplar, eucalyptus, and apple trees (Agusti *et al,* 2011; Ward *et al,* 2013; Muhr *et al,* 2016; Foster *et al,* 2018). Until now, there have been few investigations on SL effects on the cambium stimulation of *Arabidopsis*, pea, or *Eucalyptus globulus* by GR24 application (Agusti *et al,* 2011). The impact of SL hormones on the anatomy of woody plants remains unknown.

1.4. Poplar

The genus poplar has 85 different species (Jansson and Douglas, 2007). Many clones of *Populus* were commercialized in industry for timber wood, paper production, and afforestation (Rennenberg *et al,* 2010). Poplars are fast-growing trees that have been widely studied at the molecular and physiological levels as a woody plant model system, especially under biotic and abiotic stresses and their interaction (Harfouche *et al,* 2014; Jia *et al,* 2016). The responses of *Populus* species to climate change has established important knowledge for understanding and designing practical patterns for future forest plantation based on forest growth and carbon sequestration (Hozain *et al,* 2010). Perennial woody plants with long lifespan, like poplar distributed in latitudinal and altitudinal boreal and temperate regions of the northern hemisphere, are suitable for genetic and physiological investigation. Poplar is the first tree whose genome has been perfectly sequenced; hence, its genetic map is available for breeding programs. In addition, poplars can spread easily and multiple genotypes can be transformed (Taylor, 2002; AL Afas *et al,* 2007; Foster *et al,* 2015). *Populus* is used in physiological and biochemical studies for the following reasons: large leaves with high LAI (leaf area index) and expansion rates, fast growing rate, high rate of vascular bundle tissue development, wide

branched system of roots and shoots, high rates of leaf photosynthesis and respiration, quick response of stomata to environmental changes, and vertical shape of branches and leaves (Taylor, 2002). Due to the enhancement of temperatures and drought, more examinations are needed in the area of the agriculture and forest physiology on poplar plants.

1.5. Objectives of this thesis

Plants, being sessile in nature, encounter various environmental stresses that can ultimately lead to reduced growth and productivity. During these stresses, including drought and heat, the normal homeostasis of the physiological, chemical, and hormonal procedures are disturbed. *Populus* provides a good model system to understand plant biology (Jansson and Douglas, 2007). For instance, this plant can be used for studies on long-distance transport of water and nutrients (Arimura *et al,* 2004; Gerttula *et al,* 2015), adaptation to stressful environments (Brosche *et al,* 2005; Bloemen *et al,* 2016), seasonal nitrogen cycling and nitrogen storage as part of the perennial growth habit (Cooke and Weih, 2005), wood formation and xylemic structure (Love *et al,* 2009) and the impact of predicted future climate change levels on trees and forest ecosystems (Rae *et al,* 2006). Based on the facts mentioned above, I chose poplar as a model of woody plant to investigate both the abiotic stress impacts as exogenous factors and the SL deficiency effects as endogenous factors.

The first objective of this thesis was to understand the biological process involved in the xylem priming for hydraulic recovery after drought stress. I hypothesize that, if the response of xylem parenchyma cells to severe stress is a coordinated physiological and chemical process that results in the priming of xylem for hydraulic recovery, then I should observe

concurrent changes in xylem pH and, sugar concentration, as well as a correlation between ABA content and the starch degradation that generates osmotic gradients for restoration of xylem hydraulic function. To address this hypothesis, I measured a set of selected physiological and biochemical responses of poplar trees to drought stress and a recovery period. The aims of study included: i) to monitor poplar physiological modifications under drought stress and recovery; and ii) to understand the biochemical mechanisms involved in drought and rehydration periods. The study has been described in detail in Chapter 2 of this thesis.

The second objective was to realize the impact of heat on the physiological and chemical process could be similar and/or different from drought on poplars. My hypotheses were as follows: the heat stress treatment will have a highly negative effect on gas exchange and water potential; the extreme high temperature will affect whole-plant chemical functions, such as ABA, apoplastic pH, and non-structural carbohydrates, in different organs and thus heat will negatively reduce the plant growth by a constant increase in temperature. To address this hypothesis, constant heat stress was applied to poplars for 23 days, while physiological and biochemical features in different organs were monitored. The study has been described in detail in Chapter 3 of this thesis.

The third objective was to understand if strigolactones can affect the xylem vessels features and if these effects are accompanied by variation in xylem vulnerability to embolism between transgenic lines and wild type. I hypothesized that SL deficiency will result in changes in the xylem vessel's properties and total hydraulic conductivity in transgenic plants. To address this hypothesis, plants were monitored under well water condition and water shortage phase. The hydraulic conductivity, gas exchange, water potential,

and xylem anatomical features were measured among all plants. The study has been described in detail in Chapter 4 of this thesis[1].

1- More details of objectives and hypothesized are provided on the specific chapters.

CHAPTER II

Investigating the physiological and chemical responses of poplar to drought stress

2.1. Introduction

Under drought stress or periods of high transpiration demands, water tension in the xylem grows, increasing likelihood of the embolism formation. Embolism formation is a physical process influenced by a wide range of factors, including water tension, physical properties of the xylem, chemical properties of xylem sap, temperature, and previous plant embolism history (Holbrook and Zwieniecki, 1999; Hacke *et al*, 2001; Stiller and Sperry, 2002; Tyree and Zimmermann, 2002; Jensen *et al*, 2016). The presence of xylem embolism progressively reduces the stem capacity to transport water and can increase leaf water stress, forcing stomatal closure and reducing the photosynthetic activity (Brodribb and Jordan, 2008). In the event of a severe stress, when water loss by transpiration exceeds the transport capacity of xylem, the runaway cavitation may occur leading to the complete cessation of water transport and, in the worst scenario, resulting in plant death (Sperry *et al*, 1998). Therefore, it is conceivable that any strategy played out by the plant to hinder and/or minimize the negative effects of embolism, including restoration of hydraulic transport capacity during time of stress relief, could be crucial for guaranteeing plant survival (Tyree and Ewers, 1991; Choat *et al*, 2012; Klein *et al,* 2018; Barigah *et al*, 2013).

In last few decades, experimental evidences prove that restoration of xylem functionality is present in few plant species during recovery from drought, even when the bulk of water in the xylem remains under low to moderate tension (Zwieniecki and Holbrook, 2009; Brodersen *et al*, 2010; Nardini *et al*, 2011; Secchi and Zwieniecki, 2011). Thus, recovery of xylem from embolism cannot happen spontaneously and requires the presence of xylem living cells in the proximity of the empty vessels to facilitate the process and to overcome existing energy gradients (Trifilò *et al,* 2015). Consequently, both spatial arrangement and amount of woody parenchyma

become crucial for a successful embolism removal (Triflò *et al,* 2019). The majority of living cells in the xylem are located in parenchyma rays and they are often in direct contact with the vessels. Parenchyma cells provide temporary storage for non-structural carbohydrates (NSCs) in the form of sugar and starch (Salleo *et al*, 2004; Spicer, 2014) and are considered a radial water redistribution pathway. Both functions are prerequisites that can allow active repair of embolized conduits. *In vivo* observations showed that vessels fill up with water during recovery (Holbrook *et al*, 2001; Clearwater and Goldstein, 2005; Scheenen *et al*, 2007) and that water droplets preferentially form and grow on the vessel walls that are in contact with living parenchymal cells (Brodersen *et al*, 2010). However, although the direct *in vivo* observations indicated that parenchyma cells as important players in the hydraulic restoration process, the functional biology of this process remains unresolved.

According to the current models of active embolism removal, starch in parenchyma cells is hydrolyzed during water stress, and soluble sugars and ions are being released from wood parenchyma cells to apoplast embolized vessels (Secchi and Zwieniecki, 2012). Accumulation of osmoticum in apoplast lowers the apoplastic osmotic potential such that, during the relief from water stress and reduction of tension, it would allow for aquaporin-mediated water entry into empty vessels along the new water potential gradient. Once the vessels have been refilled and become functional, sugars and ions are washed away with the transpiration stream (Zwieniecki and Holbrook, 2009; Secchi and Zwieniecki, 2012; Brodersen and McElrone, 2013; Secchi and Zwieniecki, 2016). These models are consistent with observations of NSC accumulation and dynamics in parenchyma cells of drought stressed plants; it was shown that embolism presence could alter carbohydrate metabolism and carbon partitioning

between starch and soluble sugars in xylem parenchyma (Salleo *et al*, 2009; Secchi and Zwieniecki, 2011; Tomasella *et al*, 2017) with trees subjected to a short-term drought events accumulating high levels of NSC contents (Trifilo *et al*, 2017). Furthermore, the ability of plants to recover from xylem embolism is species-specific and correlated with the concentration of soluble carbohydrates accumulated at the stem level (Savi *et al*, 2016).

Alteration of carbohydrate metabolism in xylem during drought stress coincides with changes in apoplastic pH. In fact, alkalization or acidification represents one of the first chemical changes observed in the xylem sap of plants exposed to drought (Bahrun *et al*, 2002; Sobeih *et al*, 2004; Sharp and Davies, 2009) that can trigger systemic activation of whole plant response to water stress (Schachtman and Goodger, 2008). *In vivo* observations of poplar stems subjected to water stress linked drop of xylem pH to water stress level (Secchi and Zwieniecki, 2012), and, furthermore, *in vitro* analysis linked acidic apoplastic pH to increased accumulation of sugars in xylem sap of poplar stems (Secchi and Zwieniecki, 2016). These observations suggest that the accumulation of sugars in the xylem apoplast is controlled by xylem pH, where lower pH induce apoplastic sucrose hydrolyses by potential activity of acidic invertases.

The cellular increase of sucrose content triggers *de novo* efflux of sucrose from the cells by shifting the gradient of concentration and thus reversing the direction of sucrose symporters transport as the transporters are often bidirectional depending on proton (pH) and sucrose gradient across the plasma membrane (Carpaneto *et al*, 2005). The increased concentration of sucrose and the presence of lower pH in xylem apoplast result in accumulation of monosaccharide due to acidic invertase activity in the walls (Secchi and Zwieniecki, 2016). In functional vessels, such efflux would be

unnoticeable as sugars will be washed away, but in embolized vessels, sugars will accumulate in the walls, significantly lowering their osmotic potential and allowing for refilling upon relief from water stress (Secchi and Zwieniecki, 2012, 2016). In this model, changes in xylem apoplast chemistry should be coupled to membrane transport and cellular carbohydrate metabolism. The hypothesis of this research is that, if xylem parenchyma cells response to severe stress is a coordinated biological process resulting in priming xylem for hydraulic recovery, then concurrent changes in xylem pH and sugar concentration have to be observed. Indeed, this study confirmed that in poplar lower xylem apoplastic pH is linked to carbohydrate accumulation. The presented work further supports the notion that perennial woody plants biology exposed to severe water stress primes the xylem for the recovery upon re-hydration that is consistent with possibility of embolism removal (Secchi and Zwieniecki, 2014).

2.2. Material and Methods

2.2.1. Plant materials and growth conditions

Populus tremula x alba (clone 717-1B4) one-year-old, were planted in a greenhouse under controlled conditions in University of Turin (Grugliasco campus) during June 2016. Temperature was maintained in the range of 17°C to 29°C and natural daylight was provided when it was necessary by using metal halogen lamps (500–600 µmol photons m^{-2} s^{-1}) to maintain a 12/12-h light/dark cycle. Each plant grew in a 5-L pot filled with a substrate composed of sandy-loam soil/expanded clay/peat mixture (2:1:1 by weight). A total of 51 hybrid poplars were used in this study and poplars at the beginning of the experiment were 180 ± 5 cm tall with a stem diameter of 11.6 ± 0.58 mm. The plants were divided into two groups: 24 poplars, belonging to Group 1, were used to estimate the level of embolism in

response to water stress (percentage loss of hydraulic conductivity [PLC]). Those plants were further divided into three subgroups: (A) six plants watered daily (CTR), (B) six plants severely water stressed by withholding irrigation until the stem water potential (Ψ_{stem}) was below −2 MPa (STRESS), and (C) 12 plants first stressed to below −2 MPa and then watered daily (PLC was measured respectively after 1 and 7 days of recovery, REC1-7). The remaining 27 poplars, belonging to the second group, were split into nine irrigated control trees (CTR) that were irrigated to water holding capacity daily, and 18 trees severely water stressed by withholding irrigation. Once severe water stress (SS) levels were reached in these 18 trees (Day 0), half (n = 9) were sampled: xylem sap and tissues were collected and stored for further chemical analyses. The remaining half (n = 9) were watered (REC) during the morning of the same day (Day 0) and allowed to fully recover over the period of 7 days. After 1 week of stress relief (Day 7), xylem sap and tissues were collected and stored for chemical analyses. Control plants (n = 9) were sampled throughout the experiment. A detailed schematic representation of measurements/sampling timing is provided in Figure 1 (Pagliarani *et al,* 2019).

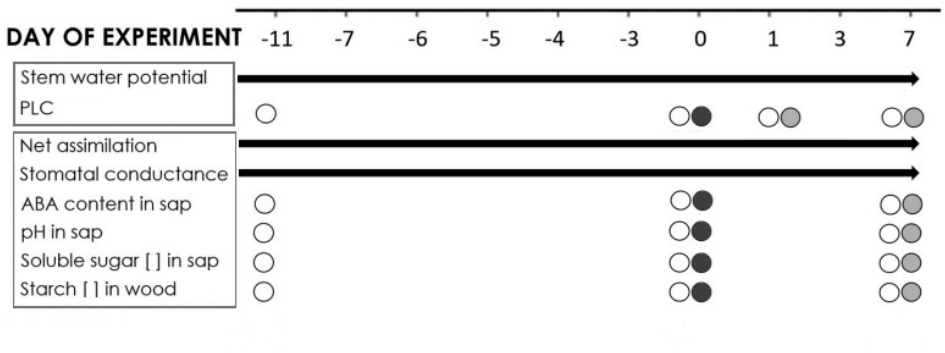

Fig 1. Timing schematic representation of measurements/sampling over the duration of the experiment. Ψ_{stem}, stomatal conductance, and photosynthesis were

monitored throughout the entire experiment, that is, from the start of the stress treatment (Day −11) until full recovery of physiological functions (Day 7). PLC was measured on stressed and recovered poplars respectively at Days 0 (black circles), 1, and 7 (grey circles), whereas on control plants, throughout the experiment duration (white circles). Chemical analyses were performed on sap and woody tissues collected at Day 0 for stressed plants (black circles) and at 7 days for recovered plants (grey circles). Sap and tissues from control plants were sampled throughout the experiment duration (white circles). ABA, abscisic acid; PLC, percent of loss of conductivity. This picture was retrieved from (Pagliarani *et al,* 2019).

2.2.2. Measurements of leaf gas exchange and stem water potential

Assimilation rate (A, µmol CO_2 m^{-2} s^{-1}), stomatal conductance (g_s, mmol H_2O m^{-2} s^{-1}) and transpiration rate (E, mmol H_2O m^{-2} s^{-1}) were measured on three fully expanded leaves per individual plant using a portable infrared gas analyzer ADC-LCPro+ system (The Analytical Development Company Ltd, Hoddesdon, UK). Measurements were performed using a 6.25 cm^2 leaf chamber equipped with artificial irradiation (1200 µmol photon m^{-2} s^{-1}) under ambient CO_2 values maintained constant at 400 ppm. Stem water pressure (Ψ_{stem}) was measured on nontranspiring leaves. Leaves were covered with aluminum foil and placed in a humidified plastic bag for at least 30 min before excision. After excision, leaves were allowed to equilibrate for more than 20 min in dark conditions before being measured for water potential with a Scholander-type pressure chamber (Soil Moisture Equipment Corp, Santa Barbara, CA). Leaf gas exchange and stem water potential were monitored during the experiment from 9:00-12:00 am.

2.2.3. Measurements of stem hydraulic conductivity

Stem hydraulic conductivity was measured using a standard approach described previously by the Secchi and Zwieniecki, (2012). In short, a long stem was cut under water, and this initial cut was followed within a few minutes by cutting a set of three stem segments, each measuring approximately 4 cm. Segments were excised under water approximately 20–30 cm from the initial cut (a distance longer than two times the length of vessels in studied poplar). The initial hydraulic conductance (k_i) of each stem segment was measured gravimetrically by determination of the flow rate of filtered 10 mM KCl solution. A water source was located on a balance (Sartorius ± 0.1 mg) and connected to the stem by a plastic tube. The stem was submerged in a water bath at a level approximately 10 cm below the water level on the balance. After a steady flow rate was reached (within a few minutes), the tube connecting the stem to the balance was closed, and a bypass was used to push water across the segment under approximately 2 bars of pressure for approximately 20 s to remove embolism. Stem conductance was then remeasured to find maximum conductance (k_{max}). The PLC was calculated as PLC = 100 × (k_{max} – ki)/k_{max}.

2.2.4. ABA measurement

ABA quantification has been performed in collaboration with different research group in the University. Briefly, ABA concentration was quantified following the method described by Siciliano *et al* (2015), with minor modifications. After being thawed, 50–100 µl of each biological replicate was centrifuged at 13,000 g and 4°C for 5 min. The obtained supernatant was filtered through a 0.2-µm syringe filter and collected in a 1-ml amber glass vial containing a glass insert (Supelco, Sigma- Aldrich) for small

sample volumes and analysed by high-performance liquid chromatography tandem mass spectrometry. High-performance liquid chromatography was carried out using a 1260 Agilent Technologies (Waldbronn, Germany) system equipped with a binary pump and a vacuum degasser. Sample aliquots (20 µl) were injected on a Luna C18 (150 × 2 mm i.d., 3 µm Phenomenex, Torrance, CA); ABA was eluted in isocratic conditions of 65:35 (H_2O:CH_3CN v/v acidified with HCOOH 0.1%) under a flow of 200 µl min^{-1} for 5 min. With the use of an electrospray ion source operating in negative ion mode, samples were introduced into a triple–quadruple mass spectrometer (Varian 310-MS TQ Mass Spectrometer). Analyses were conducted in multiple reaction monitoring mode using two transitions: 263 > 153 (CE 12 V) for quantification and 263 > 219 (CE 12 V) for monitoring, with 2 mbar of argon (Ar) as the collision gas. The external standard method was applied to quantify ABA concentration in target samples. A standard curve was generated using an original ABA standard (Sigma-Aldrich, St Louis, MO; purity 98.5%), with concentrations ranging from 10 to 500 µg L^{-1}. Limits of detection (LODs) and quantification (LOQs) were calculated on the basis of the standard deviation of the response (σ) and slope of the calibration curve (S) ratio in accordance with the ICH harmonized tripartite guideline expressed as follows: LOD = 3.3σ/S; LOQ = 10σ/S. Calculated final values were as follows: LOD = 0.87 ng ml^{-1}; LOQ = 2.90 ng ml^{-1}.

2.2.5. Non-structural carbohydrate content in tissues and xylem sap

At the end of the experiment, leaves, roots, stems and xylem sap were collected from all plants. Xylem sap was extracted from poplar stems using the procedure previously described by Secchi and Zwieniecki (2012). Briefly, after cutting the stem, leaves were removed, then the whole stem

was attached through a plastic tube to a syringe needle. The needle was threaded through a rubber cork to a small vacuum chamber with the needle tip placed in the 1.5-mL plastic tube. After generation of a vacuum (0.027 MPa absolute pressure), small pieces of stem were consecutively cut from the top, allowing liquid from open vessels to be sucked out of the stem and collected in the tube. The collected liquids were kept at -20° until analyses were performed. Sample tissues (leaf, root, stem) were oven-dried at 70 °C for 72 hours and ground into a fine powder using mortars. Non-structural sugars were quantified according to the protocol by Leyva *et al* (2008) which was later modified by Secchi and Zwieniecki (2012). Briefly, 1 ml of deionized water was added to 30 ± 2 mg of powdered tissue, vortexed, incubated at 72 °C for 15 min and centrifuged at 13.000 rpm for 10 min. The obtained supernatant was diluted and a 50 µL aliquot was mixed with 150 µL of sulfuric acid (98%) - anthrone solution (0.1%, w/v) in a 96 well micro-plate. The plate was placed on ice for 10 min and then incubated at 100°C for 20 min. After heating, the samples were allowed to cool for 20 min at room temperature. Sugar content was determined in the dry matter as glucose equivalents from the colorimetric reading (iMark™ Microplate Absorbance Reader, BIO-RAD Ltd, USA) of absorbance at 620 nm (A620) and using a predetermined glucose standard curve. Soluble sugar concentration was also determined in xylem sap samples following the same protocol by adding directly the sap aliquot to the anthrone solution.

2.2.6. Analysis of starch concentrations in wood samples

Frozen wood samples were ground to a fine powder using a tissue lyser system (TissueLyser II, Qiagen), and starch content was quantified by enzymatic assay (STA-20 kit; Sigma-Aldrich), as detailed by (Secchi and Zwieniecki, 2011). Starch content was represented by the amount of

released glucose, which was determined by colorimetric reaction using a glucose oxidase-mediated method in accordance with the manufacturer's instructions. Sample absorbance was read at 540 nm, and starch concentrations were calculated using the glucose standard curve as a reference and expressed as mg g-1 of fresh wood. Wood starch amounts were determined for all plants considered in the experiment.

2.2.7. Measurements of pH and electrical conductivity ion content in xylem sap

The pH was determined in all xylem sap samples using a micro pH electrode (PerpHect® ROSS®, Thermo Fischer Scientific, Waltham, MA USA). On the same liquids, the electrical conductivity (EC) was assessed using a portable conductivity meter (LAQUA B-700; Horiba Ltd., Kyoto, Japan).

2.2.8. Statistical analyses

Statistical analysis was performed with Sigma-plot (Systat software Inc., San Jose, USA) and IBM SPSS software (version 24). Pairwise comparisons between data were applied by using the appropriate post hoc test. Tukey's HSD test was adopted for one-way ANOVA at $p<0.05$ (Tukey, 1949).

2.3. Results

2.3.1. Leaf gas exchange and stem water potential and plant hydraulics

In the present study, water deficit imposed for 11 days in order to reach a severe stress level corresponding to -2.4 MPa (average stem water

potential; Ψ_{stem}), followed by a re-watering period of 7 days for full recovery (Fig 2). The high level of water stress resulted in losses of stem hydraulic conductivity (80 ± 9.4% of PLC; Figure 3) coincided with turgor loss in leaves. Generally, one of the primary responses of plant to water deficit is reduction of leaf gas exchange following stomatal closure. A decline in photosynthetic rate (A) was recorded in water deficit poplars throughout the stress period; also, stomatal conductance (g_s) showed significant differences between water deficit and control tree plants. During the water stress period, these values gradually declined until the day 0, which reached to the minimum amount (Fig 2 a and b; day 0); however, stomata were entirely closed at severe water stress (Fig 2b; day 0). Stem water potential (Ψ_{stem}) was significantly lower in water deficit treated plants after 6 days of water withdrawal when compared with control trees (Fig. 2c). Half of the stressed plants (nine in total) were watered during the morning of Day 0 and within several hours (Day 1), Ψ_{stem} recovered close to control-plant levels. This happened while three days after resumption of irrigation, treated plants showed unchanged values of g_s and A compare to pre-stress conditions. Moreover, 1 day after stress relief, poplars showed an uncompleted hydraulic recover (PLC = 64.2 ± 22.7), whereas a significant drop in the level of PLC, comparable with prestress levels, was measured within 7 days of watering (Fig. 3). PLC in recovered plants was not significantly different from that observed in control plants after 7 days of recovery. On the seventh day of stress relief, Ψ_{stem}, stomatal conductance and photosynthesis reached to values which were not significantly different from the control (Fig. 2a, 2b and 2c).

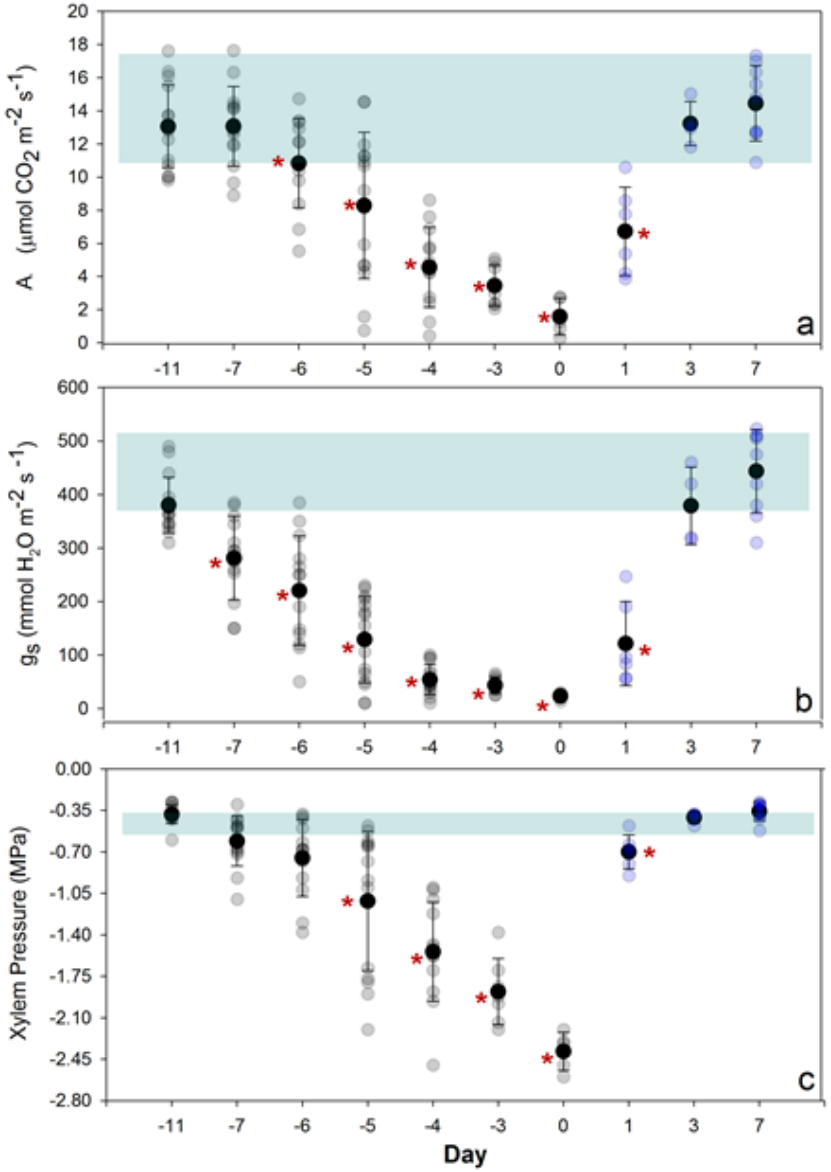

Fig. 2 Measurements of a) assimilation (A, µmol CO_2 m^{-2} s^{-1}), b) stomatal conductance (g_s, mmol H_2O m^{-2} s^{-1}) and c) xylem pressure (Ψ_{stem}, MPa) over the progression of drought stress (SS) and recovery (REC). Black dots indicate average values for each parameter, while grey and blue dots refer to single measurements of each parameter taken on SS and REC plants on each experimental day, respectively. The light blue rectangle represents the average

value of each parameter measured on well irrigated (CTR) plants. Day -11 represents the beginning of the water stress treatment; Day 0 coincides with the moment of rehydration and Day 7 with full recovery. Asterisks denote significant differences between treated (SS or REC) and irrigated (CTR) plants on each day of measurements, tested using the Student's t test ($P < 0.05$). Bars represent SD ($n = 9$). This picture was retrieved from (Pagliarani *et al,* 2019).

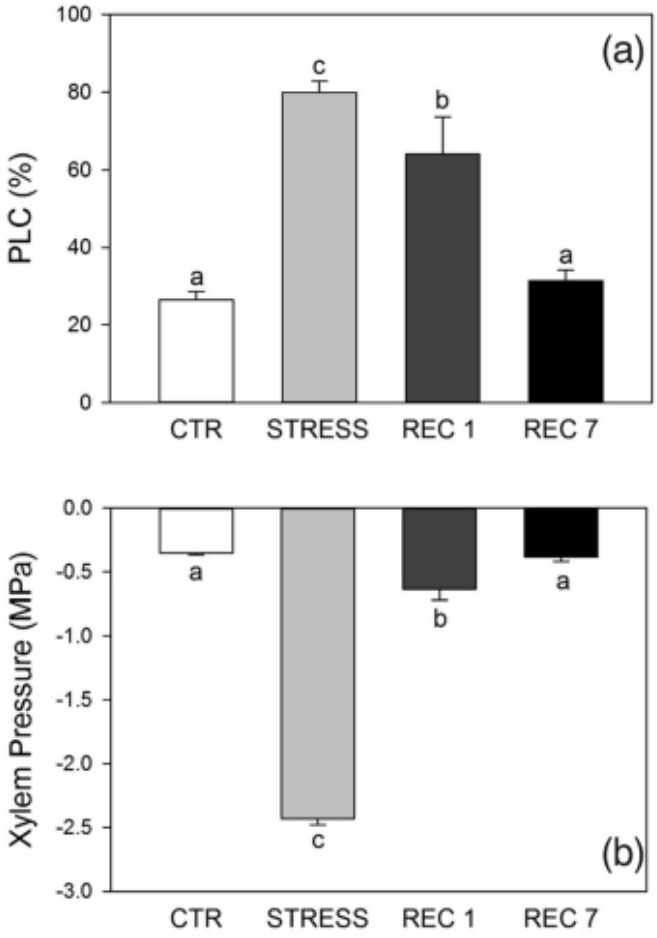

Fig 3. (a) Extent of embolism represented as percent of loss of conductivity (PLC) in stem of poplars. (b) Xylem pressure measured using balancing pressure method on transpiring leaves (Ψ_{stem}, MPa). White, grey, dark grey, and black bars indicate average values measured in CTR, SS, and 1 and 7 days of REC plants,

respectively. Uppercase letters above bars denote significant differences ($P < 0.05$), tested using Tukey's honestly significant difference test. Error bars represent SE. This picture was retrieved from (Pagliarani *et al,* 2019).

2.3.2. Measurement of xylem sap and wood biochemical contents

ABA accumulation was measured as indicator of stress adaptation to confirm the drought responses of poplar plants. As expected, ABA concentrations in the xylem sap was significantly different in stressed (up to 100-fold) and control plants at day 0 (Table 1) with higher amounts of ABA concentration in plants under severe stress. One week after re-watering, ABA decreased to prestress values, reaching levels similar to those measured in control trees (12.57 ± 5.49 µg L^{-1} and 12.41 ± 1.65 µg L^{-1}, respectively), (Table 1). Electrical conductivity of stressed xylem sap rose up (Table 1) compared to control poplars, however, after one week of re-watering, electrical conductivity of REC plant did not return to pre-stress condition (Table 1). Xylem sap acidification increased in parallel with increasing the drought stress (Table 1), consequently xylem sap pH dropped significantly under water deficit condition (5.94 ± 0.042 SS and 6.28 ± 0.037 CTR). However, pH values remained unchanged at acidic level after re-watering and recovery stress was not obtained until the end of experiment (Table 1). Plants accumulate osmolyte compounds such as soluble carbohydrate for osmotic adjustment in response to short- or long-term water deficiency or salinity stress. These low molecular compatible solutes can balance water potential and can maintain cell turgor during stress (Zhang *et al,* 2009).

Table 1. Measurements of abscisic acid (ABA), pH, electrical conductivity and total carbohydrates from xylem sap and starch in wood samples collected from well irrigated (CTR), severely stressed (SS) and recovered (REC after 7 days) poplars. Average values of stem water potential (Ψ_{stem}) were also reported for each condition.

	CTR	**SS**	**REC**
Ψ_{stem} (MPa)	-0.44 ± 0.01 b	-2.06 ± 0.06 a	-0.36 ± 0.03 b
ABA (µg L^{-1})	12.41 ± 1.65 b	1189.16 ± 165.96 a	12.57 ± 5.49 b
pH	6.28 ± 0.037 a	5.94 ± 0.042 b	5.91 ± 0.053 b
Electrical conductivity (µS cm^{-1})	0.67 ± 0.05 b	1.1 ± 0.03 a	1.01 ± 0.18 a
Total carbohydrates (mmol mL^{-1})	1.37 ± 0.154 b	7.08 ± 1.3 a	1.84 ± 0.832 b
Starch (mg g^{-1} FW)	13.2 ± 0.47 a	1.7 ± 0.10 b	4.0 ± 0.18 b

Values are means ± SE (n = 9, each biological replicate represents a different plant). Different lower-case letters following SE values indicate significant differences attested by Tukey's *HSD* test ($P < 0.05$). This table was retrieved from (Pagliarani *et al,* 2019).

A significant difference in apoplastic soluble carbohydrates content was observed between SS and CTR plants (Table 1); soluble carbohydrates level in SS plants was four times higher than in control plants (Table 1); however, after recovery, the accumulation of NSC in xylem sap declined and reached to irrigated poplar values (Table 1). Plants subjected to water stress also exhibited a lower starch concentration in wood samples (1.7 ± 0.10 mg g^{-1} FW) compared to CTR poplars (13.2 ± 0.47 mg g^{-1} FW) (Table 1).

2.4. Discussion

Trees responded to water stress with a fast decrease of both net assimilation and stomatal conductance five days after drought imposition. Although rehydration treatment did cause a fast recovery of stem water

potential to pre-stress conditions, both A and g_s took three to seven days to fully recover. This pattern of fast recovery of xylem pressure, associated with a delay in the restoring of stomatal conductance and photosynthetic processes, is consistent with previous results obtained in poplar (Secchi and Zwieniecki, 2014) and in other woody plants, such as Eucalyptus (Martorell *et al*, 2014), grapevine (Lovisolo *et al*, 2008; Chitarra *et al*, 2014), laurel (Trifilo *et al*, 2017) and conifers (Brodribb and McAdam, 2013). The xylem embolism formation in stems measured as PLC (percentage loss of hydraulic conductivity) is a parameter used to assess the impact of drought on xylem water transport in plants (Cochard *et al,* 2013; Trifilò *et al,* 2014). The results of this study indicated that more severe stress (Ψ_{stem} < −2 MPa) strongly impacted xylem hydraulic conductivity, inducing high levels of embolism formation (80% PLC), indicative of vulnerability to drought-induced cavitation in *P. tremula* × *alba* (Secchi and Zwieniecki, 2014). Twenty-four hours after soil was re-watered, a fast recovery of stem PLC was not observed in the study, consistent with an increasing number of studies that propose tree species are incapable to fast refill xylem embolisms following severe water stress (Choat *et al,* 2015; Knipfer *et al,* 2017; Creek *et al,* 2018); while after 7 days of watering, a meaningful reduction in stem PLC was recorded. Potted poplar trees grown in similar conditions were able to recover from embolism formation after water relief and under low or moderate tension; thus, the results presented here are consistent with data of xylem hydraulic recovery measured respectively in *P. trichocarpa* (Secchi and Zwieniecki, 2011), *P. nigra* (Secchi and Zwieniecki, 2012), and in the same clone used here (*P. alba* × *tremula*; Secchi and Zwieniecki, 2014).

Besides hydraulic factors, a delayed stomata opening could be attributed to non-hydraulic chemical signals, such as a slow return to pre stress-levels of

abscisic acid (ABA) previously accumulated during the progress of drought (Lovisolo *et al*, 2002; Schachtman and Goodger, 2008; Pantin *et al*, 2013). Here, analysis of ABA contents in xylem sap show that the hormone levels returned to pre-stress condition over the period of seven days. However, the delayed stomata opening could relate to the fact that the return of ABA contents from very high to low pre-stress levels did not occur in accordance to stem water potential as was shown in previous study (Lovisolo *et al*, 2008). In addition, maintenance of the low xylem pH could affect the recovery of g_s, as the increase of pH was shown *in vivo* to enhance the sensitivity of stomata to water stress by buildup of apoplastic ABA concentration in some herbaceous plants (Wilkinson and Davies, 1997). A lower pH indeed allowed for maintenance of lower stomatal aperture despite lower ABA concentration around stomata (Schachtman and Goodger, 2008). The fact that poplar and some other woody species lower their pH under water stress, unlike many herbaceous species, might be important from the perspective of their perennial habit and need to recover hydraulic losses caused by stress. Also, large quantities of ABA in the xylem sap under stress (low transpiration) can lead to sudden accumulation of this hormone in leaves during recovery and thus being responsible for the delay in g_s recovery (Perrone *et al*, 2012). All together, these results point out that the regulation of transpiration by stomata and g_s recovery from drought may be influenced by a complex network of factors (ie. changes in endogenous abscisic acid levels and/or efficiency of the photosynthetic system) other than the supply of water through the xylem and stem water pressure. Further, observed delay in g_s recovery in perennial plants might provide a necessary time buffer between water potential restoration and turning on transpiration, time that it is necessary for repair of hydraulic transport capacity lost to embolism. Ability of trees to repair xylem functionality after a

short-term drought treatment is highly correlated with carbohydrate content in the stem (Trifilo *et al*, 2017). Starch metabolism is considered to be at the forefront of plant response to embolism, and several studies have demonstrated that embolism presence alters metabolism and partitioning between starch and soluble carbohydrates as well as the related enzyme activities and gene expression (Salleo *et al*, 2004; Regier *et al*, 2009; Secchi and Zwieniecki, 2011). Here, we observed a reduction of starch content in stressed plants that is probably dependent on the increase of its degradation rate (Niittyla *et al*, 2004; Weise *et al*, 2005; Lu and Sharkey, 2006). Under drought stress, sugars in xylem apoplast could accumulate either as products of starch degradation stored in parenchyma cells or translocated from phloem to parenchyma rays. This accumulation can be either passive i.e. leak of sugars via membranes due to large difference in concentration between apoplast and living cells, or active transport facilitated by sugar membrane transporters. The sucrose transporter *SUT4*, a protein homologous to the maize *SUT1*, is a phloem-localized bidirectional transporter catalyzing both sucrose and proton transport depending on sucrose and pH gradient as well as on membrane potential (Carpaneto *et al*, 2005, 2010). The role of *SUT4* in controlling sucrose transport and partitioning was already explored in poplar and it was demonstrated that, specifically at the stem level, besides phloem cells, this transporter is also expressed in ray parenchyma cells, fibers, and secondary xylem vessels (Payyavula *et al*, 2011). Pagliarani *et al,* (2019) founded that *SUT4* transcripts were more abundant in SS (severe drought stress) poplar woody tissues; therefore, the increased activity of this symporter can facilitate the efflux of both sucrose and protons towards the apoplast, as attested by the increase of total carbohydrates content in sap and by acidification of apoplastic pH. However lower pH and accumulation of disaccharides can

halt the efflux of sugar to apoplast via SUT transporters what would hinder plant potential to build osmoticum level that would allow for refilling upon relief from stress. Nevertheless, lower pH can also trigger activity of apoplastic invertases reducing the concentration of sucrose and thus maintaining the gradient prompting sucrose efflux (Pagliarani *et al,* 2019).

Alteration of sap pH is one of the first chemical changes occurring within xylem vessels of water stressed plants (Bahrun *et al*, 2002; Sobeih *et al*, 2004). Unlike herbaceous plants, drought-induced alkalization of apoplastic pH is not common in trees, as documented in a number of woody species (Sharp and Davies, 2009) and by a recent research (Losso *et al*, 2018), where acidification of xylem sap pH was observed in conifers during the summer period at the alpine timberline. Here, it is proved that: i) poplars exposed to severe water stress respond through acidification of xylem apoplast; ii) drop of pH under drought was accompanied by the accumulation of soluble carbohydrates, iii) starch hydrolysis increases the content of soluble carbohydrates. It was previously proposed that a lower pH environment might cause accumulation of monosaccharides in xylem apoplast via sucrose hydrolysis mediated by acidic invertases (Secchi and Zwieniecki, 2016). This strongly implies that plants respond to stress with a biological control of physiological activity related to accumulation of monosaccharides in the xylem (Pagliarani *et al,* 2019). This accumulation and, in parallel, the reduction of disaccharide content results in maintence of efflux of disaccharides towards the apoplast, transport sustained by a low apoplastic sucrose concentration and by a faster buildup of osmoticum by accumulation of monosaccharide (Pagliarani *et al,* 2019). The fact that pH had not returned to the pre-stress condition within few days might reflect the lingering effect of stress or ‘memory of stress’ that would facilitate responses to consecutive droughts.

CHAPTER III

Chemical and physiological responses of poplar trees to heat stress

3.1. Introduction

Extreme heat can cause great shifts in plant vegetation, productivity, and dynamics of species communities (Smith, 2011; Ciais *et al,* 2005; Wang *et al,* 2016). There are many changes that extreme heat can cause, including DNA damage, transcriptomic reprogramming, proteomic changes, inhibition of CO_2 assimilation, altered phytohormone concentrations, and shifted homeostasis between reactive oxygen species (ROS) and antioxidants (Bita and Gerats, 2013; Jia *et al,* 2017). It has been demonstrated that temperatures higher than optimal levels can be followed by lower photosynthesis rates due to a decline in the affinity of ribulose-1,5-bisphosphate carboxylase/oxygenase (Rubisco) for CO_2, reducing carboxylation and increasing oxygenation (Ashraf and Harris, 2013; Aragao *et al,* 2005). Moreover, Rubisco is less active at high temperatures because the functionality of Rubisco activase is impaired (Sharkey, 2005, Velikova *et al*, 2012). High temperatures also significantly affect the structure and function of the thylakoid membranes (Havaux *et al*, 1996; Schrader *et al*, 2004). The thylakoid membranes are the site of electron transport within the chloroplast with high sensitivity to heat stress; thus, higher temperature stress can lead to photosystem II (PSII) impairment (Schrader *et al*, 2004; Sharkey, 2005). Reductions in the maximum (F_v/F_m) and actual (ΦPSII) quantum efficiencies of electron transport can show diminished function of PSII during heat stress (Crafts-Brandner and Salvucci, 2000; Murchie and Lawson, 2013). Heat stress can induce an increase in levels of photorespiration and dark respiration relative to photosynthesis (Wahid *et al,* 2007; Killi *et al,* 2016). Stomatal conductance and transpirative water loss are commonly enhanced with elevated temperature (Shah and Paulsen, 2003; Haworth *et al,* 2018). However, longer exposure to high temperatures may provide the chance of adaptation in stomatal behavior to

diminish stomatal conductance (Killi *et al,* 2016; Centritto *et al,* 2011). In this study, the poplar, which is a perennial plant, has been chosen to examine the impact of heat waves. Previous studies on poplar under heat treatments were implemented for a few hours or a week, mainly focused on the physiological, transcriptional, and post-transcriptional changes in gene expression involved in heat stress, heat shock proteins, hormonal biosynthesis, Rubisco activity, and sugar transporter (Hozain *et al,* 2010; Weston *et al,* 2011; Li *et al,* 2014; Jia *et al,* 2016 and 2017). All of the above studies, however, were restricted to leaves and roots. While, antioxidant activity sugar in leaves and roots, and ROS damages by heat was primarily targeted (Li *et al,* 2014; Jia *et al,* 2016 and 2017). The main objectives of this study were to determine the impact of consecutive heat waves on poplar (*P. tremula* x *P. alba*) physiology, including growth and development, along with changes in apoplast chemistry. Specifically, objectives of this study were to: i) discover whether or not the impact of heat on the physiological and chemical process could be similar or different from drought on poplar; ii) assess the effect of consecutive heat stress on physiological parameters including water potential, g_s, photosynthesis, transpiration, PSII integrity; iii) investigation of the effect of heat on total non-structural carbohydrate content; iv) detection of the impacts of progressive heat stress on apoplastic pH and electrical conductivity of xylem sap. In order to gain a better understanding of the effect of prolonged intense heat waves on the physiological and chemical processes involved in heat responses, I conducted a study based on the following hypotheses: i) prolonged heat waves would lead to limitations in g_s, photosynthesis, and water potential; ii) elevated temperature would alter concentration of non-structural carbohydrates in different organs by changing stomatal function and photosynthetic activity; iii) elevated temperature would generate

different pH values in apoplast of stressed plants. Based on the above hypotheses, I should observe detrimental effects on the leaf gas exchange and water potential concomitant with an alteration in xylem sap pH and non-structural carbohydrate contents in different plant tissues. I tested these hypotheses by evaluating the responses of potted plants to consecutive heat waves under temperatures ranging from 26 to 40 °C.

3.2. Material and Methods

3.2.1. Plant materials and growth conditions

Six- months old plants of the hybrid poplar (*P. tremula* × *P. alba* clone 717-1B4) were grown in a greenhouse under partially controlled climate conditions in University of Turin (Grugliasco campus) during April 2017. Temperature was maintained in the range of 17°C to 29°C and natural daylight was provided when it was necessary by using metal halogen lamps (500–600 µmol photons m^{-2} s^{-1}) to maintain a 12/12-h light/dark cycle. A total of 24 plants with homogeneous size (having an average height and stem diameter of 91.7 ± 2.9 cm and 4.8 ± 0.13 mm, respectively), were used in this study. Before temperature imposition treatment, all plants were acclimated to the condition in controlled growth chambers (phytotrons) for 25 days with daily irrigation (container capacity, CC) and under the following conditions: light/dark 16/8 hours; day/night temperature 24/16°C; relative humidity, 60%. The plants were then divided into two groups, the first one, consisted of 12 plants which were later distributed into two climate chambers with six plants in each. They were kept under acclimation conditions and considered as control plants. The other 12 plants (second group) were assigned to two phytotrons (six plants each) and were then subjected to heat stress. A detailed schematic representation of temperature treatment in each phytotron is provided in Figure 1. The

treatment was imposed for 23 days; the day/night temperatures of the chambers were 40/26 °C respectively with light/dark 16/8 hours. High temperature levels were obtained by allowing gradual increments during the day and the maximum value (40 °C) was maintained stable for 5 hours (Fig 2). All plants were watered daily in order to maintain container capacity.

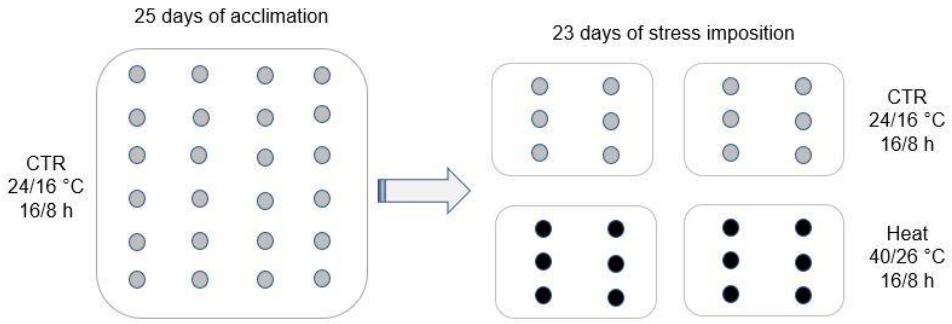

Fig 1. Timing schematic representation of temperature treatment over the duration of the experiment. Plants were monitored throughout the entire experiment, that is, from the start of the acclimation to phytotron (25 days) until end of heat stress treatment (23 days). Grey circles and black circles represent control condition (CTR) and heat stress respectively.

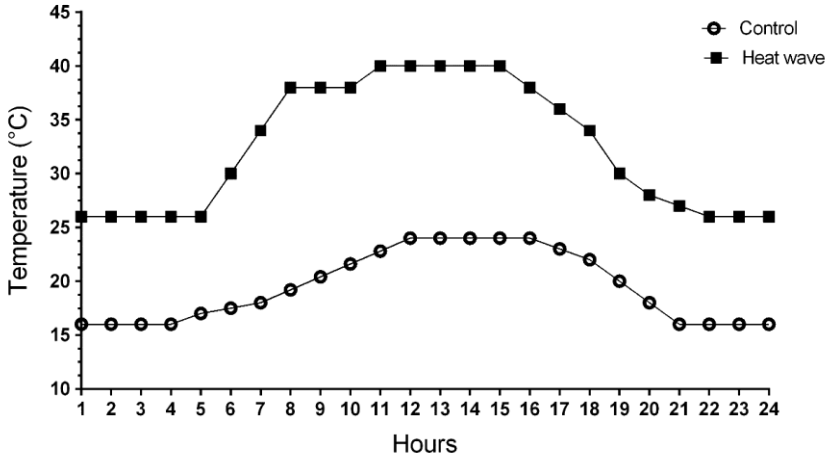

Fig 2. Daily pattern of temperature in control and heat stress phytotron.

3.2.2. Measurements of leaf gas exchange and water potential

Assimilation rate (A, µmol CO_2 m^{-2} s^{-1}), stomatal conductance (g_s, mmol H_2O m^{-2} s^{-1}) and transpiration rate (E, mmol H_2O m^{-2} s^{-1}) were measured on three fully expanded leaves per individual plant using a portable infrared gas analyzer ADC-LCPro+ system (The Analytical Development Company Ltd, Hoddesdon, UK). Measurements were performed using a 6.25 cm^2 leaf chamber equipped with artificial irradiation (1200 µmol photon m^{-2} s^{-1}) under ambient CO_2 values maintained constant at 400 ppm. Leaf water potential (Ψ_{leaf}) was measured over on the duration of the experiment on mature leaves using a Scholander-type pressure chamber (Soil Moisture Equipment Corp., Santa Barbara, CA, USA). Briefly, leaves were covered using a humidified plastic bag and excised immediately; and then Ψ_{leaf} was measured using a pressure chamber. Leaf gas exchange and leaf water potential were monitored during the experiment from 9:00-12:00 am.

3.2.3. Plant growth analysis, chlorophyll contents and chlorophyll fluorescence

Plant height and stem diameter were measured both at the beginning and at the end of the experiment. Eight young leaves (four control and four stressed poplars leaves) were labelled; from the beginning and throughout the duration of the experiment, images were taken every four days in order to estimate leaf growth. The collected images were used to calculate the Relative Leaf Expansion Rate (RLER) as it follows (Hesketh and Baker, 1969): RLER= [ln(LAe) – ln(LAb)]/ Δt, where LA is the leaf area measured at the beginning (LAb) and at the end (LAe) of the experiment and Δt is the duration of the treatment (23 days). Leaf area (LA) was calculated from digital images using the ImageJ software (http://rsbweb.nih.gov/ij/). Changes in chlorophyll concentration were also determined during the experiment by using a portable SPAD meter (SPAD 502 Plus Chlorophyll Meter, Spectrum, Plainfield, IL, USA); taking measurements on three fully expanded leaves of each plant (three control and three stressed leaves). Chlorophyll content data were collected every five days until the end of experiment. Maximal quantum yield of the PSII (F_v/F_m) was determined on the same leaves, through measurements of chlorophyll fluorescence using a portable chlorophyll fluorometer (Handy PEA, Hansatech Instruments, Ltd. UK). Before the measurements, the leaves were adapted to darkness for 45 minutes.

3.2.4. ABA measurement

ABA quantification has been performed in collaboration with different research group in the University. Briefly, ABA concentration was quantified following the method described by (Siciliano *et al*, 2015) with minor

modifications. After thawing the sap, 50-100 µL of each biological replicate was centrifuged at 13000 g and 4 °C for 5 minutes. For roots and leaves, 0.2 g dry powder of each part was transferred in 2 mL tubes with 1 mL extraction solution (80% CH_3OH acidified with 0.1% CH_3COOH) then shaken at 4 °C in the dark overnight. After that, samples were centrifuged at 15000 rpm and 4 °C for 2 min. Then the obtained supernatant from both procedures was filtered through a 0.2 µm syringe filter and collected in a 1 mL amber glass vial containing an appropriate glass insert (Supelco, Sigma-Aldrich) for small sample volumes and analyzed by HPLC-MS/MS. High Performance Liquid Chromatography was carried out using a 1260 Agilent Technologies (Waldbronn, Germany) system equipped with a binary pump and a vacuum degasser. Sample aliquots (20 µL) were injected on a Luna C18 (150 x 2 mm, 3 µ, Phenomenex, Torrance, CA, USA), ABA was eluted in isocratic conditions of 65:35 (H_2O:CH_3CN v/v acidified with HCOOH 0.1%) under a flow of 200 µL/min for 5 minutes. Using an electrospray (ESI) ion source operating in negative ion mode, samples were introduced into a triple-quadruple mass spectrometer (Varian 310-MS TQ Mass Spectrometer). Analyses were conducted in multiple reaction monitoring (MRM) mode using two transitions: 263>153 (CE 12V) for quantification, 263>219 (CE 12V) for monitoring, with 2 mbar of Argon (Ar) as collision gas. The external standard method was applied to quantify ABA concentration in target samples. In detail, a standard curve was generated using an original ABA standard (Sigma Aldrich, St Louis, MO, USA; purity 98.5%), with concentrations ranging from 10 to 500 ng mL^{-1}. The detection (LOD) and quantification (LOQ) limits were calculated based on the standard deviation of the response (σ) and slope of the calibration curve (S) ratio in accordance with the ICH harmonized tripartite guideline expressed

as: LOD=3.3σ/S; LOQ=10σ/S. Calculated final values were as follows: LOD = 0.87 ng mL^{-1}; LOQ = 2.90 ng mL^{-1}.

3.2.5. Non-structural carbohydrate content in tissues and xylem sap

At the end of the experiment, leaves, roots, stems and xylem sap were collected from all plants. Xylem sap was extracted from poplar stems using the procedure previously described by Secchi and Zwieniecki (2012). Briefly, after removing all leaves, stem was cut 20 cm above soil, whole stem was then attached through a plastic tube to a syringe needle. The needle was threaded through a rubber cork to a small vacuum chamber with the needle tip placed in the 1.5-mL plastic tube. After generation of a vacuum (0.027 MPa absolute pressure), small pieces of stem were consecutively cut from the top, allowing liquid from open vessels to be sucked out of the stem and collected in the tube. The obtained liquids were kept at -20° until analyses were performed. Sample tissues (leaf, root, stem) were oven-dried at 70 °C for 72 hours and ground into a fine powder using mortars. Non-structural sugars were quantified according to the protocol by Leyva *et al,* (2008) which was later modified by Secchi and Zwieniecki (2012). Briefly, 1 ml of deionized water was added to 30 ± 2 mg of powdered tissue, vortexed, incubated at 72 °C for 15 min and centrifuged at 13.000 rpm for 10 min. The obtained supernatant was diluted and a 50 µL aliquot was mixed with 150 µL of sulfuric acid (98%) - anthrone solution (0.1%, w/v) in a 96 well micro-plate. The plate was placed on ice for 10 min and then incubated at 100°C for 20 min. After heating, the samples were allowed to cool for 20 min at room temperature. Sugar content was determined in the dry matter as glucose equivalents from the colorimetric reading (iMark™ Microplate Absorbance Reader, BIO-RAD Ltd, USA) of absorbance at 620 nm (A620) and using a predetermined glucose standard

curve. Soluble sugar concentration was also determined in xylem sap samples following the same protocol by adding directly the sap aliquot to the anthrone solution.

3.2.6. Measurements of pH and electrical conductivity ion content in xylem sap

The pH was determined in all xylem sap samples using a micro pH electrode (PerpHect® ROSS®, Thermo Fischer Scientific, Waltham, MA USA). On the same liquids, the electrical conductivity (EC) was assessed using a portable conductivity meter (LAQUA B-700; Horiba Ltd., Kyoto, Japan).

3.2.7. Statistical analyses

Statistical analysis was performed with Sigma-plot (Systat software Inc., San Jose, USA) and IBM SPSS software (version 24). Pairwise comparisons between data were applied by using the appropriate post hoc test. Tukey's HSD test was adopted for one-way ANOVA at $p<0.05$ (Tukey, 1949).

3.3. Results

3.3.1. Leaf gas exchange and leaf water potential

After being transferred to the phytotron for acclimation, plants were maintained for 25 days in the growth chamber conditions, during which leaf gas exchange and leaf water potential measurements were conducted until the poplar plants showed similar trends in response to chamber condition

and displayed steady rates (-0.51 ± 0.1 MPa)[2]. Subsequently, heat waves were imposed for 23 days. After four days of heat treatment, a significant reduction in Ψ_{leaf} was observed in stressed plants (-0.58 ± 0.03 MPa) in comparison to CTR plants (-0.38 ± 0.02 MPa). This reduction in Ψ_{leaf} remained continuous and reached -1 (± 0.1) MPa at 23 days of stress (Fig 3 A). At the beginning of the experiment, stomatal conductance (g_s) showed fluctuations during acclimatization to the chamber; however, after two weeks, the trend of g_s remained approximately constant (167 ± 18.6 mmol H_2O $m^{-2}s^{-1}$). At the end of imposed treatment, plants almost closed their stomata. In control plants, g_s had a range from 140 (±10.5) to 280 (± 19.06) mmol H_2O $m^{-2}s^{-1}$, while heat waves induced a sharp drop of g_s ranging from 130 (± 20.5) mmol H_2O $m^{-2}s^{-1}$ at 1st day of stress to 56 (± 16.5) mmol H_2O $m^{-2}s^{-1}$ at 23rd day of stress (Fig. 3 B). In the growth chambers, photosynthesis rate (A) showed a similar steady value (10.3 ± 0.5 µmol CO_2 $m^{-2}s^{-1}$). Meanwhile, a drop-in photosynthesis rate was observed after 4 days of heat treatment in stressed plants (5.73 ±1.01 µmol CO_2 $m^{-2}s^{-1}$) relative to CTR (10.4 ± 1.2 µmol CO_2 $m^{-2}s^{-1}$), and during the 23 days of stress imposition, this value was continuously reduced and reached 2.02 (±0.67) µmol CO_2 $m^{-2}s^{-1}$ in stressed plants. Similarly, transpiration (E) was significantly affected by the treatment (Fig. 3 D). Four days of treatment diminished the amount of transpiration in stressed plants (1.5 ± 0.2 µH_2O $m^{-2}s^{-1}$) compared with the control group (2.7 ± 0.4 µH_2O $m^{-2}s^{-1}$). The results of this experiment indicated that heat stress impaired stomatal function and reduced transpiration. Changes in leaf gas exchange were accompanied by lower levels of leaf water potential in the stressed group during the experiment. Chlorophyll fluorescence measurement was performed to determine the efficiency of PSII, F_v/F_m is a parameter that can show plant

[2] data are represented by the mean and SE

photosynthetic capacity and is widely used to indicate the maximum quantum efficiency of photosystem II. However, after heat treatment, the ratio decreased gradually in plants which were exposed to high temperatures; they showed significant differences compared to the control poplars after day 16 (Fig. 4).

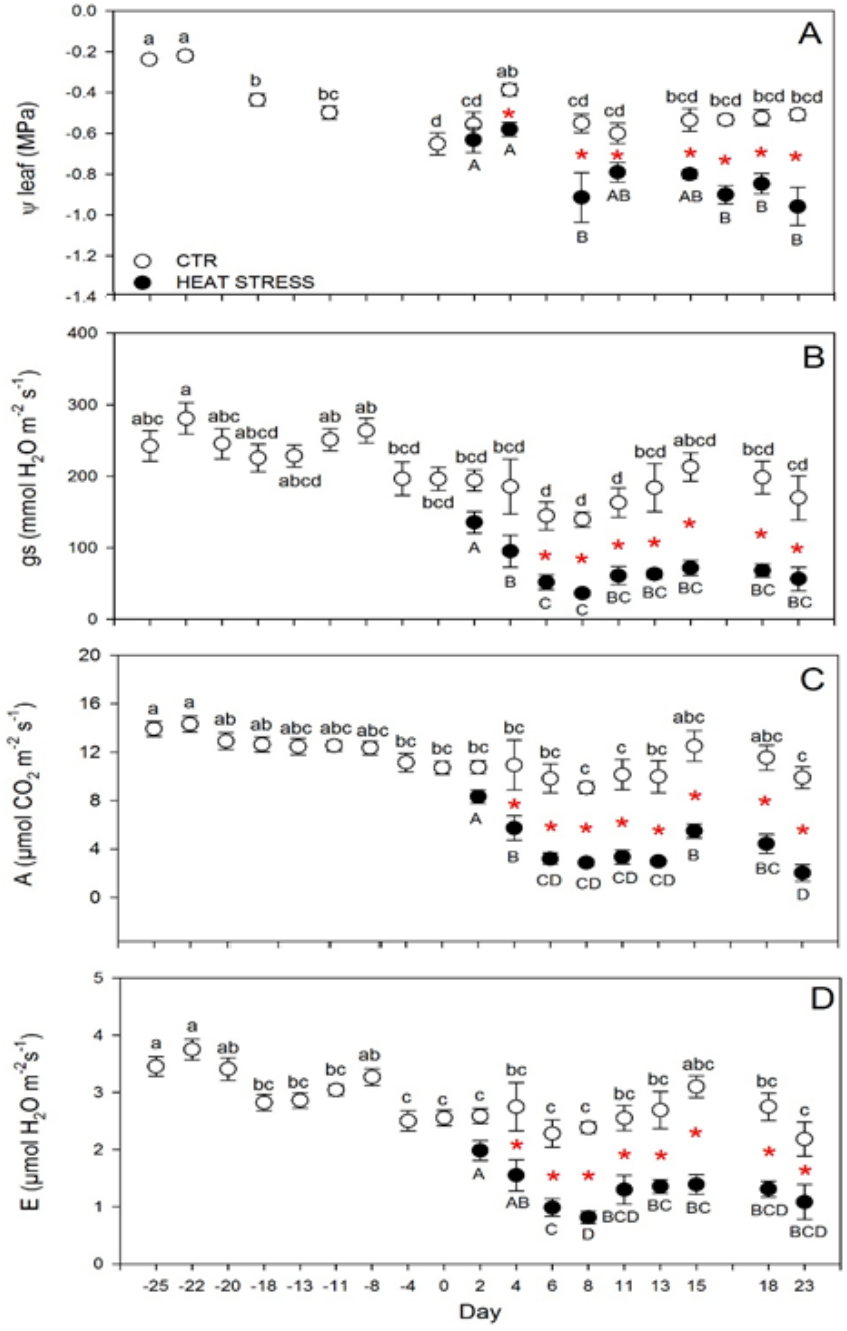

Fig. 3. A) Leaf water potential (Ψ_{leaf}) B) Stomatal conductance (g_s), C) Photosynthesis, D) Transpiration rate (E) of poplars under control and heat

condition. The values are indicating mean ± SE. Mean values were compared by using Tukey's HSD test. An asterisk indicates statistical significance *(P < 0.05) on t-test between heat treatment and control. Lower-case letters represent difference between CTR plants among days, bigger case letters represent difference between heat stress plants among days.

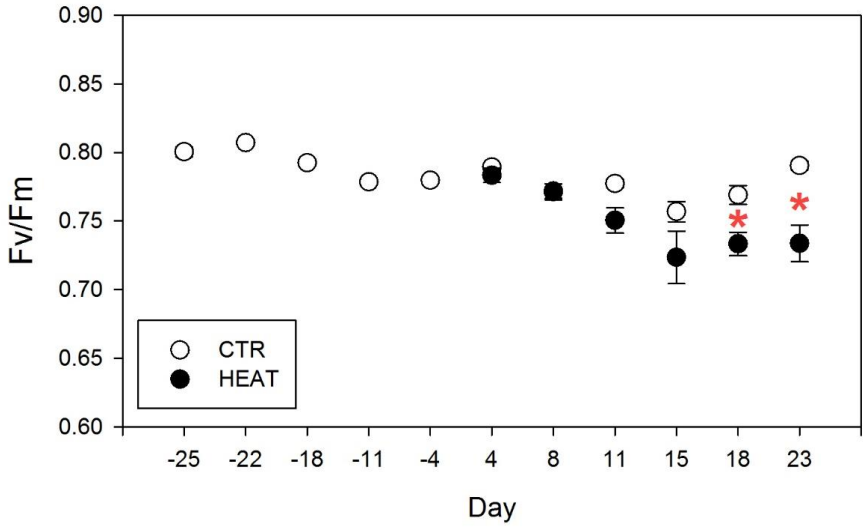

Fig. 4. Chlorophyll fluorescence, mean ± SE, an asterisk indicates significance: *P < 0.05 on t-test between heat treatment and control

3.3.2. Plant anatomical, morphological and physiological measurement

Plant height and stem diameter were recorded at the beginning and also at the end of the experiment. Both height and stem diameter were not affected by heat stress treatment (Table 1). While the height increment in control plants (3.52%) was greater than stressed plants (2.6%), the stem diameter increment was greater in control plants (15.65%) compared to stressed plants (5.39%). Elevated temperature significantly increased leaf number and leaf area; in stressed plants leaf area was smaller than the control group, but the leaf number showed greater number of leaves in heat

condition. At the end of heat treatment, leaf area increased 23.74% in control plants, whereas in stressed plants, leaf area slightly decreased under heat (+13.31%) compared to the beginning of the experiment. High temperature reduced the relative leaf expansion rate (RLER) of stressed plants compared to the control plants; however, the differences among treatments were not significant (Table 1). Leaf area per leaf number (LA/LN) data did not show any significant differences among all plants. Chlorophyll content (SPAD value) did not significantly differ across the studied plants (Fig. 5).

Table 1. Morphological and anatomical traits of poplars plant under stress and control conditions

	CTR (beginning)	**CTR (end)**	**HEAT STRESS (beginning)**	**HEAT STRESS (end)**
H_P (cm)	91 ± 5.8	94.2± 5.5	92.4 ± 2.4	94.8 ± 2.6 n.s
IRH_P %	-	+3.52 %	-	+2.6 %
D_S (mm)	4.76 ± 0.25	5.51 ± 0.24	4.85 ± 0.12	5.12 ± 0.13 n.s
IRD_S %	-	+15.65%	-	+5.39%
LA	225.2 ± 1.8 b	278.7 ± 7.9 a	259.3 ± 6.8 B	293.9 ± 2.9 A
IRLA %	-	+23.74%	-	+13.31%
LN	10 ± 0 c	11.66 ± 0.33 b	10 ± 0 c	14.33 ± 0.33 a
LA/LN	22.52	23.89	25.93	20.5 n.s
RLER	-	0.009 ± 0.001	-	0.005 ± 0.001 n.s

Values are means ± SE (n = 6, each biological replicate represents a different plant). Different lower-case and upper-case letters indicate significant differences among plants within each treatment attested by Tukey's HSD test ($P < 0.05$). H_P= Plant height, IRH_P= Increment rate of plant height, D_S= Stem diameter, IRD_S=

Increment rate of stem diameter, LA= Leaf area, IRLA= Increment rate of leaf area, LN= Leaf number, LA/LN= Leaf area/leaf number, RLER= Relative leaf expansion rate.

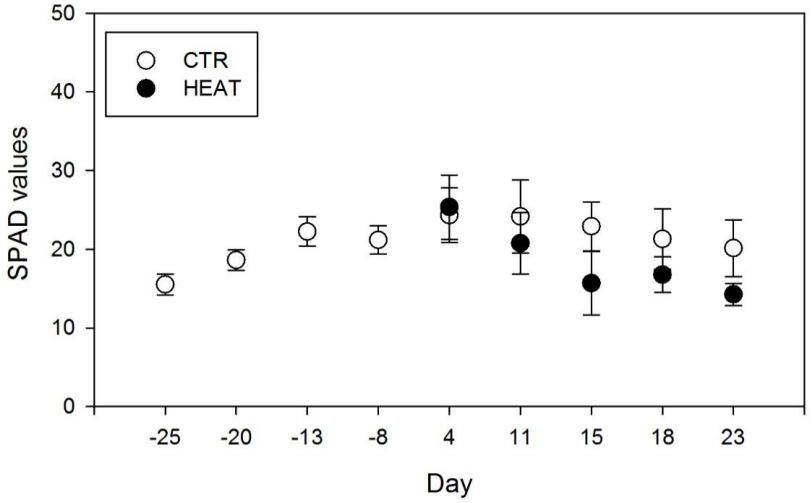

Fig. 5. Chlorophyll content, mean ± SE.

3.3.3. Biochemical measurement of leaves, stems, roots and xylem sap contents

To examine the impact of elevated temperature on biochemical properties of poplar plants, the non-structural carbohydrates concentration (NSC) was analyzed in leaves, roots, and stems. NSC content, electrical conductivity, pH, and ABA were also measured in xylem sap. The analysis of NSC content in leaves and roots did not indicate any statistically significant differences among all plants (Table 2). In contrast, heat stress triggered a remarkable drop in non-structural carbohydrates concentration in the stem of stressed plants compared to control poplars with 55.4 (± 3.1) and 83.8 (± 11.14) mg g^{-1} respectively (Table 2). Abscisic acid (ABA), known as stress phytohormone, can be induced in plants after sensing stresses, playing an

important role in stomatal closure. ABA content did not show any significant differences in roots and leaves across the tested plants (Table 2).

Table 2. Biochemical contents measurement of leave, stem and root

	CTR	**HEAT STRESS**
NSC_{leaf} (mg g^{-1})	172.2 ± 5.1	167.7 ± 13.6 n.s
NSC_{stem} (mg g^{-1})	83.8 ± 11.14 b	55.4 ± 3.1 a
NSC_{root} (mg g^{-1})	48.7 ± 9.6	44.1 ± 11.0 n.s
ABA_{leaf} (ng g^{-1} DW)	9.56 ± 1	10.4 ± 2 n.s
ABA_{root} (ng g^{-1} DW)	6.23 ± 0.2	6.3 ± 0.1 n.s

Values are means ± SE (n = 6, each biological replicate represents a different plant). Different lower-case letters following SE values indicate significant differences attested by Tukey's HSD test ($P < 0.05$). NSC_{leaf}= NSC content in leaves, NSC_{stem}= NSC content in stems, NSC_{root}= NSC content in roots, ABA_{leaf}= ABA content in leaves, ABA_{root}= ABA content in roots.

Non-structural carbohydrate content in the xylem sap increased under heat stress (Table 3). Similarly, electrical conductivity of stressed xylem sap increased (Table 3). It has been demonstrated that xylem apoplastic pH in plants under drought stress show symptoms of alkalization or acidification, and in some cases remained unchanged based on plants' response to the stress (Sharp and Davies, 2009). However, changes in apoplastic pH under heat stress are still poorly understood. In the current study, the results of pH measurement showed that high temperatures caused a significant drop in xylem pH (5.95 ± 0.05) compared to control (6.15 ± 0.02). ABA quantification of xylem sap showed that ABA concentration was increased slightly under heat in the stressed group; however, the difference was not remarkable (Table 3).

Table 3. Biochemical analysis of poplar sap exposed to stress and control conditions

	CTR	HEAT STRESS
pH	6.15 ± 0.02 b	5.95 ± 0.05 a
NSC_{XP} (mg ml^{-1})	0.52 ± 0.11 b	3.8 ± 1.1 a
EC (µS cm^{-1})	0.56 ± 0.03 b	0.98± 0.16 a
ABA_{XP} (µg L^{-1})	41.7± 17.5	63.5 ± 34.4 n.s

Values are means ± SE (n = 6, each biological replicate represents a different plant). Different lower-case letters following SE values indicate significant differences attested by Tukey's HSD test ($P < 0.05$). NSC_{XP}= NSC in xylem sap, EC= Electrical conductivity, ABA_{XP}= ABA content in xylem sap.

3.4. Discussion

Plant exposure to abiotic stresses in the natural environment induces changes in plant growth, performance, and product (Szymańska *et al,* 2017). Plants regularly face extreme high temperature, one of the consequences of climate change in most parts of the world. In this study, plants were subjected to prolonged heat wave treatment for almost three weeks. The obtained results demonstrated that plants were affected by heat waves; the treatment had strong effects on leaf gas exchange and decreased the parameters measured (g_s, A, E). In a number of studies, heat stress has been shown to inhibit gas exchange in different plant species (Song *et al,* 2014; Marias *et al,* 2017). Accordingly, some experiments were conducted to identify the relationship between stomatal conductance (g_s) and photosynthesis restriction under high temperature (Ashraf and Harris, 2013; Ameye *et al,* 2012; Jia *et al,* 2016; Correia *et al,* 2018). Moreover, it has been proven that environmental stresses can inhibit photosynthesis performance by stomatal or nonstomatal (alterations in enzyme activity) inhibition, or both (Ashraf and Harris, 2013; Song *et al,* 2014). Mostly, the

nonstomatal limitation is linked with the alteration in enzyme activity (Larkindale *et al,* 2005). In this study, heat stress triggered a reduction in photosynthesis and g_s that was accompanied by an increase in the leaf water potential. Due to high demand of evapotranspiration under elevated temperature, stressed plants had a negative value of leaf water potential (Ψ_{leaf}), even with daily irrigation. These results are consistent with the findings of research on other plant species (Wahid 2007; Nduwimana and Wei, 2017; Wahid and Close, 2007; Sarwar *et al,* 2019). The reduction of water potential could be related to inability of the roots to uptake water and nutrients upon high temperature (Pie *et al,* 2000; Ghorbanpoure *et al,* 2018; Sarwar *et al,* 2019). One of the strategies to cope with heat stress is to keep their stomata open for transpirational cooling in most species of plants (Salvucci and Crafts-Brandner, 2004; Ameye *et al,* 2012). However, in this study, different results were recorded as plants diminished the rate of transpiration; the same results have been reported in wheat (Feng *et al,* 2014), tomato (Duan *et al,* 2017), simon poplar (*P. simonii*) (Song *et al,* 2014), and canadian goldenrod (*Solidago canadensis* L.) (Wang *et al,* 2016). High temperature has been shown to cause an increase in transpiration rates (Prasad *et al,* 2008; Ameye *et al,* 2012); here, transpiration decreased during the initial onset of heat stress. Generally, the most destructive effects of heat stress on photosynthesis apparatus has been reported on the chlorophyll content and maximum photochemical efficiency of PSII (F_v/F_m); therefore, efficiency of photosynthesis can be inhibited by these damages, which enhances photorespiration rate in plant species (Yamada *et al,* 1996; Ameye *et al,* 2012; Song *et al,* 2014). Chlorophyll fluorescence analysis has become one of the most powerful and reliable assessments of plant responses to the environmental changes, which gives us insight into the function and efficiency of photosynthesis

during stresses (Maxwell and Johnson, 2000; Crain and Trembly, 2017). Moreover, it is the most common indicator of photoinhibition degree and the level of damage to the photosynthesis system under temperature stress (Yamada *et al,* 1996). This study demonstrated that a slight decline in F_v/F_m ratio started after heat treatment, but significant damage was only observed after sixteen days of treatment. It has been indicated that, in some species which are exposed to heat waves, electron transport in PSII remained functional in the thylakoid membrane, regardless of reduction in net photosynthesis rate (Ameye *et al,* 2012; Ashraf and Harris, 2013).

In general, the total plant growth and development, foliar growth and expansion can be affected by long-term heat stress. However, some studies reported greater vegetative growth rate under elevated temperature in some non-perennial crops such as maize and soybean (Hatfield *et al,* 2011; Hatfield and Prueger, 2015). The data of the present study showed an increase in the number of leaves along with a remarkable reduction in leaf area in stressed plants. In this regard, shortening of leaves and smaller leaf area have been reported in many studies upon heat stress (Prasad *et al,* 2006; Niinemets, 2010; Tao and Zhang, 2013; Chen *et al,* 2018). SPAD value measurement (an indicator of chlorophyll content) did not show any significant damage in leaves' chlorophyll and photosynthetic pigments and leaves remained green during heat stress. This finding is in contrast to Dhyani *et al,* (2013) and Liu *et al,* (2013) results in wheat and rice, respectively. They reported that high thermal treatment distracted chlorophyll content dramatically. During the three-week period of heat treatment, plants adapted to stress; the exposure wasn't long enough to damage leaves' chlorophyll. However, long-term stress exposure may lead to significant chlorophyll content destruction in poplar.

Stored non-structural carbohydrates (NSC) have been suggested as a key determinant of stress resistance in plants (Rosas *et al,* 2013). NSC performs different functional roles, including transport, energy metabolism, and osmoregulation, while also supplying substrates for the synthesis of defense compounds (Hartmann and Trumbore, 2016; Tomasella *et al,* 2017). The result of NSC concentrations in different tissues revealed that NSC content was not changed in leaves and roots. Similar to the results of this study, NSC in leaves of sweet orange did not change dramatically under high temperature (Vu *et al,* 2002). In contrast, stressed plants showed a remarkable reduction of non-structural carbohydrates concentration in stem cells in the present work. In addition, a decline in sap pH was observed in heat stress plants, along with increased carbohydrates concentration and elevated electrical conductivity. The results of the present study are consistent with the results of Secchi and Zwieniecki (2012) research on *Populus nigra* under drought stress. They reported a simultaneous reduction in xylem sap pH, carbohydrates enhancement, and ions accumulation in the apoplast of poplars with symptoms of severe drought stress. The findings of the present study suggest that drought stress occurred together with prolonged heat waves, and xylem sap acidification was induced by drought in plants under high thermal stress. Generally, changes in the xylem sap pH observed in plants under drought stress are one of the primary responses to dry soil (Bahrun *et al*, 2002; Sobeih *et al*, 2004). The regulatory mechanisms of apoplastic pH variation are still unknown (Jia and Davies, 2007; Gloser *et al*, 2016). Various mechanisms were suggested to explain the mechanism change of xylem sap pH which mostly were associated with the ion transport modifications in xylem sap and/or minerals content, the respiration rate (Salomón *et al,* 2016), flow rate (Peuke, 2016), and ABA signals (Roelfsem and Hedrich,

2002; Gloser *et al*, 2016; Boursiac *et al,* 2013; Brunetti *et al,* 2019). In some plants, especially annual species, xylem sap alkalization was reported under drought stress (Sharp and Davies, 2009). In contrast to herbaceous, some woody trees showed acidification of sap under drought stress in *Populus nigra* (Secchi and Zwieniecki, 2012; Brunetti *et al,* 2019); in conifer during summer period at the alpine timberline (Losso *et al*, 2018) and also in *Eucalyptus globulus* L. under water shortage regime (Hernandez *et al,* 2016). However, pH alteration under heat waves condition is less considered.

Change in phytohormones concentration is one of the first environmental responses to different stresses and accumulation of abscisic acid (ABA) is known as the fastest symptom of thermal stress in plants (Yamaguchi-Shinozaki and Shinozaki, 2006). Several researchers demonstrated the effects of ABA on abiotic stress (Hasanuzzaman *et al,* 2013; McAdam and Brodribb, 2014; Sah *et al,* 2016; Vishwakarma *et al,* 2017; Bita and Gerats, 2013). Briefly, ABA has a crucial role in acclimation to the high thermal stress by regulating physiological process and molecular pathway in annual and perennial plants (Jia *et al,* 2017). Stomatal regulation, seed dormancy and germination, modulation of root architecture, leaf senescence, synthesis of storage proteins and lipids and many other roles are attributed to ABA role in plants (Tuteja, 2007; Sah *et al,* 2016; Vishwakarma *et al,* 2017). Escandón *et al,* (2016) reported that in a short-term heat stress, ABA acted as a protector against oxidative destruction in *Pinus radiata*. Moreover, accumulation of ABA under high temperature treatment induced stomatal closure, inhibited CO_2 assimilation, and decreased soluble sugar in leaves (Jia *et al,* 2016). However, in this study, ABA accumulation measurement in different tissues did not demonstrate remarkable changes. Similar results have been obtained in *Eucalyptus*, with ABA content

remaining unchanged after heat stress imposition (Correia *et al,* 2018). Overall, the results of the present study highlight that heat stress induced stomatal closure, higher negative rate of Ψ_{leaf}, and lower transpiration rates, even with daily irrigation. In addition, acidification of xylem sap occurred, along with a significant increment of apoplastic soluble carbohydrates content and enhancement of xylem sap electrical conductivity, which confirmed the drought occurrence. Previous observations conducted on poplar suggest that such a drop in xylem apoplast pH, coinciding with higher NSC concentrations and ions in xylem sap, could be a symptom of severe drought in poplar (Secchi and Zwieniecki, 2012). Altogether, in the future climate scenario, which is characterized by rising temperatures, we can expect a reduction in the non-structural carbohydrate pool, which results in reduced growth and yield, as well as higher rates of mortality.

CHAPTER IV

Effects of strigolactones deficiency on xylem anatomy of poplar plants

4.1. Introduction

Strigolactones (SLs) are terpenes lactones derived from apocarotenoids as cleavage products, recently discovered as plant hormones with dual biological roles in plants as well as in rhizosphere. SLs act in roots and shoots, regulating plant growth and architecture (Gomez-Roldan *et al,* 2008; Czarnecki *et al,* 2014). SLs can control the shoot development by suppressing bud outgrowth (Cardinale *et al,* 2018). Recent findings on genetic mutants of SLs showed enhanced branching and bushy phenotype in Arabidopsis, pea, petunia and rice (Foster *et al,* 2017). The phenotypes resulting from SL deficiencies are well characterized in annual plants, but less so in woody perennials. *MORE AXILLARY GROWTH* genes *MAX1*, *MAX2*, *MAX3*, and *MAX4* are four members of strigolactone pathway genes in the model plant Arabidopsis (Stirnberg *et al,* 2002; Booker *et al,* 2004). *MAX1*, *MAX3* and *MAX4* and its orthologues and paralogues were shown to be involved in the SL biosynthesis, and *MAX2* was shown to be a key gene in SL signaling (Booker *et al*, 2005; Seto *et al*, 2014; Zhang *et al,* 2014). In poplar (*Populus* × *canescens*), the corresponding orthologs involved in SL biosynthesis are *MAX4* which has a role in the monitoring of shoot architecture (control of internode length), root alteration, and signaling in the rhizosphere (Czarnecki *et al,* 2014; Muhr *et al,* 2016). More recently, *MAX4 knockdown* lines (*amiMAX4*) were generated in poplar (*Populus* × *canescens*) with typical symptoms of SL deficiencies such as increased branch numbers, reduced plant height, reduced average internode length and increased number of adventitious root formation (Muhr *et al,* 2016).

In trees, the xylem network integrates all parts of plants and this network transports water from one vessel to another through lateral pits and

distributes nutrients along the roots to stems, trunk and leaves (Jacobsen *et al,* 2019). The xylem network consists of a long-distance system of parenchyma cells, fibers, and conductive elements (vessels or tracheids) (Tyree and Zimmermann; 2002; Jupa *et al,* 2015). The knowledge of xylem components and its structure for instant conduits number, diameter, density, dimensions, length of vessels, porosity, and pit characteristics are necessary in the assessment of water transport rate efficiency, estimation of conduit vulnerability to cavitation or pathogen, and disruption of water in conduits which may result in water and nutrient limitations (Sperry *et al,* 2006; Choat *et al,* 2008). Many studies on the water transport in xylem and bordered pit structure showed the relationship between embolism resistance and bordered pit structure (Sperry and Tyree, 1990; Cochard *et al,* 1992; Sperry and Hacke, 2004). Bordered pits are responsible for more than 50% of total xylem hydraulic resistance (Wheeler *et al,* 2005; Hacke *et al,* 2006; Choat *et al,* 2008) accordingly, alterations in the thickness and pit porosity has an important impact on the total hydraulic resistance in the plant (Marciszewska and Tulik, 2013). Vessel diameter is a determinant of xylem conductivity and hydraulic function in plants, and it can influence the vulnerability of drought-induced cavitation (Davis *et al,* 1999). Multiple researchers have suggested that long and wide vessels are more vulnerable to embolism than narrower vessels (Davis *et al,* 1999; Hacke *et al,* 2017). The vulnerability of larger and wider vessels is consistent with the pit area hypothesis predictions; based on this hypothesis, larger vessels are predicted to contain more vessels wall area, and more inter-vessel pits, and are thus speculated to have vulnerability to embolism spread because of larger pit membrane pore (Sperry *et al,* 2005; Wheeler *et al,* 2005; Zwieniecki and Secchi, 2014; Christman *et al,* 2009, 2012; Hargrave *et al,* 1994). In addition, the relationship between conduit diameter and freezing-

induced embolism has been found by Davis and colleagues (1999). Analysis of aspen anatomical features has shown that vessels with wider diameter were prone to embolism at higher pressures compared to vessels with narrower diameters (Cai and Tyree, 2010). Consequently, the minimal increase of the vessel cross-sectional lumen area and the bordered pits could result in substantially enhanced hydraulic conductivity, but the larger diameter of vessels could increase the risk of cavitation and diminish the safety of water flow (Tyree and Zimmermann, 2002; Marciszewska and Tulik, 2013). Vessel density is defined as the number of vessels per transverse area, directly impacting the bulk of xylem composition, which can in turn affect resistance to vessel implosion under negative pressure both in stems and roots (Jacobsen *et al,* 2005; Preston *et al,* 2006). Scientists are particularly interested in the study of xylem structure in woody plants such as poplar, since their fast growth rate makes them suitable as a model plant (Plavcová and Hacke, 2012). In this study, we used two *MAX4* knockdown lines (T14-4A and T22-5A), which were generated by Muher and colleague (2016). These transgenic lines were selected based on the stability of the phenotypes at different growth conditions of their study. Until now, SL deficiency effects on anatomical changes of woody perennials plants had not been studied. The objective was to determine the anatomical differences of stems and roots between wild type and transgenic poplars. Vessel diameter, vessel density, vessel length and xylem competent changes in stems and roots were examined in detail. Since the total conductive capacity of a stem is closely connected to anatomical parameters of xylem (Jupa *et al*, 2015), alteration of stem architecture can influence stem hydraulic properties due to variations in the xylem components and its structure in transgenic poplars. Accordingly, an evaluation of the anatomical variability in resistance and/or vulnerability to

embolism of SL transgenic plants is crucial in order to forestall the response of these plants to different conditions of water availability. It was hypothesized that those features will lead to great vulnerability to embolism formation in SL transgenic plants, and higher vulnerability can be determined by wider vessels, higher vessel density, and/or longer vessels.

4.2. Material and Methods

4.2.1. Plant material and experimental setup

Populus × *canescens* (Aiton) wild type trees and T14-4A and T22-5A (*MORE AXILLARY BRANCHING4, MAX4,* knock down plants) transgenic lines provided by the "Department of Plant Cell Biology, Albrecht- von-Haller-Institute for Plant Sciences, Georg-August-University, Gottingen 37077, Germany, were used in this experiment. The German group generated, through a microRNA technique, the *MAX4* knockdown lines. The present experiment was conducted in the greenhouse of University of Turin (Grugliasco campus) in the middle of June 2018. Initially, poplars were “in vitro propagated” in the lab and subsequently, each plant potted in a 2.5-L container filled with a substrate composed of sandy-loam soil/expanded clay/peat mixture (2:1:1 by weight) and grew in a greenhouse. Ambient conditions in the greenhouse were: temperature maintained in the range of 29 - 17 °C and natural day light supplemented by metal halogen lamps (500–600 µmol photons m^{-2} s^{-1}) to maintain a 12/12-h light/dark cycle of photoperiod. The plants were watered daily to keep container capacity. In total, 150 poplars of the same age (six months old) were used in this study (50 per each line). Plants were further divided into three groups; the first group (Group A, 10 plants per each line) was used for biomass analysis and biometric characteristics. The second group (Group B, 10 plants per each line) was used for hydraulic conductivity and xylem anatomical

measurements; the third group (Group C, 30 plants per each line) was used for assessing the percent loss of hydraulic conductivity (PLC), the vessel length and to measure leaf gas exchange and stem water potential. The plants of the third group were gradually subjected to drought by stopping irrigation and the duration of water stress treatment depended on the levels of desired drought, from moderate to severe water stress. Physiological parameters were monitored throughout the entire experiment. A detailed schematic representation of measurements/sampling of each group is provided in Figure 1.

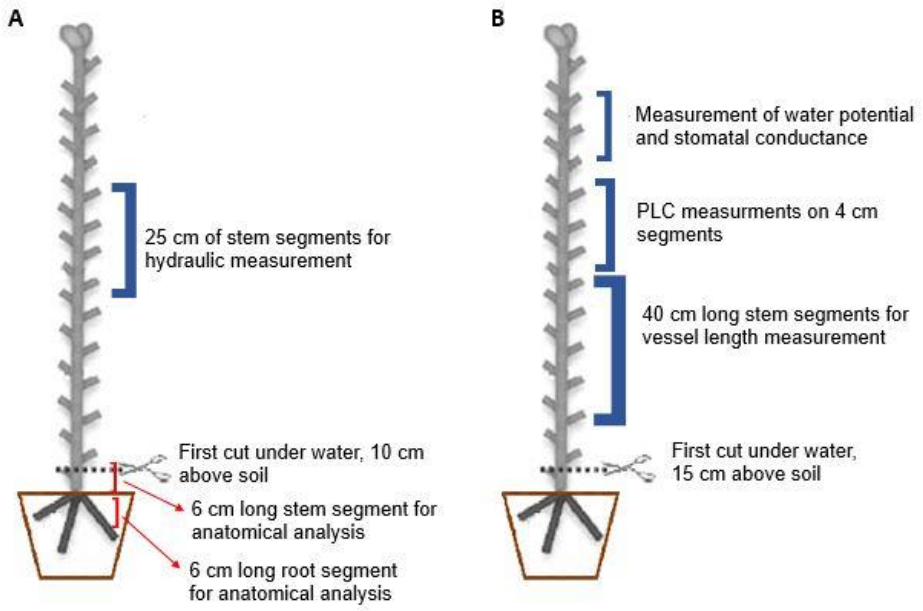

Fig 1. Schematic representation of the experiments: A) this group was used for determining the specific hydraulic conductivity and xylem anatomical measurements, B) plants belonging to group C were used to determine the percent loss of hydraulic conductivity, leaf gas exchange measurements and vessel length assessment.

4.2.2. Biometric characteristics and biomass analysis

Plant height, stem diameter, length of internodes and number of nodes were measured on plants belonging to group A. Then, leaves were collected to calculate the total leaf area (cm^2) using the leaf area meter (LI-3100C Area Meter). Finally, the leaves, stems and roots were sampled and harvested. To obtain the dry weight of each tissue, samples were oven dried at 70 ° C for 72 h and the dry weight of each tissue was recorded.

4.2.3. Measurements of stem water potential and leaf gas exchange

Stem water potential was measured on nontranspiring leaves. Leaves were covered with aluminum foil and placed in a humidified plastic bag for 15 min before excision. After excision, leaves were allowed to equilibrate for an additional 20 min before the xylem pressure was measured using a Scholander type pressure chamber (Soil Moisture Equipment Corp, Santa Barbara, CA). Stomatal conductance (g_s) and net photosynthesis (A) were measured on three fully expanded leaves per individual plant using a portable infrared gas analyzer ADC-LCPro+ system (The Analytical Development Company Ltd, Hoddesdon, UK). Measurements were performed using a 6.25 cm^2 leaf chamber equipped with artificial irradiation (1200 µmol photon m^{-2} s^{-1}) under ambient CO_2 values maintained constant at 400 ppm. The physiological parameters were monitored during the experiment from 9:00-13:00 am.

4.2.4. PLC measurement

The percent loss of hydraulic conductivity (PLC) was measured on plants belonging to the group “C” using a standard approach that was previously described (Secchi and Zwieniecki, 2010). Briefly, a 1.5-m-long shoot was

cut under water. Within a few minutes, this initial cut was followed with cutting a set of three stem segments. Segments were excised under water approximately 20–30 cm from the initial cut (distance longer than 2 times the length of vessels in studied poplar). Each segment was approximately 4-cm long. The initial hydraulic conductance (k_i) of each stem segment was measured gravimetrically by determining the flow rate of filtered 10 mM KCl solution. A water source was located on a balance (Sartorius ± 0.1 mg) and connected to the stem by a plastic tube. During measurements, stems were submerged in a water bath with a water level approximately 10 cm below the level of water on the balance. After a steady flow rate was reached (within a few minutes), the tube connecting the stem to the balance was closed, and a bypass tube was used to push water across the segment under approximately 0.2 MPa pressure for approximately 20 s to remove embolism. The chosen segment length used for determining PLC was short enough to have the majority of vessels open in poplar stems (vessel length is usually approximately 5 cm), thus making removal of embolism very easy and complete within a few seconds. Stem conductance was then remeasured to find maximum conductance (k_{max}). The PLC was calculated as $PLC = 100 \times (k_{max} - k_i)/k_{max}$.

The PLC data and stem water potential has been used for making the vulnerability curve. The curve was fitted with a four-parameter logistic curve (dose response), where

$PLC = \text{initial}_{PLC} + (\text{maximum}_{PLC} - \text{initial}_{PLC})/(1 + (P_x/EC50_{PLC})^{SlopeEC50PLC})$ and $g_s = \text{minimum}_{gs} + (\text{intial}_{gs} - \text{minimum}_{gs})/(1 + (P_x/EC50_{gs})^{SlopeEC50gs})$.

This function was preferred over other sigmoidal shapes, because it allows for treating xylem pressure as a treatment (dose) and allows for the fit of initial values to true preexisting conditions. $EC50_{PLC(gs)}$ is the parameter describing a 50% change in the curve between the initial value of PLC or g_s

and the corresponding final value at very low xylem pressures (PLC - maximum and g_s - minimum). $Slope_{PLC(gs)}$ describes the rate of change in PLC or g_s at the inclination point of the curve (Secchi and Zwieniecki, 2014). To compare wild-type and transgenic plants, PLC, and g_s response to xylem water pressure, the $EC50_{PLC(gs)}$ parameters of fitted curves were compared using the statistical Z test for the equality of regression coefficients (Paternoster *et al,* 1998).

4.2.5. Stem specific hydraulic conductivity

Well-watered plants belonging to group B were used to determine the specific hydraulic conductivity using a standard approach previously described by Sperry *et al* (1988). A 1.5-m-long shoot was cut under water, leaves were removed, and within a few minutes this initial cut was followed with cutting a 25 cm long segment. Segments was excised under water approximately 20 cm from the initial cut. Specific conductivity (k_s, $m^2 \cdot s^{-1} \cdot MPa^{-1}$) was calculated by measuring the flow rate (Q, $m^3 \cdot s^{-1}$) under a known pressure gradient (ΔP, MPa), the length of the stem segment (L, m), and the area of the xylem (A, m^2):

$$Ks = \frac{QL}{\Delta PA}$$

Flow rates were measured on stem segments trimmed under water to about 25 cm long under a gravimetric pressure with a degassed, 0.22µ filtered 10 mM KCl solution. Stems were connected to a balance (Sartorius ± 0.1 mg) and connected to the stem by a plastic tube. The segments were acclimated for 10 minutes to allow flow rates to stabilize before measurements and segments were subjected to the pressure 0.5 MPa for 15-20 minutes, in order to remove all the native embolism and reach to maximum flow rate

and then the maximum hydraulic conductivity samples (K_{max}) were calculated using:

$$K_{max} = \frac{Qmax \times L}{\Delta P \times A}$$

where Q_{max} is the maximum flow rate.

4.2.6. Anatomical analyses

For anatomical analyses, segments were excised from stem base (approximately 6 cm long) and 1st order roots of plants from group B and immediately put in falcon tubes filled with a fixative solution (formalin free fixative, Sigma-Aldrich Co). From the other plants (group C), 40 cm long stem segments were excised, placed in a plastic bag with moist paper tissue and stored in a fridge. All these samples were without delay transferred to the Masaryk University (Czech Republic), where they were further processed. In the lab, the samples (group B) stored in the fixative solution were thoroughly washed with distilled water. Afterwards, stem and root cross sections (~50 µm thick) were prepared with a sliding microtome (GSL 1; Swiss Federal Research Institute WSL, Birmensdorf, Switzerland). The sections were stained with a mixture of 0.35% safranin (dissolved in 50% ethanol, w/v) and 0.65% alcian blue (dissolved in distilled water, w/v) for 3 min, thoroughly washed in distilled water, and mounted on a slide. Sections were observed in bright field microscope (Olympus BX 51; Olympus, Tokyo, Japan) at 4x and 20× objective magnifications. Cross sections were photographed with a digital camera (SLT-A35; Sony, Japan). For sections observed at 4x objective magnification, the whole cross-sectional area was photographed while a representative 90° wedge was photographed in sections observed at 20x objective magnification. The photographs were merged in PTGui v. 8.3.7. PRO (New House Internet

Services. Rotterdam, The Netherlands) and image analysis software, namely- Adobe Photoshop CS6 (Adobe Systems, Mountain View, USA) and ImageJ v 1.51k (https://imagej.nih.gov/ij), was used to quantify individual anatomical traits.

To assess relative proportions of individual tissues in roots and stem, areas of whole section, bark, xylem and pit (in stems) were precisely selected in cross sections observed at 4x objective magnification and quantified in ImageJ software. The relative proportions of individual tissues were calculated as:

Relative proportion of xylem: RP_X (%) = $\frac{\text{xylem area}}{\text{section area}} \times 100$

Relative proportion of pith area: RP_P (%) = $\frac{\text{pith area}}{\text{section area}} \times 100$

Relative proportion of bark area: RP_B (%) = $\frac{\text{bark area}}{\text{section area}} \times 100$

Lumina of vessels present in the 45° wedge observed at 20x objective magnification were precisely selected in Adobe Photoshop and the vessel area (A) was quantified in ImageJ software. Vessels were assumed as ideal capillaries of precisely circular shape. Vessel diameter (D) was calculated accordingly to the following equation: $D=\sqrt{\frac{4A}{\pi}}$

In addition, theoretical hydraulic conductivity (K_{ht}) was calculated for individual vessels as: $K_{ht} = \frac{\pi D^4}{128\eta}$

where D is the diameter of vessel and ŋ is the dynamic viscosity of water at 20°C (1.002×10^{-9} MPa s). The analyzed vessels were sorted into classes according to their diameter to assess relative distribution of vessel diameters in individual organs and contributions of individual diameter classes to total organ conductive capacity.

Among the other vessel characteristics, relative proportion of xylem vessels (RP_{XV}), vessel density (VD), relative intervessel lateral contact (F_{VV}), relative vessel-to-parenchyma lateral contact (F_{VP}) and relative vessel-to-fiber lateral contact (F_{VF}) were calculated according to the following equations:

$$RP_{XV}\ (\%) = \frac{\text{total vessel cross sectional area}}{\text{xylem area}} \times 100$$

$$VD = \frac{number\ of\ vessel}{xylem\ area}$$

$$F_{VV} = \frac{\text{cell wall lenght in contant between vessels}}{\text{vessel perimeter}} \times 100$$

$$F_{VP} = \frac{\text{cell wall lenght in contant between vessels and parenchyma}}{\text{vessel perimeter}} \times 100$$

$$F_{VF} = \frac{\text{cell wall lenght in contant between vessels and fibres}}{\text{vessel perimeter}} \times 100$$

Stem vessel lengths (group C) were assessed using the silicone injection method described by Jupa *et al* (2016). Briefly, a two-component silicone QSil 218 (ACC silicones, Bridgwater, UK) was mixed with a 0.04% (v/v) fluorescent dye (Tinopal OB) and let to degas in an ultrasonic cleaner for 5 min. Then, the segments were shortened for 2 cm from their base using a sharp razor blade and the degassed silicone mixture was injected into these segments at a pressure of 70 kPa for 12 h. After 72 h of silicone hardening, samples were cut with a sliding microtome at regular 2 cm intervals starting from the injection point. The cross sections were obsserved with an epifluorescence microscope equipped with a mercury lamp (Olympus BX 51, Olympus, Tokyo, Japan; filter set U-MNUA2) at 10x objective magnification. The whole cross sections were photographed using the SLT-A35 camera, merged in PTGui software and the number of silicone-filled vessels was counted for each section. The vessel length distribution was estimated using exponential decay function (for details, see Nijsse, 2004 and Sperry *et al,* 2005). The relationship between number of vessel (N_L)

and distance from the injection (L) point was fitted with the following exponential function:

$N_L=N_0\, e^{(-kL)}$,

where N_0 is the number of vessels at the injection point and k is the best fit extinction coefficient.

Also, relative distribution of vessels length was determined according to the following equation:

$P_{LC} = - (1+ kL_2)\, e^{(-kL_2)} + (1+ kL_1)\, e^{(-kL_1)}$,

Where P_{LC} is fraction of vessels in a length class determined by lengths L_1 and L_2.

4.2.7. Statistical analyses

Statistical analyses were performed with IBM SPSS and Statistica software v. 13.2. (TIBCO Software, Palo Alto, CA, USA). The results are presented in the form of mean ± standard deviation. Pairwise comparisons between data were applied by using the appropriate post hoc test. Tukey's HSD test was adopted for one-way ANOVA at $p<0.05$ (Tukey, 1949).

4.3. Results

4.3.1. Biometric characteristics

Growth measurements showed that plant height and average internode length were significantly different in Wild type (WT) compared to the transgenic lines; WT plants were taller than both transgenic lines and their stems also contained longer internodes (Table 1). Other significant differences in the biometric parameters between WT and either T14-4 or T22-5 were also measured. Stem diameter, stem base diameter, and dry biomass of the root of T22-5 were significantly higher compared with WT

and T14-4 (Table 1). A smaller number of nodes, smaller leaf area and lower biomass in leaf and stem were recorded for T14-4 compared to WT and T22-5 (Table 1).

Table 1. Measurements of biometric traits of wild type (WT) and SLs deficient T22-5 and T14-4 transgenic lines

Biometric characteristics	**WT**	**T22-5**	**T14-4**
H_P (cm)	124.4 ± 6.2 a	105.3 ± 5.3 b	93.7 ± 1.7 c
D_S (mm)	4.7 ± 0.3 a	5.3 ± 0.5 b	4.6 ± 0.03 a
D_{SB} (mm)	6.1 ± 0.6 a	7.7 ± 0.6 b	6.6 ± 1.01 a
N_{node}	43.2 ± 2.04 ab	45.6 ± 5.2 b	38.5 ± 6.6 a
AL_{node} (cm)	2.8 ± 0.1 a	2.3 ± 0.2 b	2.4 ± 0.3 b
LA (cm^2)	2266.2 ± 293.5 a	2044.1 ± 261.5 a	1749.7 ± 198.2 b
DW_L (g)	7.02 ± 1.4 a	6.8 ± 1.08 a	5.3 ± 1.04 b
DW_S (g)	6.9 ± 1.03 ab	7.5 ± 2.1 a	5.6 ± 1.3 b
DW_R (g)	7.2 ± 2.2 a	14.3 ± 6.2 b	9.6 ± 4.3 a

Values are means ± SD (n = 10, each biological replicate represents a different plant). Different lower-case letters following SD values indicate significant differences among individual plants tested by Fisher LSD post-hoc test ($P < 0.05$). H_P= Plant Height, D_S= Stem diameter, D_{SB}= Stem base diameter, N_{node}= Number of nodes, AL_{node}= Average internode length, LA= Leaf area, DW_L= DW leaf biomass, DW_S= DW stem biomass, DW_R= DW roots biomass

4.3.2. Specific hydraulic conductivity

The analyses of the specific hydraulic conductivity measured in native state (without high pressure flash) indicated significantly greater values in T14-4 line compared to WT, while there were no obvious statistical differences between WT and T22-5. After embolism removing by high-pressure flush, both transgenic lines showed a higher maximum specific hydraulic conductivity compared to WT. Apparently, high-pressure flush resulted in significant increases in specific hydraulic conductivity in all plants

suggesting the presence of native embolism. The greatest increase of specific conductivity after flushing was detected in T22-5 (Fig 2).

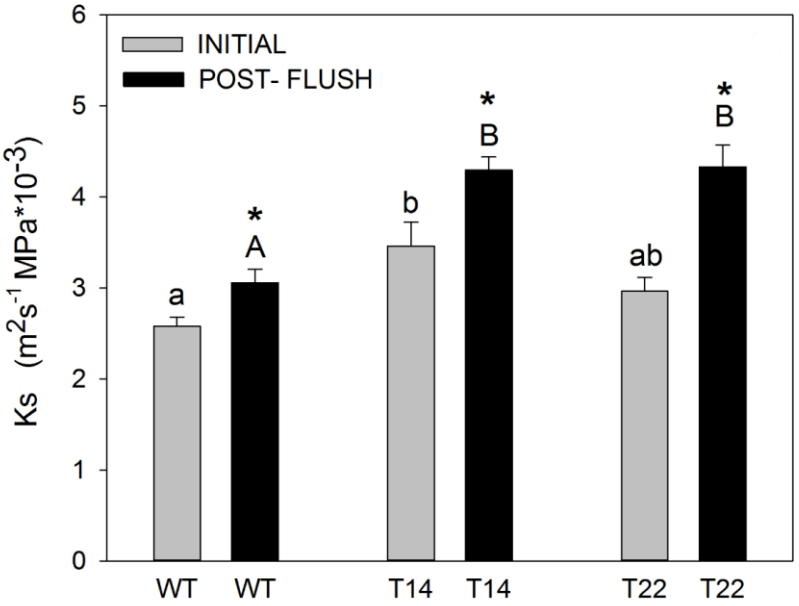

Fig 2. Values of specific hydraulic conductivity of stems measured in native state (grey columns) and after high-pressure flush (black columns) in wild type (WT) and T22-5 and T14-4 transgenic lines. Columns and error bars represent means and SD (n= 5 each biological replicate represents a different plant). Different lower-case and upper-case letters indicate significant differences among plants within initial and maximum conductivities tested by Fisher LSD test at $P < 0.05$. Asterisks indicate the significant differences between the initial and maximum conductivities at $P < 0.05$.

4.3.3. Xylem vulnerability to embolism

There were two main differences found in xylem vulnerability to embolism across the studied plants (Fig 3). An increase in water stress resulted in additional loss of stem hydraulic in parallel with more negative values of stem water potential (Fig 3). The 50% loss of stem conductivity (EC50) described by the $EC50_{PLC}$ parameter occurred at -1.99 MPa (SE=0.0906,

t=22.0025, p<0.0001) for WT, -1.75 MPa (SE=0.1, t=17.44, p<0.0001) for T22-5 and –1.67 (SE=0.094, t=17.083, p<0.0001) for T14-4. Based on the $EC50_{PLC}$ parameters, the stem of transgenic lines was more vulnerable to embolism than the stem of the WT. Paternoster test results (df=44, p<0.01) showed that only the $EC50_{PLC}$ value of the T14-4 line was statistically different from the WT lines. Decrease of xylem water potential below -2.5 MPa resulted in more than 80% of percentage loss of hydraulic conductivity for all plants tested.

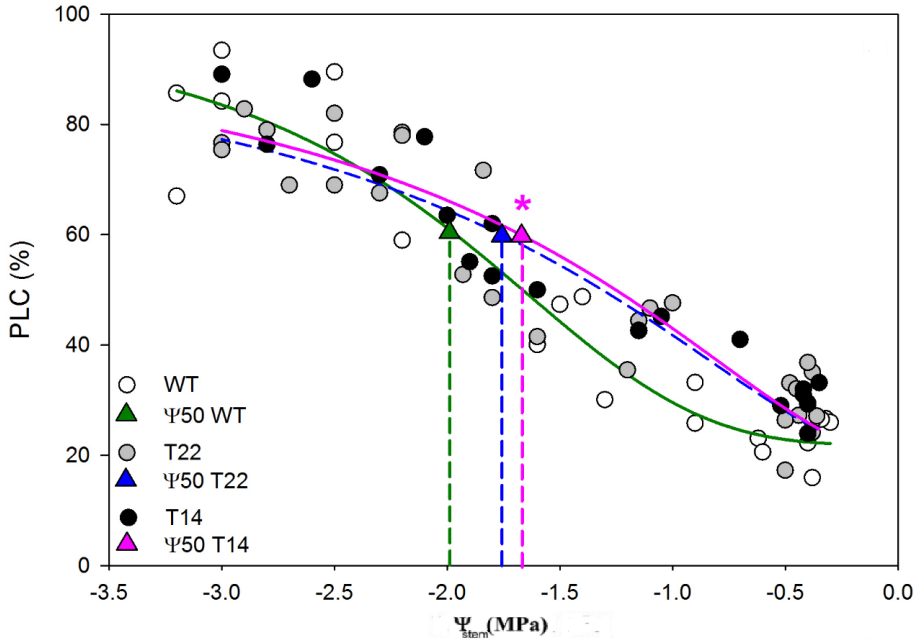

Fig. 3. Xylem vulnerability curves for WT and two SLs deficient transgenic lines. Data were fitted with the four-parameter logistic curves (dose-response curve). The white circles represent the WT plants, while the gray and black circles represent the T22-5 line and the T14-4 line, respectively. The triangles (green for WT, Blue for T22-5 and pink for T14-4) represent value of Ψ_{50}.

The level of native embolism in well water condition obtained from the vulnerability curves indicated that both transgenic lines had similar level of native embolism (~32% of PLC), and these values were significantly higher than those measured in WT (~25% of PLC) (Table 2).

Table 2. Stem water potential and corresponding values of native PLC in well-watered wild type (WT) plants and T22-5 and T14-4 transgenic lines.

Plant	Ψ (MPa)	PLC (%)
WT	-0.36 ± 0.01 a	24.3 ± 1.3 a
T22-5	-0.41 ± 0.01 a	30.6 ± 1.5 b
T14-4	-0.41 ± 0.02 a	33.3 ± 1.6 b

Values are means ± SD (n=10). Different lower-case letters represent significant differences among plants tested by Fisher LSD post-hoc test ($P < 0.05$).

4.3.4. Photosynthesis and stomatal conductance

The net photosynthesis rate (A) in transgenic lines was greater than WT plants under well water condition (Fig 4). A gradual reduction in photosynthesis rate was induced by drought in all plants. A correlation between stem water potential and photosynthesis is represented in Figure 4.

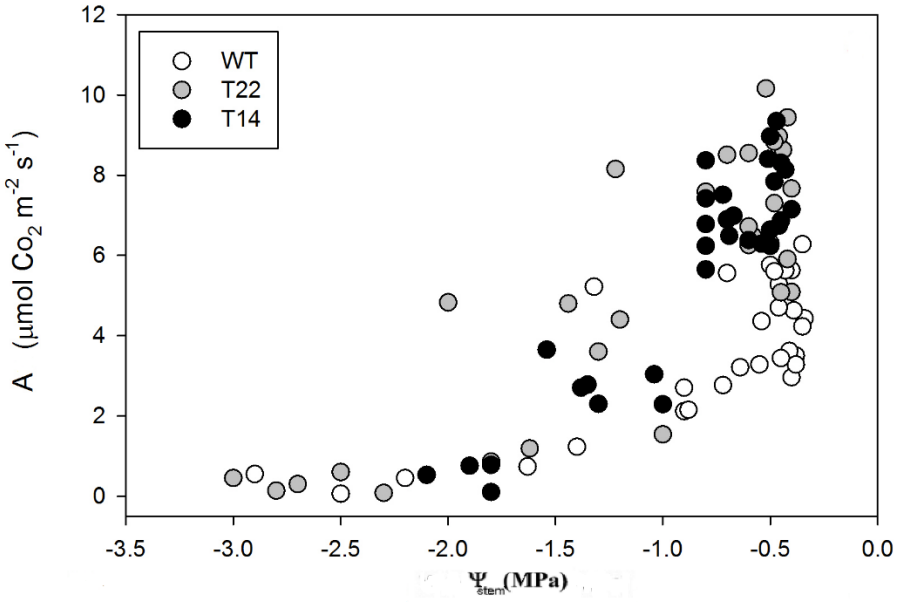

Fig. 4. Measurements of photosynthesis (A, µmol CO_2 m^{-2} s^{-1}) over the progression of water stress. The white circles represent the WT plants, while the gray and black circles represent the T22-5 line and the T14-4 line, respectively.

The data of stomatal conductance revealed that under well-watered conditions, both T22-5 and T14-4 lines had higher values of maximum g_s (~450 mmol H_2O m^{-2} s^{-1}) relative to WT (~150 mmol H_2O m^{-2} s^{-1}). In terms of stomata response to drought, an exponential decrease in g_s was observed along decreasing stem water potential, (Fig 5). The WT plants showed 50% loss of g_s ($EC50_{gs}$) at -0.78 MPa (SE=0.089, t=8.73, p<0.0001), whereas T22-5 line reached $EC50_{gs}$ at -0.97 MPa (SE=0.2095, t=4.64, p<0.0001) and T14-4 at -0.94 MPa (SE=0.073, t=12.86, p<0.0001).

WT plants closed their stomata by 50% ~1.4 MPa, before $EC50_{PLC}$, providing a relatively wide PLC safety margin (approx. 0.6 MPa wider safety margins [a difference between $EC50_{PLC}$ and $EC50_{gs}$] compared to both transgenic lines), while transgenic lines closed stomata at only ~ 0.8 MPa ahead of $EC50_{PLC}$, providing a very narrow safety margin. However, all plant

groups completely closed their stomata and reduced g_s to minimum before the EC50PLC (Fig 5).

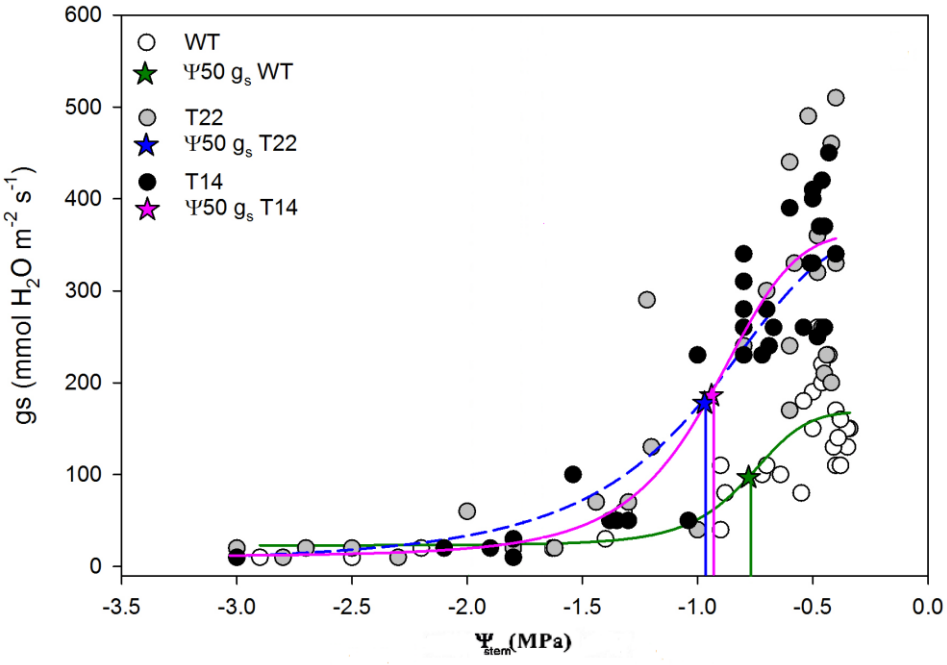

Fig 5. Measurements of stomatal conductance (mmol H_2O m^{-2} s^{-1}) over the progression of water stress. The white circles represent the WT plants, while the gray and black circles represent the T22-5 line and the T14-4 line, respectively. The stars (green for WT, Blue for T22-5 and pink for T14) represent $\Psi 50 g_s$.

4.3.5. Wood anatomy

In order to explain differences in physiological parameters related to xylem transport and to describe differences in anatomical structure between WT and both transgenic lines, xylem anatomy was examined, with the main focus on xylem vessel properties. In terms of plant organs, the greatest differences in xylem anatomy between WT and both transgenic lines were observed in stems, compared to roots. Stems of both transgenic lines

contained vessels of greater diameter, compared with WT (Table 3). Similarly, relative proportions of vessels in xylem were also higher in both transgenic plants, compared to WT. In contrast, there were no statistically significant differences in the vessel density across the tested plants of stems from both transgenic lines and WT (Table 3).

Besides differences in vessel characteristics, T22-5 transgenic line showed greater proportions of xylem and oppositely smaller proportions of bark, compared to WT and T14-4 (Table 3). No differences were detected in relative proportions of pith, across the studied plants. An overview on stem cross sections of poplar (line T14-4, as an example) is shown in Figure 6.

Table 3. Selected anatomical parameters analyzed in stem cross-sections of wild type (WT) and SLs deficient transgenic lines T22-5 and T14-4.

Anatomical characteristics	**WT**	**T22-5**	**T14-4**
D (µm)	26.2 ± 1.03 b	32.03 ± 1.2 a	30.5 ± 1.9 a
VD (number of vessels. mm^{-2})	185.5 ± 19.1 a	190.3 ± 23.5 a	189.8 ± 9.1 a
RP_{XV} (%)	11.01 ± 1.05 b	16.2 ± 1.7 a	15.1 ± 1.1 a
RP_X (%)	59.06 ± 2.7 b	66.1 ± 1.8 a	63.7 ± 3.3 ab
RP_P (%)	0.36 ± 0.2 a	0.86 ± 0.7 a	0.26 ± 0.1 a
RP_B (%)	40.5 ± 2.6 a	32.9 ± 2.4 b	35.9 ± 3.1 ab

Values are means ± SD (n = 4, each biological replicate represents a different plant). Different lower-case letters represent significant differences among plants tested by Tukey's HSD test ($P < 0.05$). D= Vessel diameter, VD= Vessel density, RP_{XV} = relative proportion of xylem vessels, RP_X= Relative proportion of xylem, RP_P = Relative proportion of pith area, RP_B = Relative proportion of bark area.

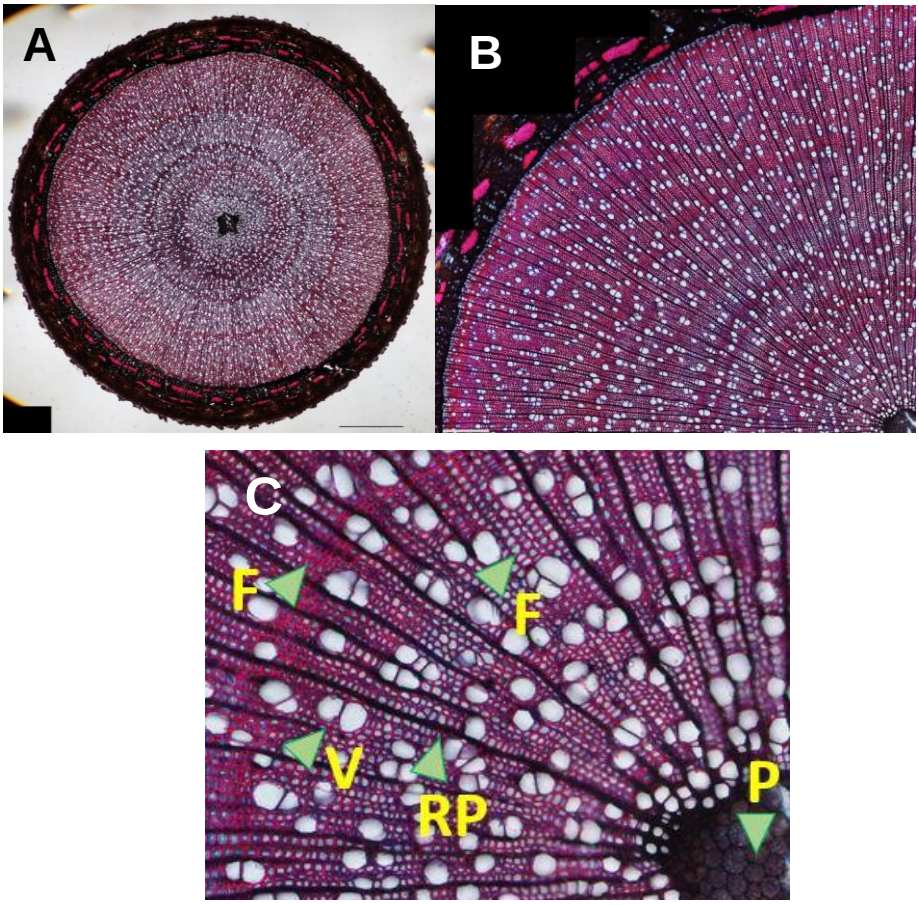

Fig 6. Stem cross sections of T14-4 transgenic line observed with a light microscope. The section was stained with a mixture of Safranine and Alcian blue. A) whole stem cross section, B) detail of stem xylem in a 90° wedge, C) detail of xylem with individual xylem cell types: F: fiber, V: vessels, RP: ray parenchyma and P: pith. Scale bar: A) 1 mm, B) 230 µm C) 50 µm.

In roots, both transgenic lines showed a higher vessel density, compared to WT plants. Other anatomical traits such as vessel diameter, relative proportion of xylem and bark, and relative proportion of vessel in xylem of root segments - did not significantly differ across the studied plants (Table 4). An overview of the root cross sections of T14-4 are shown in Figure 7.

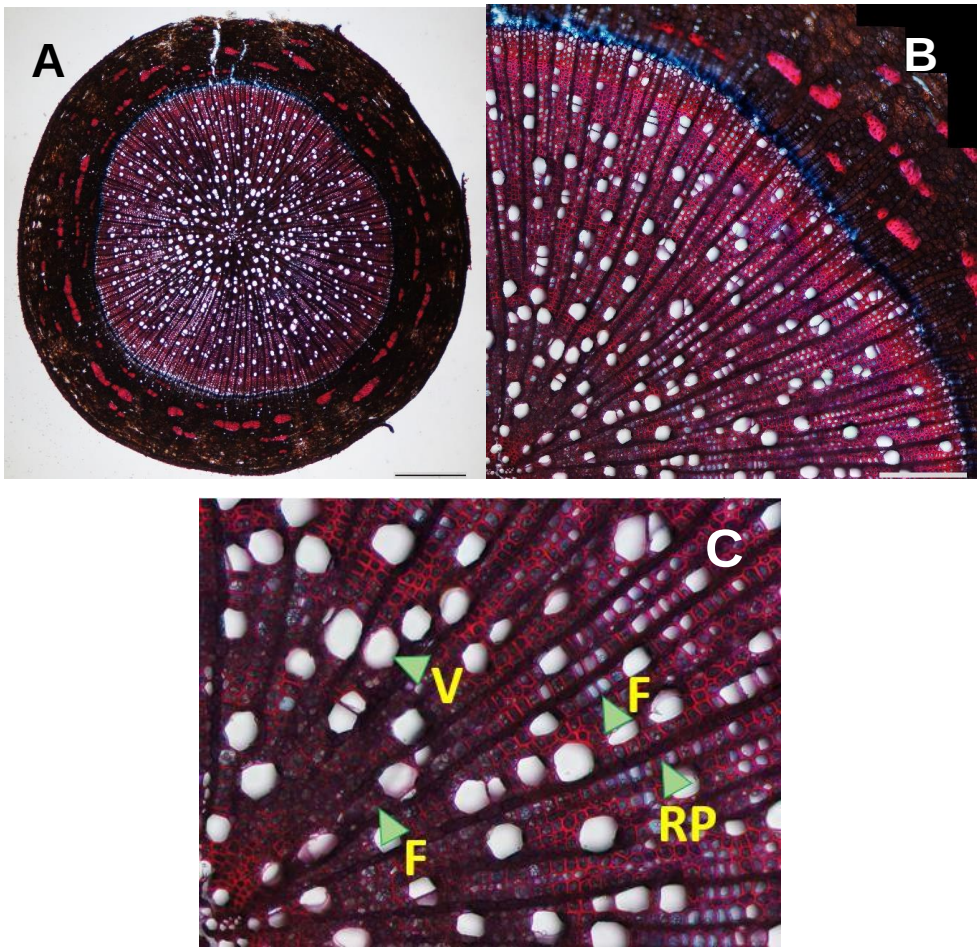

Fig 7. Root cross sections of T14-4 transgenic line observed with a light microscope. The section was stained with a mixture of Safranine and Alcian blue. A) whole stem cross section, B) detail of root xylem in a 90° wedge, C) detail of xylem with individual xylem cell types: F: fiber, V: vessels and RP: ray parenchyma. Scale bar: A) 1 mm, B) 230 µm C) 50 µm.

Table 4. Selected anatomical parameters analyzed in root cross-sections of wild type (WT) and SLs deficient transgenic lines T22-5 and T14-4

Anatomical characteristics	WT	T22-5	T14-4
D (µm)	37.4 ± 1.8 a	35.8 ± 3.7 a	36.1 ± 2.2 a
VD (number of vessels. mm^{-2})	82.6 ± 9.3 b	112.6 ± 9.4 a	105.5 ± 12.1 a
RP_{XV} (%)	10.04 ± 0.2 a	12.2 ± 1.8 a	11.8 ± 1.6 a
RP_X (%)	48.9 ± 3.04 a	50.5 ± 4.01 a	49.1 ± 4.01 a
RP_B (%)	51.05 ± 3.04 a	49.4 ± 4.01 a	50.8 ± 4.01 a

Values are means ± SD (n = 4, each biological replicate represents a different plant). Different lower-case letters represent significant differences among plants tested by Tukey's HSD test ($P < 0.05$). D= Vessel diameter, VD= Vessel density, RP_{XV} = relative proportion of xylem vessels, RP_X= Relative proportion of xylem, RP_B = Relative proportion of bark area.

Significant differences were observed in the distribution of stem vessel diameters between WT and both transgenic lines (Fig 8 A). Specifically, the distribution of vessel diameters in WT was shifted toward lower diameters, compared to T22-5 and T14-4. Wild type stems contained a high proportion of vessels in the 10-20 µm class, while both transgenic lines had the highest proportion of vessels in the median diameter size classes (30-40 and 40-50 µm). Both transgenic lines had very few vessels in high diameter size classes (60-70 µm), while WT had no vessels in the same diameter size class (Fig 8 A). In roots, no significant differences were found in the distribution of vessel diameters across the tested plants (Fig 8 B).

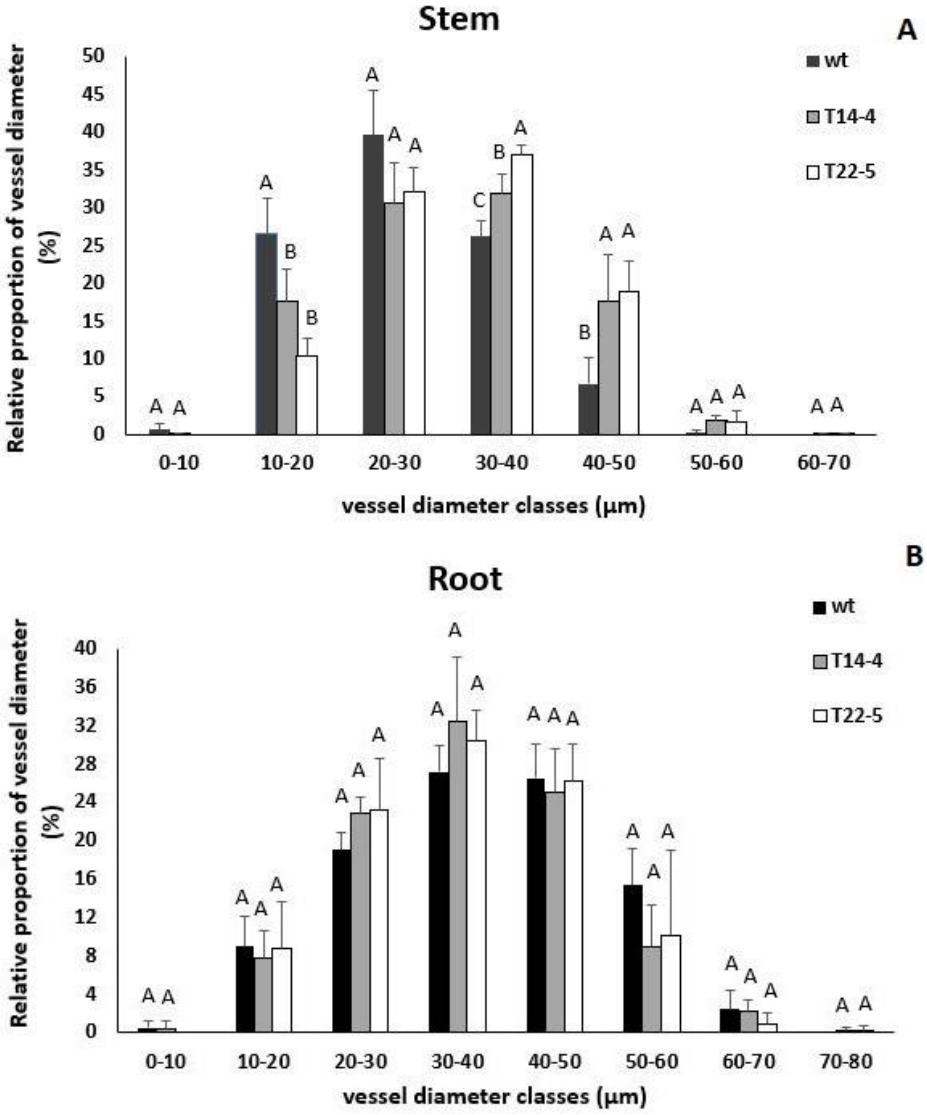

Fig 8. Distribution of vessel diameter in A) stem and B) root sections of WT and two SLs deficient lines. Different letters above denote significant differences within individual diameter classes (WT, T14-4 and T22-5), tested by Tukey's HSD test ($P < 0.05$). Columns and bars represent means and SD ($n = 4$).

Similarly, relative contribution of individual diameter classes to total stem K_{ht} was shifted toward lower diameter classes in WT, compared to both transgenic lines. (Fig 9).

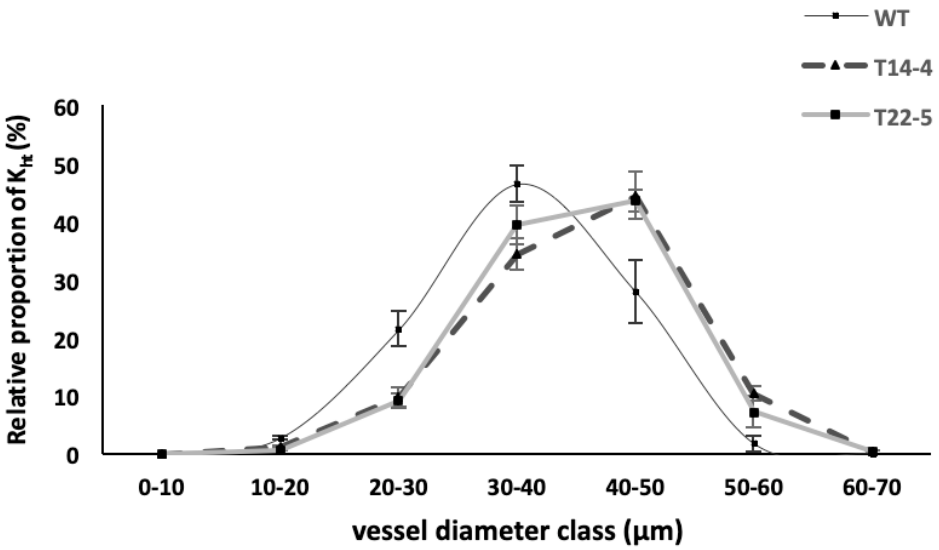

Fig 9. Distribution of theoretical hydraulic conductivity (K_{ht}) of vessels in stems of WT and two SLs deficient transgenic lines. Black dots on the line and bars represent means and SE (n = 4).

Vessel connectivity analyses revealed significantly lower intervessel lateral contact in line T22-5, in comparison with WT (Table 5). In contrast, there was no difference in the vessel-to-parenchyma lateral contact among all plants (Table 5). However, analyses of vessel-to-fiber lateral contact showed substantially higher value in line T22-5, compared to WT. Interestingly, very similar effects were also observed in the evaluation of vessel connectivity in roots (Table 5).

Table 5. Lateral contact of vessel with neighboring xylem cell types in stem and root of wild type (WT) and SLs deficient transgenic lines T22-5 and T14-4.

		WT	T22-5	T14-4
Stem	F_{VV} (%)	15.8 ± 2.1 a	10.1 ± 2.1 b	12.2 ± 2.4 ab
	F_{VP} (%)	16.3 ± 2.8 a	15.7 ± 2.1 a	14.2 ± 2.5 a
	F_{VF} (%)	67.8 ± 4.9 b	74.1 ± 1.7 a	73.5 ± 1.6 ab
Root	F_{VV} (%)	13.3 ± 0.6 a	9.2 ± 2.3 b	10.2 ± 1.9 ab
	F_{VP} (%)	21.6 ± 1.9 a	18.9 ± 1.1 a	22.3 ± 2.6 a
	F_{VF} (%)	64.9 ± 2.04 b	71.8 ± 3.3 a	67.3 ± 4.01 ab

Values are means ± SD (n = 4, each biological replicate represents a different plant). Different lower-case letters represent significant differences among plants tested by Tukey's HSD test ($P < 0.05$). F_{VV}= relative intervessel lateral contact, F_{VP}= relative vessel-to-parenchyma lateral contact, F_{VF}= relative vessel-to-fiber lateral contact.

While no statistically remarkable differences were found in average vessel length among all plants, both transgenic lines showed a slightly lower value of this parameter compared to WT (Fig 10). An overview of the silicon filled vessels of T14-4 is shown in Figure 11.

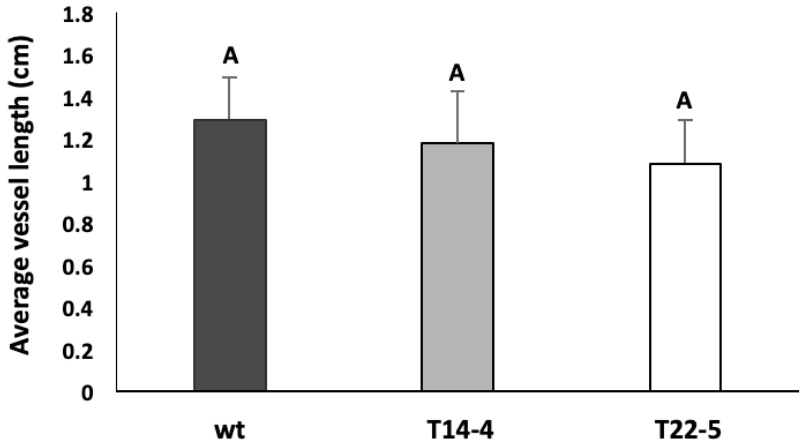

Fig 10. Average vessel length in stems of wild type (WT) and two SLs deficient transgenic lines. Columns and bars represent means and SD (n = 4).

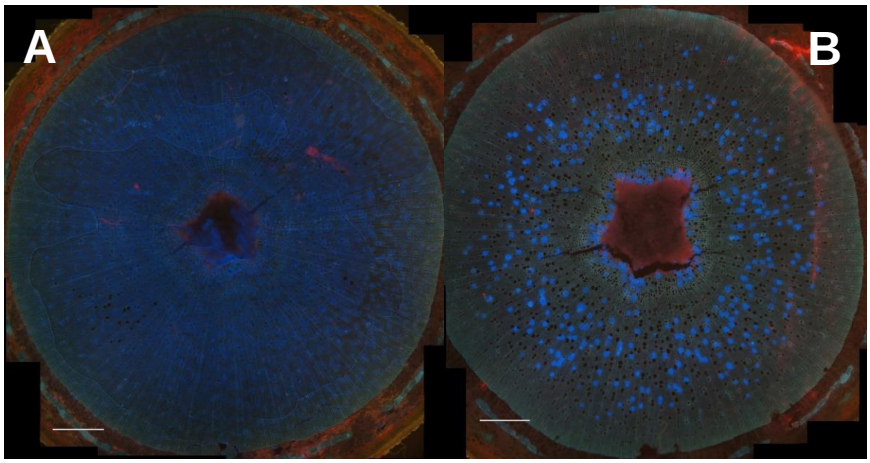

Fig 11. Cross section of the silicon filled vessel in stem of T14-4 transgenic line observed with an epifluorescence microscope equipped with a mercury lamp. A) stem cross section at the injection point 0 cm, B) stem cross section at the distance of 2 cm from injection point. Scale bar: 470 µm.

As with mean vessel length, no significant differences in vessel length distribution were observed across all tested plants. Stems of all plants contained very short vessels (approx. 50% of vessels were shorter than 2 cm). Interestingly, both transgenic lines contained few long vessels (12-20) cm, which were not present in WT. In WT, the maximum vessel length did not exceed 12 cm (Fig 12).

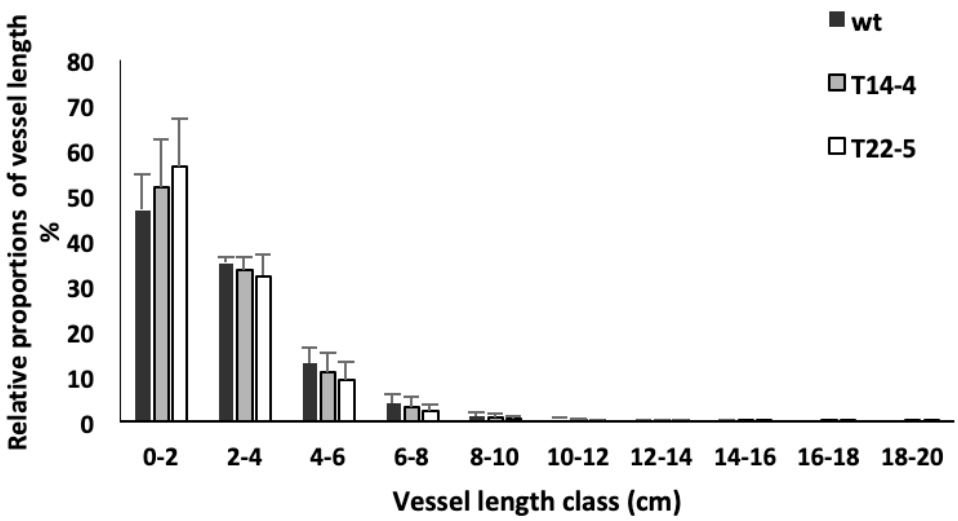

Fig 12. Distribution of vessel lengths in stems of wild type (WT) and two SLs deficient transgenic lines. Columns and error bars represent means and SD (n = 4).

4.4. Discussion

Recently, several roles of strigolactones (SLs) in plants and rhizosphere such as suppression of shoot branching by inhibiting the outgrowth of axillary buds (Gomez-Roldan *et al,* 2008; Umehara *et al,* 2008), enhancement of symbiosis between plants and arbuscular mycorrhizal fungi (*AMF*) (Akiyama *et al,* 2005), stimulation of seed germination (Xie *et al,* 2010) and alteration of root architecture (Ruyter-Spira *et al,* 2011) – have been demonstrated in many studies. It has been proposed by Visentin *et al* (2016) that SLs can act as signal mediators in drought stress. In tomato, *Arabidopsis*, and *Lotus*, the drought sensitivity of SLs deficient and their physiological responses to water stress were reported (Ha *et al,* 2014; Liu *et al,* 2015; Visentin *et al,* 2016). It was found that SLs can be synthesized in poplar (Czarnecki *et al,* 2014; Muhr *et al,* 2016), and poplar *BRC1* genes can also be regulated by SLs, which leads to complex regulation of bud outgrowth in trees (Muhr *et al,* 2016). *MAX4* knockdown lines in poplar have

been generated with typical symptoms of SL deficiency, such as higher branch patterns and shorter internode length (Muhr *et al,* 2016); however, the hydraulic conductivity variations and SL-induced xylem anatomical changes haven't been studied yet, either in herbaceous or woody plants.

To investigate of the SL deficiency impacts in the hydraulic conductance and anatomical features of poplar, transgenic and WT plants were monitored. In this study, the shoot architecture of transgenic poplars (T14-4 and T22-5) showed SL deficiency features, compared to WT (*Populus* × *canescens* (Aiton), including shorter plant height, shorter internode length and a smaller number of nodes. These findings are in agreement with studies conducted on model plants with SL deficiency, such as *Arabidopsis thaliana* and *Solanum lycopersicum* (Al-Babili and Bouwmeester*,* 2015; Xie *et al,* 2010; Brewer *et al,* 2013; Waters *et al,* 2017). Anatomical analysis revealed that SL deficiency poplars had stems with wider vessel diameter. On the basis of the phenotypical and anatomical alterations of the transgenic plants, a change in the hydraulic conductivity was hypothesized; therefore, the native and maximum hydraulic conductivity of the stem in all plants were measured. Native K_{sx} indicates the real hydrulic conductivity of each line in the water availability condition (David-Schwartz *et al,* 2016). The result of the study showed that T14-4 line had a greater value of K_{sx} in native state while after embolism removal, both transgenic lines had a higher value of K_{sxmax} (increase by 33%) than WT. It has been demonstrated that, in each species, the maximum xylem specific hydraulic conductivity has strong correlation with vessel diameter, and higher conductivity is accompanied by larger vessel diameters (Ewers *et al,* 1989; Vander Willigen *et al,* 2000; Ayup *et al,* 2012). The data from the present study suggests that SL deficiency leads to larger vassels in diameter, which could be attributed to an increase of maximum K_{sx} in transgenic lines. The

potential effect of differences in xylem characteristics on hydraulic conductance were reflected in the theoretical hydraulic conductivity (Tombesi *et al,* 2010). The distribution of theoretical hydraulic conductivity (K_{ht}) variation was shifted to bigger diameter classes. Simultaneously, larger proportions of xylem containing wider vessels provides greater conductive capacity of the stem, which is consistent with higher specific hydraulic conductivity and theoretical hydraulic conductivity in both transgenic lines, compared to WT. Many studies suggest that the larger vessels contain more pitted wall area, which might make them more vulnerable to embolism spread (Wheeler *et al,* 2005; Hacke *et al,* 2006, 2017; Loepfe *et al,* 2007; Brodersen *et al,* 2013). Although not quantified in this study, it is also possible that an increment in bordered pit area adjacent to wider conduits altered the probability of embolism formation [rare pit hypothesis] (Hargrave *et al,* 1994; Christman *et al,* 2009, 2012; Jacobsen *et al,* 2019). Embolism can be impelled by drought during dry periods and winter time when freeze-thaw events occur (Nardini *et al,* 2011). These two situations may happen frequently in wider vessels compared to narrower conduits (Montwé *et al,* 2014; Cai and Tyree, 2010). In this sense, the susceptiblity of poplar to the embolism and water stress via vulnerability curves has been shown by Secchi and Zwieniecki (2014). Accordingly, the result of PLC curve analysis here showed that transgenic lines were more susceptible to xylem embolism and displayed a 50% loss of PLC at less negative xylem water potential (-1.99 MPa for WT versus -1.75 MPa for T22-5 and -1.67 MPa for T14-4). The former studies showed that more embolism-resistant species possess narrower conduits (Hajek *et al,* 2014; Cai and Tyree, 2010), and a positive relationship between P50 and narrower conduits was reported (Lobo *et al,* 2018). In addition, Gleason and colleague (2016) examined the trade-off between angiosperms and gymnosperm species and showed a

positive relationship among P50 and hydraulic conductivity, as well as an infirm tradeoff across hydraulic efficiency and safety in those species. Both transgenic lines had greater native PLC; thus, it seems that the native embolism value of transgenic lines increased with the absence of SL in the stem organ.

Photosynthesis and stomatal conductance of transgenic lines under well water conditions showed higher values compared to WT plants which agrees with former studies in Arabidopsis thaliana and Solanum lycopersicum SL deficient mutants (Liu *et al,* 2015, Visentin *et al,* 2016). The increased vulnerability to embolism in transgenic plants was associated with their reduced capacity to control stomatal conductance during stress development. In T22-5 and T14-4 lines, 50% of stomatal shutdown occurred at -0.97 and -0.94 MPa, respectively, while in wild-type plants, 50% of stomatal shutdown occurred at -0.78 MPa. In agreement with this result, the stomata of SL deficient plants such as tomato, *Arabidopsis*, and *Lotus* were found to be hypersensitive to drought condition (Ha *et al,* 2014; Liu *et al,* 2015; Visentin *et al,* 2016). One of the mechanisms that plants could have adapted to reduce water loss is stomatal closure (Hochberg *et al,* 2017). The stomata behavior in transgenic plants suggests that they were less likely to control transpiration rates to protect xylem from embolism formation; this means, the absence of SL in transgenic lines could induce a significant reduction of the xylem vulnerability safety margin. The effect of phytohormones, such as auxin and cytokinin, in the initiation of vascular tissues and the formation of xylem, especially auxin, on vessel diameter have been discussed in many studies (Hacke *et al,* 2017; Růžička *et al,* 2015; Yoshida *et al,* 2009; Kaneda *et al,* 2011; Johnson *et al,* 2018), including in *Arabidopsis* and *Populus* (Yamagushi *et al,* 2011; Endo *et al,* 2015; Ohtani *et al,* 2011). However, to our knowledge, no previous study

has tested the relationship between SLs as phytohormone and its role in vessels differentiation and stem hydraulic capacity. Analysis of anatomical structure between WT and both transgenic lines indicated that the existence of wider vessels in transgenic stems was accompanied by shifted distributions of vessel diameters toward greater diameter classes, as well as larger proportions of xylem. Moreover, SL deficiency also resulted in denser vessels in roots. Altogether, wider vessels in stems and denser vessels in roots could presumably be a kind of disadvantage among transgenic lines, which may result in increased vulnerability to embolism formation (Tyree *et al,* 1994; Hacke *et al,* 2001; Sperry *et al,* 2006). This association was recently observed with microCT technic (high-resolution computed tomography) by Jacobsen *et al* (2019) who showed that larger vessels were prone to embolize at higher water potential in poplar plants. In aspen stems, it was found that conduits with wider diameter tended to embolize at higher pressure compared to conduits with smaller diameter (Cai and Tyree, 2010). The anatomical studies on poplar under water shortage demonstrated that narrower vessels were potentially resistant to embolism formation (Arend and Fromm, 2007; Jacobsen *et al,* 2019). In contrast with these results, it has been reported that narrow conduits were associated with greater vulnerabilities to embolism in the genus *Cistus* at Mediterranean area (Torres-Ruiz *et al,* 2017). The role of pits and their structure in resistance to embolism should be considered here. According to pit hypothesis, conduits with smaller diameters have smaller pit area per conduit so they tend to reduce the risk of cavitation (Sperry *et al,* 2005; Wheeler *et al,* 2005). Meanwhile, larger and wider conduits with higher porous pit membrane are more prone to air seeding. Hence, structural alterations in pit porosity or thickness of bordered pits could affect the total hydraulic resistance (Wheeler *et al,* 2005; Hacke *et al,* 2006; Choat *et al,*

2008). A negative association between vessel density and plant height was found by Preston *et al* (2006); consequently, shorter plant species were more prone to have heavier wood despite their higher vessel density, which is consistent with the results of the present study in transgenic lines, with regard to shorter plants and denser vessels in roots. There was a clear difference in the proportion of the bark area between WT and transgenic lines, particularly in T22-5, and it seems SL deficiency resulted in a thinner bark area. In total, larger proportions of xylem in T22-5 lines suggested that this line tended to possess larger xylem area in order to have wider vessels, even at the cost of thinner bark area.

The connectivity between vessels is one of the most important xylem characteristics (Scholz *et al,* 2013). The lateral connection of individual xylem components or connection of xylem with the parallel tissues is essential for numerous physiological processes (Scholz *et al,* 2013). The most notable of these important mechanisms includes the cycling of water, solutes, and ions in plant body, which builds upon an interaction between xylem and phloem (Zwieniecki *et al,* 2004). The vessel connectivity measurement showed a lower intervessel lateral contact with other vessels in T22-5 line; thus, solitary vessel was more pronounced in this transgenic line compared to WT. Analysis of vessel-to-parenchyma lateral contact showed that the SL deficiency did not have any impacts on this feature. However, vessel-to-fiber lateral contact showed higher value in T22-5 line, which means vessels were surrounded with more fibers in this line. Fibers are slender, longitudinally elongated cells with typically thick walls and narrow lumina (Morris *et al,* 2016). Fibers became dead after their maturity which is consistent with their significant role in xylem strengthening and mechanical support of plant body (Jacobsen *et al,* 2005; Sperry *et al,* 2006). Many anatomical studies showed that vessel implosion resistance can be

raised by an increase in the amount of fibers (Plavcová *et al,* 2011; Jacobsen *et al,* 2005; Jupa *et al,* 2016; Hacke, 2015). Based on the above facts, the T22-5 line can be presumed to have more rigidity structure and mechanical safety when it experiences extreme negative pressure (Jacobsen *et al,* 2005). There was no difference in the average vessel length among all plants. However, a slight tendency toward shorter vessels was observed in transgenic lines, suggesting there might be a subtle effect of SL deficiency. Overall, the initial hypothesis that there is a link between the absence of SLs in transgenic lines and alteration in hydraulic conductivity and xylem vessel properties corresponded to the lack of this hormone has been supported. Stimulation of cambial cell activity and divisions in *Arabidopsis*, pea, and *Eucalyptus globulus* by GR24 (synthetic SL analog) exogenous application has been observed in previous studies, which GR24 promoted the secondary vascular tissues production and cambium zone lateral extension (Agusti *et al,* 2011; Ramírez *et al,* 2018). Also, GR24 application in *Arabidopsis*, Lotus and maize showed increased tolerance to water deficit condition, while SL deficient plants displayed more sensitivity to drought (Van Ha *et al,* 2014; Liu *et al,* 2015; Davidson *et al,* 2015). Those results can indirectly confirm the sensitivity of SL deficient lines based on the wider diameter in stem, denser vessels in root, and also higher stem hydraulic conductivity data. In this study, the anatomical data represented that absence of SLs in transgenic lines could lead to xylem changes with corresponding morphological variations, particularly in the stem of transgenic plants in comparison with roots.

CHAPTER V

General Conclusions

5.1. Conclusions

In this thesis, poplar has been chosen to study the abiotic stress impacts as exogenous factors and SL deficiency effects as endogenous factors. Ongoing global climate warming is leading to an increase in frequency and intensity of heat waves and also increasing drought in several areas of the globe, having a huge impact on woody plant survival (Chmura *et al,* 2011; Anderegg *et al,* 2016). In order to characterize drought and heat effects on the physiological and chemical responses of poplar trees, two separate experiments were carried out under drought stress in a greenhouse and also under heat stress conditions in controlled growth chambers (phytotrons). The results of the drought experiment were consistent with the previous studies and supported a proposed scenario, wherein dynamic changes occur in the xylem sap under water stress and during recovery (Secchi and Zwieniecki, 2016).

In response to water deficit stress, poplars showed significant declines in g_s, A, and stem water potential after only five days of drought imposition. After rehydration, g_s and A did not recover immediately as full recovery took three to seven days. The delayed recovery in stomatal conductance and photosynthetic processes, despite a quick recovery in xylem pressure, can indicate that during water stress, hormonal changes in plants, such as increase in ABA, cause a lag in the stomatal function. After re-watering, the decrease of xylem ABA sap content to prestress levels, which occurred over the period of seven days, coincided with the delayed increase in stomatal opening. Therefore, the time discrepancy between stem water potential and stomatal opening in returning to pre-stress conditions can be explained by the lingering presence of ABA, as has been previously shown by Lovisolo *et al* (2008). Such stomatal regulation after rehydration can be considered as a safety mechanism, which allows the plant to regain full turgor more

efficiently (Mansfield and Davies, 1981; Ortuño *et al,* 2006). During severe drought stress when stomatal closure happens, a reduction in transpiration stream rates occurs in plants (Brodribb and McAdam, 2011; McDowell *et al,* 2008; Urli *et al,* 2013). This interruption in transpiration stream can change the balance of carbohydrate fluxes in xylem tissues, so that carbohydrates are not washed away in the transpiration stream and an accumulation of sugar in the apoplast can trigger a response leading to starch degradation (Secchi and Zwieniecki 2011, 2016). Starch degradation can result in enhanced soluble sugar content, which supplies osmotic protection against stress. Shifts in carbohydrate concentration during drought stress coincide with changes in apoplastic pH. In vivo observations of poplar stems subjected to water stress exhibited a relation between a drop in xylem pH and water stress level (Secchi and Zwieniecki, 2012). Furthermore, in vitro analysis linked an acidic apoplastic pH to an increased accumulation of sugars in the xylem sap of poplar stems (Secchi and Zwieniecki, 2016). After re-watering, the presence of sugars and lower pH in apoplast continue until full xylem functional recovery happens, producing high levels of osmoticum that promote the refilling process (Secchi and Zwieniecki, 2012). During recovery from stress, in the presence of water, transpiration resumes, sugars wash away, and pH changes in xylem. I characterize, from a physiological and biochemical perspective, the functional link between drought-induced xylem sap acidification and sugar accumulation, demonstrating that these synergetic events are crucial for triggering plant responses to water stress, including the restoration of xylem functionality (Fig. 1). All events suggest the potential priming of the xylem for fast recovery during the rehydration period. The presented study highlights the importance of studying mobilization of carbohydrate reserves to sustain high-energy processes involved in plant defense responses.

Plants subjected to heat stress showed significantly lower eco-physiological traits after four days. Lower values of leaf water potential were reported in poplars exposed to heat stress, along with impaired stomatal conductance, photosynthesis, and transpiration rates, even with the access to daily water. Normally, transpiration rate increases during the heat waves (Prasad *et al,* 2008; Ameye *et al,* 2012), but lower rates of transpiration were observed in our experiment. Concentrations of soluble sugars in leaves and roots slightly decreased under heat stress conditions, while sugar content significantly dropped in the stem of stressed samples. Furthermore, under heat stress, poplars increased the sugar content as well as electrical conductivity in the xylem sap, with simultaneously decreased sap pH. After perceiving stress, the poplars initiated osmotic adjustment by increasing the concentrations of NSC in sap and reducing apoplastic pH. High temperature, along with drought stress, induces the same physiological and chemical responses. The results obtained here suggest that heat stress can stimulate water stress. Drought probably enhanced the effects of heat stress on plant responses, as confirmed by the measured sap acidification (Secchi and Zwieniecki, 2011). One of the symptoms/signals of stress in poplars experiencing severe drought and low transpiration rate might be related to the presence of water stress. Figure 1 shows an overall view of the study that was carried out in this thesis.

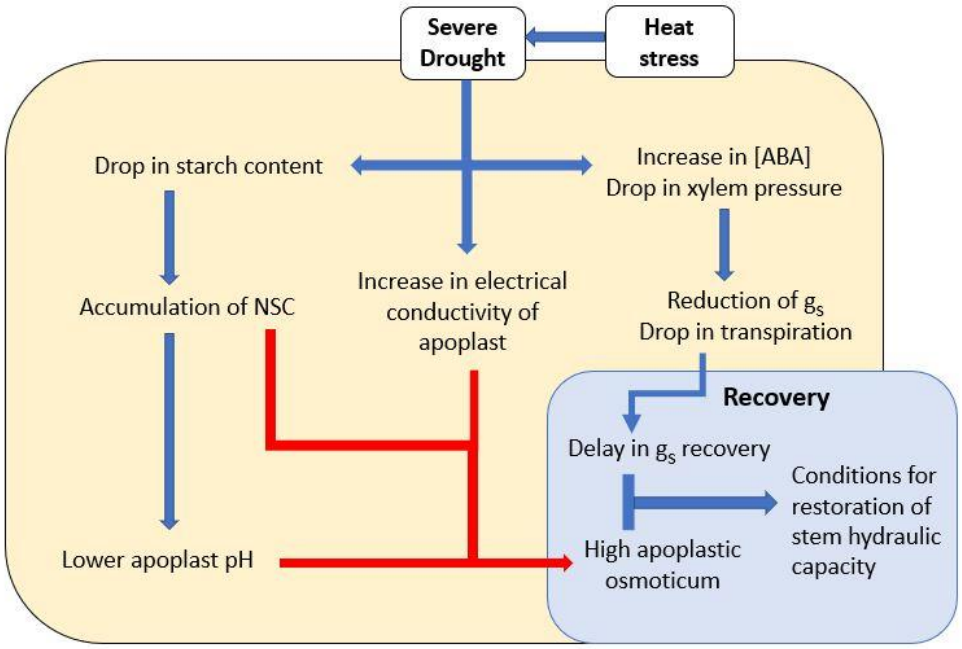

Fig. 1. Schematic representation of physiological and chemical responses of poplar stems to severe water stress and heat stress analyzed in this thesis. In heat stress the recovery part should consider excluded.

In plants, strigolactones (SLs), as a novel class of plant hormones, regulate various aspects of plants' growth and development (Cardinale *et al,* 2018). Xylem formation and development were studied in a wide range of different species (Wheeler *et al,* 2007; Sperry *et al,* 2006). A complex network of hormones such as auxins, cytokinins, gibberellins, and brassinosteroids are involved in xylem and its components' formation (Fukuda, 2004). However, the role of SLs in xylem vessel development, along with hydraulic conductivity, is still unknown. This study provided a preliminary analysis of SL deficiency effects on xylem proprieties and total hydraulic capacity of poplars. The results of this study suggested that there is a correlation between the absence of SLs, vessel dimensions of xylem, and the shift in

vulnerability to xylem embolism of transgenic conduits. The results also showed that transgenic poplar stems have greater diameter vessels, higher actual and theoretical hydraulic conductivity, higher proportion of xylem area, higher proportion of xylem vessel in stems, and denser vessels in roots compared to wild type plants. In addition, a lower proportion of bark in transgenic lines was observed. Variation in vessel diameter and density impacts xylem transport and function; wider and denser vessels are considered efficient conduits but by lumen diameter enhancement, vessels are more susceptible to dysfunction when water stress occurs (Jacobsen *et al,* 2012, 2019). Here, higher maximum specific hydraulic conductivity observed in transgenic lines was accompanied by wider vessels in stem. The vessel length measurements did not show any significant differences between lines. Vessels and associated elements play important roles in plant water relations and mechanical protection. The data showed greater vessel-to-fiber lateral contact, and the proportion of solitary conduits was higher in transgenic lines. Fiber-rich stem can make stiffer organs more resistant to breakage (Chave *et al,* 2009). In addition, those connected fibers to vessel might supply more water by their lumina under cavitation and/or embolism experiences. The results of this research suggested that most variation in xylem occurred in the stem of transgenic plants (T22-5) and SL deficiency had a greater impact on the stem, in comparison to the roots.

Chapter VI

References

6.1. References

Adams HD, Zeppel MJB, Anderegg WRL et al. 2017. A multi-species synthesis of physiological mechanisms in drought-induced tree mortality. Nat Ecol Evol 1:1285–1291.

Aguilar-Martínez JA, Poza-Carrión C, Cubas P. 2007. Arabidopsis *BRANCHED1* acts as an integrator of branching signals within axillary buds. Plant Cell 19: 458–472.

Agusti J, Herold S, Schwarz M, Sanchez P, Ljung K, Dun E A, et al. 2011. Strigolactone signaling is required for auxin-dependent stimulation of secondary growth in plants. Proc Natl Acad Sci USA 13: 20242-20247.

Akiyama K, Matsuzaki K, Hayashi H. 2005. Plant sesquiterpenes induce hyphal branching in arbuscular mycorrhizal fungi. Nature 435: 824–827.

Akiyama K, Ogasawara S, Ito S, Hayashi H. 2010. Structural requirements of strigolactones for hyphal branching in AM fungi, Plant Cell Physiol 51: 1104-1117.

Al Afas N, Marron N, Ceulemans R. 2007. Variability in *Populus* leaf anatomy and morphology in relation to canopy position, biomass production, and varietal taxon. Ann For Sci 64: 521-532.

Al-Babili S, Bouwmeester HJ. 2015. Strigolactones, a novel carotenoidderived plant hormone. Annu Rev Plant Biol 66: 161–186.

Allen CD, Macalady AK, Chenchouni H, Bachelet D, Vennetier NM, Kitzberger et al. 2010. A global overview of drought and heat-induced tree mortality reveals emerging climate change risks for forests. For Ecol Manag 259: 660-684.

Ameye M, Wertin TM, Bauweraerts I, McGuire MA, Teskey RO, Steppe K. 2012. The effect of induced heat waves on *Pinus taeda* and *Quercus rubra* seedlings in ambient and elevated CO_2 atmospheres. New Phytol 196: 448–461.

Anderegg WR, Hicke JA, Fisher RA, Allen CD, et al. 2015. Tree mortality from drought, insects, and their interactions in a changing climate. New Phytol 208 (3): 674-83.

Anderegg WRL, Klein T, Bartlett M, Sack L, Pellegrini AFA, Choat B, Jansen S. 2016. Meta-analysis reveals that hydraulic traits explain cross-species patterns of drought-induced tree mortality across the globe. PNAS 113(18): 5024–5029.

Andreo-Jimenez B, Ruyter-Spira C, Bouwmeester HJ. et al. 2015. Ecological relevance of strigolactones in nutrient uptake and other abiotic stresses, and in plant-microbe interactions below-ground. Plant Soil 394: 1.

Aragao DV, Fortini LB, Mulkey S, Zarin DJ. et al. 2005. Correlation but no causation between leaf nitrogen and maximum assimilation: The role of drought and reproduction in gas exchange in an understory tropical plant *Miconia ciliata* (Melastomataceae). Am J Bot 92: 456-461.

Arend M, Fromm J. 2007. Seasonal change in the drought response of wood cell development in poplar. Tree Physiol 27, 985–992.

Arimura G, Huber DPW, Bohlmann J. 2004. Forest tent caterpillars (*Malacosoma disstria*) induce local and systemic diurnal emissions of terpenoid volatiles in hybrid poplar (*Populus trichocarpa x deltoides*): cDNA cloning, functional characterization, and patterns of gene expression of (−)-germacrene D synthase, PtdTPS1. Plant J 37:603–16.

Ashraf M, Harris PJC. 2013. Photosynthesis under stressful environments: An overview. Photosynthetica 51 (2): 163-190.

Ayup M, Hao X, Chen Y, Li W, Su R. 2012. Changes of xylem hydraulic efficiency and native embolism of *Tamarix ramosissima* Ledeb. seedlings under different drought stress conditions and after rewatering. S Afr J Bot 78: 75–82.

Badger MR, Andrews TJ. 1987. CO-Evolution of Rubisco and CO_2 Concentrating Mechanisms. In: Biggins J. (eds) Progress in Photosynthesis Research. Springer, Dordrecht.

Bahrun A, Jensen CR, Asch F, Mogensen VO. 2002. Drought-induced changes in xylem pH, ionic composition, and ABA concentration act as early signals in field-grown maize (*Zea mays* L.). J Exp Bot 53: 251–263.

Bandurska H, Stroiński A. 2005. The effect of salicylic acid on barley response to water deficit. Acta Physiol Plant 27:379-386.

Barigah TS, Charrier O, Douris M, Bonhomme M, Herbette S, et al. 2013. Water stress-induced xylem hydraulic failure is a causal factor of tree mortality in beech and poplar. Ann Bot 112(7): 1431-1437.

Bauweraerts I, Ameye M, Wertin TM, McGuire MA, Teskey RO, Steppe K. 2014. Water availability is the decisive factor for the growth of two tree species in the occurrence of consecutive heat waves. Agric For Meteorol (189–190): 19–29.

Beaudette PC, Chlup M, Yee J, Emery RJN. 2007. Relationships of root conductivity and aquaporin gene expression in Pisum sativum: diurnal patterns and the response to $HgCl_2$ and ABA. J Exp Bot 58: 1291-1300.

Bernacchi CJ, Portis AR, Nakano H, von Caemmerer S, Long SP. 2002. Temperature response of mesophyll conductance: implications for the determination of Rubisco enzyme kinetics and for limitations to photosynthesis in vivo. Plant Physiol 130: 1992-1998.

Beveridge CA, Dun EA, Rameau C. 2009. Pea has its tendrils in branching discoveries spanning a century from auxin to strigolactones. Plant Physiol 151: 985–990.

Bird IF, Cornelius MJ, Keys AJ. 1982. Affinity of RuBP carboxylases for carbon dioxide and inhibition of the enzymes by oxygen. J Exp Bot 33: 1004–1013.

Bita CE, Gerats T. 2013. Plant tolerance to high temperature in a changing environment: scientific fundamentals and production of heat stress-tolerant crops. Front Plant Sci 4: 273.

Blackman CJ, Brodribb TJ, Jordan GJ. 2009. Leaf hydraulics and drought stress: response, recovery and survivorship in four woody temperate plant species. Plant Cell Environ 32: 1584–1595.

Bloemen J, Fichot R, Horemans JA, Broeckx LS, Verlinden et al. 2017. Water use of a multi-genotype poplar short-rotation coppice from tree to stand scale. GCB Bioenergy 9: 370-384.

Booker J, Auldridge M, Wills S, McCarty D, Klee H, et al. 2004. *MAX3*/*CCD7* is a *carotenoid cleavage dioxygenase* required for the synthesis of a novel plant signaling molecule. Curr Biol 14: 1232-1238.

Booker J, Sieberer T, Wright W, Williamson L, Willett B, Stirnberg P, et al. 2005. *MAX1* encodes a cytochrome P450 family member that acts downstream of *MAX3/4* to produce a carotenoid-derived branch-inhibiting hormone. Dev Cell 8: 443–449.

Bota J, Flexas J, Keys AJ, Loveland J, Parry MAJ, Medrano H. 2002. CO_2/O_2 specificity factor of ribulose-1,5-bisphosphate carboxylase/oxygenase in grapevines (*Vitis vinifera* L.): first in vitro determination and comparison to in vivo estimations. Vitis 41: 163.

Boursiac Y, Léran S, Corratgé-Faillie C, Gojon A, Krouk G, Lacombe B. 2013. ABA transport and transporters. Trends Plant Sci 18: 325–333.

Braun N, de Saint Germain A, Pillot JP, Boutet-Mercey S, Dalmais M, Antoniadi I, et al. 2012. The pea TCP transcription factor *PsBRc1* acts downstream of strigolactones to control shoot branching. Plant Physiol 158: 225–238.

Brewer PB, Koltai H, Beveridge CA. 2013. Diverse roles of strigolactones in plant development. Mol Plant 6: 18-28.

Brodersen CR, McElrone AJ, Choat B, Lee EF, Shackel KA, Matthews MA. 2013. In vivo visualizations of drought-induced embolism spread in *Vitis vinifera*. Plant Physiol 161: 1820–1829.

Brodersen CR, McElrone AJ, Choat B, Matthews MA, Shackel KA. 2010. The dynamics of embolism repair in xylem: in vivo visualizations using high-resolution computed tomography. Plant Physiol 154:1088–1095.

Brodersen CR, McElrone AJ. 2013. Maintenance of xylem network transport capacity: a review of embolism repair in vascular plants. Front Plant Sc 4:108.

Brodribb TJ, Cochard H. 2009. Hydraulic failure defines the recovery and point of death in water-stressed conifers. Plant Physiol 149:575–584.

Brodribb TJ, Jordan GJ. 2008. Internal coordination between hydraulics and stomatal control in leaves. Plant Cell Environ 31(11): 1557-1564.

Brodribb TJ, McAdam SA. 2011. Passive origins of stomatal control in vascular plants. Sci 331: 582–585.

Brodribb TJ, McAdam SAM. 2013. Abscisic Acid Mediates a Divergence in the Drought Response of Two Conifers. Plant Physiol 162(3): 1370-1377.

Brosche M, Vinocur B, Alatalo ER, Lamminmaki A, Teichmann T, et al. 2005. Gene expression and metabolite profiling of Populus euphratica growing in the Negev desert. Genome Biol 6: R101.

Brunetti C, Gori A, Marino G, Latini P. et al. 2019. Dynamic changes in ABA content in water-stressed *Populus nigra*: effects on carbon fixation and soluble carbohydrates, Ann Bot mcz005.

Buckley TN. 2016. Stomatal responses to humidity: has the ‘black box’ finally been opened? Plant Cell Environ 39, 482–484.

Cai J, Tyree MT. 2010. The impact of vessel size on vulnerability curves: data and models for within species variability in saplings of aspen, *Populus tremuloides* Michx. Plant Cell Environ 33: 1059–1069.

Cardinale F, Korwin Krukowski P, Schubert A, Visentin I. 2018. Strigolactones: mediators of osmotic stress responses with a potential for agrochemical manipulation of crop resilience. J Exp Bot 69(9): 2291-2303.

Carpaneto A, Geiger D, Bamberg E, Sauer N, Fromm J, Hedrich R. 2005. Phloem-localized, proton-coupled sucrose carrier *ZmSUT1* mediates sucrose efflux under the control of the sucrose gradient and the proton motive force. J Biol Chem 280(22): 21437-21443.

Carpaneto A, Koepsell H, Bamberg E, Hedrich R, Geiger D. 2010. Sucrose- and H+-Dependent Charge Movements Associated with the Gating of Sucrose Transporter ZmSUT1. Plos One 5(9).

Centritto M, Brilli F, Fodale R, Loreto F. 2011. Different sensitivity of isoprene emission, respiration and photosynthesis to high growth temperature coupled with drought stress in black poplar (*Populus nigra*) saplings. Tree Physiol 31: 275–286.

Chapin FS, Schulze E, Mooney HA. 1990. The ecology and economics of storage in plants. Annu Rev Ecol Syst 21: 423-447.

Chaves MM, Flexas J, Pinheiro C. 2009. Photosynthesis under drought and salt stress: regulation mechanisms from whole plant to cell. Ann Bot 103:551–560.

Chaves MM, Maroco JP, Pereira JS. 2003. Understanding plant responses to drought - from genes to the whole plant. Funct Plant Biol 30:239–264

Chaves MM.1991. Effects of water deficits on carbon assimilation. Environ Exper Bot 42: 1–16.

Chen Y, Zhang Z, Tao F, Palosuo T, Rötter RP. 2018. Impacts of heat stress on leaf area index and growth duration of winter wheat in the North China Plain. Field Crops Res 222: 230–237.

Chitarra W, Balestrini R, Vitali M, Pagliarani C, Perrone I, Schubert A, Lovisolo C. 2014. Gene expression in vessel-associated cells upon xylem embolism repair in *Vitis vinifera* L. petioles. Planta 239(4): 887-899.

Chmura DJ, Anderson PD, Howe GT, Harrington CA, Halofsky JE, Peterson DL, Shaw DC, St.Clair JB. 2011. Forest responses to climate change in the northwestern United States: ecophysiological foundations for adaptive management. For Ecol Manag 261: 1121-1142.

Choat B, Brodersen CR, McElrone AJ 2015. Synchrotron x-ray microtomography of xylem embolism in Sequoia sempervirens saplings during cycles of drought and recovery. New Phytol 205: 1095–1105.

Choat B, Brodribb, TJ, Brodersen, CR. et al. 2018 Triggers of tree mortality under drought. Nature 558, 531–539.

Choat B, Cobb AR, Jansen S. 2008. Structure and function of bordered pits: new discoveries and impacts on whole-plant hydraulic function. New Phytol 177: 608–625.

Choat B, Jansen S, Brodribb TJ, Cochard H et al. 2012. Global convergence in the vulnerability of forests to drought. Nature 491(7426):752-5.

Christman MA, Sperry JS, Adler FR. 2009. Testing the “rare pit” hypothesis for xylem cavitation resistance in three species of Acer. New Phytol 182 664–674.

Christman MA, Sperry JS, Smith DD. 2012. Rare pits, large vessels and extreme vulnerability to cavitation in a ring-porous tree species. New Phytol 193 713–720.

Christmann A, Weiler EW, Steudle E, Grill E. 2007. A hydraulic signal in root-to-shoot signalling of water shortage. Plant J 52: 167–174.

Ciais PH, Reichstein M, Viovy N, Granier A, Ogée J, Allard V, et al. 2005. Europe-wide reduction in primary productivity caused by the heat and drought in 2003. Nature 437: 529–533.

Clearwater MJ, Goldstein G. 2005. “Embolism repair and long distance water transport,” in Vascular Transport in Plants, eds Holbrook N. M., Zwieniecki M. A., editors. (Burlington: Elsevier Academic Press) 375–399.

Cochard H, Badel E, Herbette S, Delzon S, Choat B, Jansen S. 2013. Methods for measuring plant vulnerability to cavitation: a critical review. J Exp Bot 64(15):4779-91.

Cochard H, Cruizat P, Tyree MT. 1992. Use of positive pressures to establish vulnerability curves. Further support for the air-seeding hypothesis and implications for pressure-volume analysis. Plant Physiol 100: 205–209.

Comstock JP. 2002. Hydraulic and chemical signaling in the control of stomatal conductance and transpiration. J Exp Bot 53: 195–200.

Cooke JE, Weih M. 2005. Nitrogen storage and seasonal nitrogen cycling in *Populus*: bridging molecular physiology and ecophysiology. New Phytol 167:19–30

Cornic G, Fresneau C. 2002. Photosynthetic carbon reduction and carbon oxidation cycles are the main electron sinks for photosystem II activity during a mild drought. Ann Bot 89: 887–894.

Correia B, Hancock RD, Amaral J, Gomez-Cadenas A, Valledor L, Pinto G. 2018. Combined drought and heat activates protective responses in *Eucalyptus globulus* that are not activated when subjected to drought or heat stress alone. Front. Plant Sci 9: 819.

Correia MJ, Pereira JS, Chaves MM, Rodrigues ML, Pacheco CA. 1995. ABA xylem concentrations determine maximum daily leaf conductance of field-grown *Vitis vinifera* L. plants. Plant Cell Environ 18: 511–521.

Couée I, Sulmon C, Gouesbet G, Amrani AE. 2006. Involvement of soluble sugars in reactive oxygen species balance and responses to oxidative stress in plants. J Exp Bot 57: 449–459.

Coumou D, Robinson A. 2013. Historic and future increase in the global land area affected by monthly heat extremes. Environ Res Lett 8: 034018.

Crafts-Brandner SJ, Salvucci ME. 2000. Rubisco activase constrains the photosynthetic potential of leaves at high temperature and CO_2. Proc Natl Acad Sci USA 97: 13430–13435.

Crain BJ, Tremblay RL. 2017. Hot and bothered: changes in microclimate alter chlorophyll fluorescence measures and increase stress levels in tropical Epiphytic Orchids. Int J Plant Sci 178(7): 503–511.

Creek D, Blackman Chris J, Brodribb TJ, Choat B, Tissue DT. 2018. Coordination between leaf, stem, and root hydraulics and gas exchange in three arid-zone angiosperms during severe drought and recovery. Plant Cell Environ 41:2869–2881.

Cutler SR, Rodriguez PL, Finkelstein RR, Abrams SR. 2010. Abscisic acid: emergence of a core signaling network. Annu Rev Plant Biol 61: 651.

Czarnecki O, Yang J, Wang X, Wang S, Muchero W, Tuskan GA, Chen J. 2014. Characterization of *MORE AXILLARY GROWTH* Genes in *Populus*. PLoS ONE 9(7): e102757.

David-Schwartz R, Paudel I, Mizrachi M, et al. 2016 Indirect evidence for genetic differentiation in vulnerability to embolism in *Pinus halepensis*. Front Plant Sci 7:768.

Davidson EA, Bayer TS, Windram O, Hleba Y. 2015. Formulations de strigolactone et leurs utilisations. Patent WO 2015061764 A1.

Davies WJ, Zhang JH. 1991. Root signals and the regulation of growth and development of plants in drying soil. Annu Rev Plant Physiol Plant Mol Biol 42: 55–76.

Davis SD, Sperry JS, Hacke UG. 1999. The relationship between xylem conduit diameter and cavitation caused by freezing. Am J Bot 86: 1367-1372.

Dbara S, Haworth M, Emiliani G, Mimoun MB, Gómez-Cadenas A, Centritto M. 2016. Partial root-zone drying of olive (*Olea europaea* var. ‘Chetoui’) induces reduced yield under field conditions. PloS One 11: e0157089.

de Saint Germain A, Ligerot Y, Dun E A, Pillot JP, Ross JJ, Beveridge CA et al. 2013. Strigolactones stimulate internode elongation independently of gibberellins. Plant Physiol 163: 1012–1025.

Delgado E, Medrano H, Keys AJ, Parry MAJ. 1995. Species variation in Rubisco specificity factor. J Exp Bot 46: 1775–1777.

Dhyani K, Ansari MW, Rao YR, Verma RS, Shukla A, Tuteja N. 2013. Comparative physiological response of wheat genotypes under terminal heat stress. Plant Signal Behav 8(6), e24564.

Dietze MC, Sala A, Carbone MS, Czimczik CI et al. 2014. Nonstructural carbon in woody plants. Annu Rev Plant Biol 65: 667-687.

Ding W, Song L, Wang X, Bi Y. 2010. Effect of abscisic acid on heat stress tolerance in the calli from two ecotypes of *Phragmites communis*. Biol plant. 54: 607–613.

Dodd IC, Theobald JC, Bacon MA, Davies WJ. 2006. Alternation of wet and dry sides during partial rootzone drying irrigation alters root-to-shoot signaling of abscisic acid. Funct Plant Biol 33:1081–1089.

Doebley J, Stec A, Hubbard L. 1997. The evolution of apical dominance in maize. Nature 386: 485–488.

Duan H, Wu J, Huang G, Zhou S, et al. 2017. Individual and interactive effects of drought and heat on leaf physiology of seedlings in an economically important crop. AoB Plants 9(1): plw090.

Duan H, Wu J, Huang G, Zhou S, Liu W, Liao Y, Yang X, Xiao Z, Fan H. 2017. Individual and interactive effects of drought and heat on leaf physiology of seedlings in an economically important crop. AoB PLANTS 9: plw090; 10.1093/aobpla/plw090

Dun EA, de Saint Germain A, Rameau C, Beveridge CA. 2012. Antagonistic action of strigolactone and cytokinin in bud outgrowth control. Plant Physiol 158: 487-498.

Endo H, Yamaguchi M, Tamura T, Nakano Y. et al. 2015. Multiple classes of transcription factors regulate the expression of *VASCULAR-RELATED NAC-DOMAIN7*, a master switch of xylem vessel differentiation. Plant Cell Physiol 56, 242–254.

Escandón M, Cañal MJ, Pascual J, Pinto G, Correia B, Amaral J, Meijón M. 2016. Integrated physiological and hormonal profile of heat-induced thermotolerance in *Pinus radiata*. Tree Physiol 36(1): 63-77.

Ewers FW, Fischer JB, Chiu ST. 1989. Water transport in the liana *Bauhinia fassoglensis* (Fabaceae). Plant Physiol 91: 1625-1631.

Fahad S, Bajwa AA, Nazir U, Anjum SA, Farooq A, Zohaib A, Sadia S et al. 2017. Crop production under drought and heat stress: plant responses and management options. Front Plant Sci 8:1147.

Farmer RE Jr. 1996. The genecology of *Populus*. Biology of *Populus* and its implications for management and conservation, pp 33–55. In: Stettler RF, Bradshaw HD Jr, Heilman PE, Hinckley TM. Eds, NRC Research Press, Ottawa, Ontario, Canada,

Farquhar GD, von Caemmerer S, Berry JA. 1980. A biochemical model of photosynthetic CO_2 assimilation in leaves of C_3 species. Planta 149: 78–90.

Farrar J, Pollock C, Gallagher J. 2000. Sucrose and the integration of metabolism in vascular plants. Plant Sci 154:1-11.

Feng B, Liu P, Li G, Dong ST, Wang FH, Kong LA, Zhang JW. 2014. Effect of heat stress on the photosynthetic characteristics in flag leaves at the grain-filling stage of different heat-resistant winter wheat varieties. J Agron Crop Sci 200:143–155.

Fischer EM, Schär C. 2010. Consistent Geographical patterns of changes in high-impact European heatwaves. Nat Geosci 3: 398-403.

Foster AJ, Pelletier G, Tanguay P, Séguin A. 2015. Transcriptome analysis of poplar during leaf spot infection with *Sphaerulina* spp. PLoS ONE 10(9): e0138162.

Foster TM, Ledger SE, Janssen BJ, et al. 2018. Expression of *MdCCD7* in the scion determines the extent of sylleptic branching and the primary shoot growth rate of apple trees. J Exp Bot 69(9): 2379-2390.

Frich P, Alexander LV, Della-Marta P, Gleason B, Haylock M, Tank A, Peterson T. 2002. Observed coherent changes in climatic extremes during the second half of the twentieth century. Clim Res 19: 193–212.

Galmés J, Hermida-Carrera C, Laanisto L, Niinemets Ü. 2016. A compendium of temperature responses of Rubisco kinetic traits: variability among and within photosynthetic groups and impacts on photosynthesis modeling. J Exp Bot 67:5067–5091.

Galmés J, Kapralov MV, Andralojc PJ, Conesa MÀ, et al. 2014. Expanding knowledge of the Rubisco kinetics variability in plant species: environmental and evolutionary trends. Plant Cell Environ 37, 1989–2001.

Gerttula S, Zinkgraf M, Muday GK, Lewis RD. 2015. Transcriptional and hormonal regulation of gravitropism of woody stems in *Populus*. Plant Cell 27 (10) 2800-2813.

Ghorbanpour A, Salimi A, Ghanbary M. AT, Pirdashti H, Dehestani A. 2018. The effect of Trichoderma harzianum in mitigating low temperature stress in tomato (*Solanum lycopersicum* L.) plants. Sci Hortic 230, 134–141.

Gleason SM, Westoby M, Jansen S, Choat B, Hacke UG, et al. 2016. Weak tradeoff between xylem safety and xylem-specific hydraulic efficiency across the world's woody plant species. New Phytol 209: 123–136.

Gloser V, Korovetska H, Martín-Vertedor AI, et al. 2016. The dynamics of xylem sap pH under drought: a universal response in herbs? Plant Soil 409:259–272.

Gomez-Roldan V, Fermas S, Brewer PB, et al. 2008. Strigolactone inhibition of shoot branching. Nature 455: 189-194.

Goodsman DW, Lusebrink I, Landhäusser SM, Erbilgin N, Lieffers VJ. 2013. Variation in carbon availability, defense chemistry and susceptibility to fungal invasion along the stems of mature trees. New Phytol 197: 586–594.

Grant OM. 2012. Understanding and exploiting the impact of drought stress on plant physiology. Pages 89-104 in P. Ahmad, Prasad MNV eds. Abiotic Stress Responses in Plants: Metabolism, Productivity and Sustainability. Springer Science+Business Media, LLC, NY, USA.

Guan JC, Koch KE, Suzuki M, Wu S, Latshaw S, et al. 2012. Diverse roles of strigolactone signaling in maize architecture and the uncoupling of a branching-specific subnetwork. Plant Physiol 160: 1303-1317.

Guha A, Han J, Cummings C, McLennan DA, Warren JM. 2018. Differential ecophysiological responses and resilience to heat wave events in four co-occurring temperate tree species. Environ Res Lett 13: 065008.

Guilioni L, Wery J, Lecoeur J. 2003. High temperature and water deficit may reduce seed number in field pea purely by decreasing plant growth rate. Funct Plant Biol 30: 1151-1164.

Ha CV, Leyva-González MA, Osakabe Y, Tran UT, Nishiyama R, Watanabe Y et al. 2014. Positive regulatory role of strigolactone in plant responses to drought and salt stress. Proc Natl Acad Sci USA 111: 851–856.

Hacke UG, Sperry JS, Wheeler JK, Castro L. 2006. Scaling of angiosperm xylem structure with safety and efficiency. Tree Physiol 26: 689–701.

Hacke UG, Spicer R, Schreiber SG, Plavcová L. 2017. An ecophysiological and developmental perspective on variation in vessel diameter. Plant Cell Environ 40:831-845.

Hacke UG, Stiller V, Sperry JS, Pittermann J, McCulloh KA. 2001. Cavitation fatigue. Embolism and refilling cycles can weaken the cavitation resistance of xylem. Plant Physiol 125: 779–786.

Hacke, 2015. Functional and ecological xylem anatomy. Springer International Publishing AG, Switzerland.

Harfouche A, Meilan R, Altman A. 2014. Molecular and physiological responses to abiotic stress in forest trees and their relevance to tree improvement. Tree Physiol 34: 1181-1198.

Hargrave K, Kolb K, Ewers F, Davis S. 1994. Conduit diameter and drought-induced embolism in *Salvia mellifera* Greene (Labiatae). New Phytol126 695–705

Hartmann H, Trumbore S. 2016. Understanding the roles of nonstructural carbohydrates in forest trees from what we can measure to what we want to know. New Phytol 211:386–403.

Hartmann H, Trumbore S. 2016. Understanding the roles of nonstructural carbohydrates in forest trees - from what we can measure to what we want to know. New Phytol 211:386–403.

Hartmann H, Ziegler W, Kolle O, Trumbore S. 2013. Thirst beats hunger – declining hydration during drought prevents carbon starvation in Norway spruce saplings. New Phytol 200:340–349.

Hartung W, Wilkinson S, Davies W. 1998. Factors that regulate abscisic acid concentrations at the primary site of action at the guard cell. J Exp Bot 51:361–367.

Hasanuzzaman M, Nahar K, Alam MM, Roychowdhury R, Fujita M. 2013. Physiological, biochemical and molecular mechanisms of heat stress tolerance in plants. Int J Mol Sci 14: 9643-9684.

Hatfield JL, Boote KJ, Kimball BA, Ziska LH, Izaurralde RC, Ort D, Thomson AM, Wolfe DW. 2011. Climate impacts on agriculture: implications for crop production. Agron J 103: 351–370.

Hatfield JL, Prueger JH. 2015. Temperature extremes: Effect on plant growth and development. Weather Clim Extrem 10: 4-10.

Havaux M, Tardt F, Ravenel I, Chamu D, Parot P. 1996. Thylakoid membrane stability to heat stress studied by flash spectroscopic measurements of the electronic shift in intact potato leaves: influence of the xanthophyll content. Plant Cell Environ 19, 1359–1368.

Haworth M, Marino G, Brunetti C, Killi D, De Carlo A, Centritto M. 2018. The impact of heat stress and water deficit on the photosynthetic and stomatal physiology of olive (*Olea europaea* L.)— a case study of the 2017 heat wave. Plants 7: 76.

Hermida-Carrera C, Kapralov MV, Galmés J. 2016. Rubisco catalytic properties and temperature response in crops. Plant Physiol 171(4): 2549–2561.

Hesketh JD, Baker DN. 1969. Relative rates of leaf expansion in seedlings of species with differing photosynthetic rates. J Arizona Acad Sci 5(4) 216-221.

Hoch G, Richter A, Körner C. 2003. Non-structural carbon compounds in temperate forest trees. Plant Cell Environ 26:1067–1081.

Hochberg U, Windt WC, Ponomarenko A, Zhang YJ et al. 2017. Stomatal closure, basal leaf embolism, and shedding protect the hydraulic integrity of grape stems. Plant Physiol 174(2): 764–775.

Holbrook NM, Ahrens ET, Burns MJ, Zwieniecki MA. 2001. In vivo observation of cavitation and embolism repair using magnetic resonance imaging. Plant Physiol 126(1): 27-31.

Holbrook NM, Zwieniecki MA. 1999. Embolism repair and xylem tension: Do we need a miracle? Plant Physiol 120(1): 7-10.

Hozain MI, Salvucci ME, Fokar M, Holaday AS. 2010. The differential response of photosynthesis to high temperature for a boreal and temperate *Populus* species relates to differences in Rubisco activation and Rubisco activase properties. Tree Physiol 30(1): 32–44.

Hurkman WJ, DuPont FM, Altenbach SB, Combs A, Chan R et al. 1998. BiP, HSP70, NDK and PDI in wheat endosperm. II. Effects of high temperature on protein and mRNA accumulation. Physiol Plant 103: 80–90.

IPCC. 2007. Core Writing Team, Pachauri RK, Reisinger A, eds. Climate change 2007: synthesis report. Contribution of Working Group I, II and III to the fourth assessment report of the Intergovernmental Panel on Climate Change. Cambridge, UK and New York, NY, USA: Cambridge University Press.

IPCC. 2014. Climate change 2014: synthesis report. In: Pachauri, R.K., Meyer, L.A. (Eds.), Contribution of Working Groups I, II and III to the Fifth Assessment Report of the Intergovernmental Panel on Climate Change. IPCC, Geneva, Switzerland.

Ishikawa C, Hatanaka T, Misoo S, Fukayama H. 2009. Screening of high kcat Rubisco among Poaceae for improvement of photosynthetic CO_2 assimilation in rice. Plant Prod Sci 12: 345–350.

Jacobsen AL, Ewers FW, Pratt RB, Paddock WA, Davis SD. 2005. Do xylem fibers affect vessel cavitation resistance? Plant Physiol 139: 546–556.

Jacobsen AL, Pratt RB, Tobin MF, Hacke UG, Ewers FW. 2012. A Global analysis of xylem vessel length in woody plants. Am J Bot 99(10): 1583-1591.

Jacobsen AL, Pratt RB, Venturas MD, Hacke UG. 2019. Large volume vessels are vulnerable to water-stress-induced embolism in stems of poplar. IAWA J 40 (1): 4–22.

Jang JY, Kim DG, Kim YO, Kim JS, Kang H. 2004. An expression analysis of a gene family encoding plasma membrane aquaporins in response to abiotic stresses in *Arabidopsis thaliana*. Plant Molecular Biology 54: 713–725.

Jansson S, Douglas CJ. 2007. *Populus*: a model system for plant biology. Annu Rev Plant Biol 58: 435–458.

Jensen KH, Berg-Sørensen K, Bruus H, Holbrook NM, et al. 2016. Sap flow and sugar transport in plants. Rev Mod Phys. 88: 035007.

Jia J, S Li, X Cao, H Li, W Shi, A Polle, TX Liu, C Peng, ZB Luo. 2016. Physiological and transcriptional regulation in poplar roots and leaves during acclimation to high temperature and drought. Physiol Plant 157: 38–53.

Jia J, Zhou J, Shi W, Cao X, Luo J, Polle A, Luo ZB. 2017. Comparative transcriptomic analysis reveals the roles of overlapping heat-/drought-responsive genes in poplars exposed to high temperature and drought. Sci Rep 7: 43215.

Jia W, Davies WJ. 2007. Modification of leaf apoplastic pH in relation to stomatal sensitivity to root-sourced abscisic acid signals. Plant Physiol 143(1):68–77.

Johnson D, Eckart P, Alsamadisi N, Noble H, Martin C, Spicer R. 2018. Polar auxin transport is implicated in vessel differentiation and spatial patterning during secondary growth in *Populus*. Am J Bot 105(2): 186–196.

Jupa R, Didi V, Hejátko J, Gloser V. 2015. An improved method for the visualization of conductive vessels in *Arabidopsis thaliana* inflorescence stems. Front Plant Sci 6:211.

Jupa R, Plavcová L, Flamiková B, Gloser V. 2016. Effects of limited water availability on xylem transport in liana *Humulus lupulus* L. Environ Exp Bot 130:22-32.

Kamanga RM, Mbega E, Ndakidemi P. 2018. Drought tolerance mechanisms in plants: physiological responses associated with water deficit stress in *Solanum lycopersicum*. Adv Crop Sci Tech 6:3.

Kaneda M, Schuetz M, Lin BSP, Chanis C, Hamberger B, et al. 2011. ABC transporters coordinately expressed during lignification of *Arabidopsis* stems include a set of ABCBs associated with auxin transport. J Exp Bot 62: 2063–2077.

Kasuga J, Arakawa K, Fujikawa S. 2007. High accumulation of soluble sugars in deep supercooling Japanese white birch xylem parenchyma cells. New Phytol 174: 569–579.

Kempa S, Krasensky J, Dal Santo S, Kopka J, Jonak C. 2008. A central role of abscisic acid in stress- regulated carbohydrate metabolism. PLoS One 3: 39.

Keys A.J. 1986. Rubisco – its role in photorespiration. Philosophical transactions of the royal society of London. Series B, Bio Sci 313 325–336.

Killi D, Bussotti F, Raschi A, Haworth M. 2016. Adaptation to high temperature mitigates the impact of water deficit during combined heat and drought stress in C_3 sunflower and C_4 maize varieties with contrasting drought tolerance. Physiol Plant 10.1111/ppl.12490.

Kim MD, Kim YH, Kwon SY, Yun DJ, Kwak SS, Lee HS. 2010. Enhanced tolerance to methyl viologen-induced oxidative stress and high temperature in transgenic

potato plants overexpressing the *CuZnSOD*, *APX* and *NDPK2* genes. Physiol Plant 140: 153–162.

Kiorapostolou N, Da Sois L, Petruzzellis F, Savi T, et al. 2019. Vulnerability to xylem embolism correlates to wood parenchyma fraction in angiosperms but not in gymnosperms. Tree Physiol tpz068, https://doi.org/10.1093/treephys/tpz068.

Klein T, Zeppel MJB, Anderegg WRL, Bloemen J, De Kauwe MG, et al. 2018. Xylem embolism reflling and resilience against drought-induced mortality in woody plants: processes and trade-offs. Ecol Res 33: 839–855.

Klein T. 2014. The variability of stomatal sensitivity to leaf water potential across tree species indicates a continuum between isohydric and anisohydric behaviours. Funct Ecol 28:1313–1320.

Knipfer T, Brodersen CR, Zedan A, Kluepfel DA, McElrone AJ. 2015. Patterns of drought induced embolism formation and spread in living walnut saplings visualized using X-ray microtomography. Tree Physiol 35:744–755.

Knipfer T, Cuneo IF, Earles JM, Reyes C, Brodersen CR, McElrone AJ. 2017. Storage compartments for capillary water rarely refill in an intact woody plant. Plant Physiol 175: 1649–1660.

Koolhaas JM, Bartolomucci A, Buwalda B, DeBoer SF, Flugge G et al. 2011. Stress revisted: acritical evaluation of the stress concept. Neurosci Biobehav Rev 35:1291-1301.

Krishnan HB. Natarajan SS. Bennett JO, Sicher RC. 2011. Protein and metabolite composition of xylem sap from field-grown soybeans (*Glycine max*). Planta 233 921–931.

Kubien DS, Whitney SM, Moore PV, Jesson LK. 2008. The biochemistry of Rubisco in Flaveria. J Exp Bot 59: 1767–1777.

Lahr EC, Krokene P. 2013. Conifer stored resources and resistance to a fungus associated with the spruce bark beetle *Ips typographus*. PLoS ONE 8: e72405.

Landhäusser SM, Lieffers VJ. 2012. Defoliation increases risk of carbon starvation in root systems of mature aspen. Trees 26, 653–661.

Larkindale J, Knight MR. 2002. Protection against heat stress-induced oxidative damage in Arabidopsis involves calcium, abscisic acid, ethylene, and salicylic acid. Plant Physiology 128(2): 682–695.

Larkindale J, Mishkind M, Vierling E. 2005. Plant responses to high temperature. Pages: 100-144. In M. Jenks and P. Hasegawa eds. Plant Abiotic Stress. Blackwell Publishing Ltd.

Ledger SE, Janssen BJ, Karunairetnam S, Wang T, Snowden KC. 2010. Modified *CAROTENOID CLEAVAGE DIOXYGENASE8* expression correlates with altered branching in kiwifruit (*Actinidia chinensis*). New Phytol 188: 803–813.

Leopfe L, Martinez-Vilalta JM, Pinol J, Mencuccini M. 2007. The relevance of xylem network structure for plant hydraulic efficiency and safety. J Theor Biol 247 788-803.

Lewis JM, Mackintosh CA, Shin S, Gilding E, et al. 2008. Overexpression of the maize *TEOSINTE BRANCHED1* gene in wheat suppresses tiller development. Plant Cell Rep 27: 1217–1225.

Leyva A, Quintana A, Sánchez M, Rodríguez EN, Cremata J, Sánchez JC. 2008. Rapid and sensitive anthrone-sulfuric acid assay in microplate format to quantify carbohydrate in biopharmaceutical products: method development and validation. Biologicals 36: 134–141.

Li X, Yang Y, Sun X, Lin H, Chen J et al. 2014. Comparative physiological and proteomic analyses of Poplar (*Populus yunnanensis*) plantlets exposed to high temperature and drought. PLoS ONE 9(9): e107605.

Lipiec J, Doussan C, Nosalewicz A, Kondracka K. 2013. Effect of drought and heat stresses on plant growth and yield: a review. Int Agrophys 27: 463-477.

Liu J, He H, Vitali M, Visentin I, Charnikhova T, Haider I, Schubert A, Ruyter-Spira C, Bouwmeester HJ, Lovisolo C. 2015. Osmotic stress represses strigolactone

biosynthesis in Lotus japonicus roots: exploring the interaction between strigolactones and ABA under abiotic stress. Planta 241: 1435e1451.

Liu QH, Wu X, Li T, Ma JQ, Zhou XB. 2013. Effects of elevated air temperature on physiological characteristics of flag leaves and grain yield in rice. Chil J Agric Res 73(2): 85-90.

Lobo A, Torres-Ruiz JM, Burlett R, Lemaire C, Parise C, et al. 2018. Assessing inter- and intraspecific variability of xylem vulnerability to embolism in oaks. For Ecol Manage 424: 53–61.

Long SP, Zhu XG, Naidu SL, Ort DR. 2006. Can improvement in photosynthesis increase crop yields? Plant, Cell Environ 29: 315–330.

Loreto F, Velikova V, Di Marco G. 2001. Respiration in the light measured by $^{12}CO_2$ emission in $^{13}CO_2$ atmosphere in maize leaves. Aust J Plant Physiol 28: 1103-1108.

Losso A, Nardini A, Dämon B, Mayr S. 2018. Xylem sap chemistry: seasonal changes in timberline conifers *Pinus cembra*, *Picea abies*, and *Larix decidua*. Biol Plantarum 62(1): 157-165.

Love J, Bjorklund S, Vahala J, Hertzberg M, Kangasjarvi J, Sundberg B. 2009. Ethylene is an endogenous stimulator of cell division in the cambial meristem of *Populus*. PNAS 106: 5984–5989.

Lovisolo C, Hartung W, Schubert A. 2002. Whole-plant hydraulic conductance and root-to-shoot flow of abscisic acid are independently affected by water stress in grapevines. Funct Plant Biol 29(11): 1349-1356.

Lovisolo C, Perrone I, Hartung W, Schubert A. 2008. An abscisic acid-related reduced transpiration promotes gradual embolism repair when grapevines are rehydrated after drought. New Phytol 180(3): 642-651.

Lu Y, Sharkey TD. 2006. The importance of maltose in transitory starch breakdown. Plant Cell Environ 29(3): 353-366.

Manzi M, Lado J, Rodrigo MJ, Zacarías L, Arbona V, Gómez-Cadenas A. 2015. Root ABA accumulation in long-term water-stressed plants is sustained by hormone transport from aerial organs. Plant Cell Physiol 56: 2457–2466.

Marciszewska K, Tulik M. 2013. Hydraulic efficiency and safety of xylem sap flow in relation to water stress in woody plants. pp 1-32. In Vanderlei Rodrigues da Silva Eds. Hydraulic Conductivity. DOI: 10.5772/56656.

Marias DE, Meinzer FC, Still C. 2017. Impacts of leaf age and heat stress duration on photosynthetic gas exchange and foliar nonstructural carbohydrates in *Coffea arabica*. Ecol Evol 7: 1297–1310.

Marino G, Brunetti C, Tattini M, et al. 2017. Dissecting the role of isoprene and stress-related hormones (ABA and ethylene) in *Populus nigra* exposed to unequal root zone water stress. Tree Physiol 12: 1637–1647.

Martínez-Vilalta J, Garcia-Forner N. 2017. Water potential regulation, stomatal behaviour and hydraulic transport under drought: deconstructing the iso/anisohydric concept. Plant Cell Environ 40: 962-976.

Martín-Trillo M, Cubas P. 2010. TCP genes: a family snapshot ten years later. Trends Plant Sci. 15: 31–39.

Martorell S, Diaz-Espejo A, Medrano H, Ball MC, Choat B. 2014. Rapid hydraulic recovery in *Eucalyptus pauciflora* after drought: linkages between stem hydraulics and leaf gas exchange. Plant Cell Environ 37(3): 617-626.

Marzec M, Melzer M. 2018. Regulation of root development and architecture by strigolactones under optimal and nutrient deficiency conditions. Int J Mol Sci 19(7). pii: E1887.

Mathur S, Agrawal D, Jajoo A. 2014. Photosynthesis: response to high temperature stress. Photochem Photobiol B Biol 137:116–126.

Maxwell K, Johnson GN. 2000. Chlorophyll fluorescence-a practical guide. J Exp Bot 51:659–668.

Mayr S, Bertel C, Dämon B, Beikircher B. 2014. Static and dynamic bending has minor effects on xylem hydraulics of conifer branches (*Picea abies*, *Pinus sylvestris*). Plant Cell Environ 37: 2151–2157.

McAdam SA, Brodribb TJ. 2014. Separating active and passive influences on stomatal control of transpiration. Plant Physiol 164: 1578–1586.

McAdam SAM Manzi M, Ross JJ, Brodribb TJ, Gomez-Cadenas A. 2016. Uprooting an abscisic acid paradigm: Shoots are the primary source. Plant Signal Behav 11:6-e1169359.

McAdam SAM. Brodribb TJ. 2015. The evolution of mechanisms driving the stomatal response to vapor pressure deficit. Plant Physiol 167(3): 833-843.

McDowell N, Pockman WT, Allen CD, Breshears D. 2008. Mechanisms of plant survival and mortality during drought: why do some plants survive while others succumb to drought? New Phytol 178: 719–739.

Mencuccini M, Minunno F, Salmon Y, Martínez-Vilalta J, Hölttä T. 2015. Coordination of physiological traits involved in drought-induced mortality of woody plants. New Phytol Trust 208: 396-409.

Mishra S, Upadhyay S, Shukla RK. 2017. The role of strigolactones and their potential cross-talk under hostile ecological conditions in plants. Front Physiol. 7:691.

Mitchell PJ, McAdam SA, Pinkard EA, Brodribb TJ. 2016. Signifcant contribution from foliage-derived ABA in regulating gas exchange in *Pinus radiata*. Tree Physiol 37: 236–245.

Montwé D, Spiecker H, Hamann A. 2014. An experimentally controlled extreme drought in a Norway spruce forest reveals fast hydraulic response and subsequent recovery of growth rates. Trees 28: 891–900.

Morris H, Plavcová L, Cvecko P, Fichtler E, Gillingham M AF. et al. 2016. A global analysis of parenchyma tissue fractions in secondary xylem of seed plants. New Phytol 209 1553–1565.

Muhr M, Prüfer N, Paulat M, Teichmann T. 2016. Knockdown of strigolactone biosynthesis genes in *Populus* affects *BRANCHED1* expression and shoot architecture. New phytol 212 (3): 613-626.

Munemasa S, Hauser F, Park J, Waadt R, et al. 2015. Mechanisms of abscisic acid-mediated control of stomatal aperture. Curr Opin Plant Biol. 28: 154-62.

Murchie EH, Lawson T. 2013. Chlorophyll Fluorescence Analysis: A Guide to Good Practice and Understanding Some New Applications. J Exp Bot 13: 3983-3998.

Murchie EH, Pinto M, Horton P. 2009. Agriculture and the new challenges for photosynthesis research. New Phytol 181: 532–552.

Nakamura SI. Akiyama C. Sasaki T. Hattori H. Chino M. 2008. Effect of cadmium on the chemical composition of xylem exudate from oilseed rape plants (*Brassica napus* L.). Soil Sci Plant Nutr 54: 118–127.

Nardini A, Battistuzzo M, Savi T. 2013. Shoot desiccation and hydraulic failure in temperate woody angiosperms during an extreme summer drought. New phytol 200 (2): 322-9.

Nardini A, Casolo V, Dal Borgo A, Savi T, et al. 2016. Rooting depth, water relations and non-structural carbohydrate dynamics in three woody angiosperms differentially affected by an extreme summer drought. Plant Cell Environ 39:618–627

Nardini A, Lo Gullo MA, Salleo S. 2011. Refilling embolized xylem conduits: Is it a matter of phloem unloading? Plant Sci 180(4): 604-611.

Nardini A, Savi T, Trifilò P, Lo Gullo MA. 2018. Drought stress and the recovery from xylem embolism in woody plants. Prog Bot 79: 197–231.

Nduwimana A, Wei SM. 2017. The effects of high temperature regime on cherry tomato plant growth and development when cultivated in different growing substrates systems. Biol Chem Res 173-186.

Nelson DC, Scaffidi A, Dun EA, Waters MT, Flematti GR, Dixon KW, et al. 2011. F-box protein *MAX2* has dual roles in karrikin and strigolactone signaling in *Arabidopsis thaliana*. Proc. Natl Acad. Sci 108: 8897-8902.

Niinemets U. 2010. Responses of forest trees to single and multiple environmental stresses from seedlings to mature plants: Past stress history, stress interactions, tolerance and acclimation. For Ecol Manag 260: 1623–1639.

Niittyla T, Messerli G, Trevisan M, Chen J, Smith AM, Zeeman SC. 2004. A previously unknown maltose transporter essential for starch degradation in leaves. Sci 303(5654): 87-89.

Nijsse J. 2004. On the mechanism of xylem vessel length regulation. Plant Physiol 134:32-34.

Niu S, Luo Y, Li D, Cao S, Xia J, Li J, Smith MD. 2014. Plant growth and mortality under climatic extremes: An overview. Environ Exper Bot 98: 13-19.

Ohtani M, Nishikubo N, Xu B, Yamaguchi M. et al. 2011. A NAC domain protein family contributing to the regulation of wood formation in poplar. Plant J 67, 499–512.

Ort DR, Merchant SS, Alric J, Barkan A, Blankenship RE, Bock R, Croce R, Hanson MR, Hibberd JM, Long SP, et al. 2015. Redesigning photosynthesis to sustainably meet global food and bioenergy demand. Proc Natl Acad Sci USA 112: 8529–8536.

Pagliarani C, Casolo V, Ashofteh Beiragi M, Cavalletto S et al. 2019. Priming xylem for stress recovery depends on coordinated activity of sugar metabolic pathways and changes in xylem sap pH. Plant Cell Environ 42:1775–1787.

Palatnik JF, Allen E, Wu X, Schommer C, Schwab, et al. 2003. Control of leaf morphogenesis by microRNAs. Nature 425: 257–263.

Pantin F, Monnet F, Jannaud D, et al. 2013. The dual effect of abscisic acid on stomata. New Phytol 197: 65–72.

Pareek A, Singla SL, Grover A. 1998. Proteins alterations associated with salinity, desiccation, high and low temperature stresses and abscisic acid application in seedlings of Pusa 169, a high-yielding rice (*Oryza sativa* L.) cultivar. Curr Sci 75: 1023-1035.

Parent B, Hachez C, Redondo E, Simonneau T, Chaumont F, Tardieu F. 2009. Drought and abscisic acid effects on aquaporin content translate into changes in hydraulic conductivity and leaf growth rate: A trans-scale approach. Plant Physiol 149: 2000-2012.

Parniske M. 2008. Arbuscular mycorrhiza: the mother of plant root endosymbioses. Microbiology 6 763–775.

Parry MA, Andralojc PJ, Scales JC, Salvucci ME, Carmo-Silva AE, Alonso H, Whitney SM. 2013. Rubisco activity and regulation as targets for crop improvement. J Exp Bot 64: 717–730.

Paternoster R, Brame R, Mazerolle P, Piquero A. 1998. Using the correct statistical test for the quality of regression coefficients. Criminology 36: 859–866

Payyavula RS, Tay KHC, Tsai CJ, Harding SA. 2011. The sucrose transporter family in Populus: the importance of a tonoplast *PtaSUT4* to biomass and carbon partitioning. Plant J 65(5): 757-770.

Peguero-Pina JJ, Sancho-Knapik D, Barrón E, Camarero JJ, Vilagrosa A, Gil-Pelegrín E. 2014. Morphological and physiological divergences within *Quercus ilex* support the existence of different ecotypes depending on climatic dryness. Ann Bot 114:301–313.

Pei ZM. et al. 2000. Calcium channels activated by hydrogen peroxide mediate abscisic acid signalling in guard cells. Nature 406: 731–734.

Pelleschi S, Guy S, Kim JY, et al. 1999. Ivr2, a candidate gene for a QTL of vacuolar invertase activity in maize leaves. Gene-specific expression under water stress. Plant Mol Bio 39: 373–380.

Perdomo JA, Conesa MÀ, Medrano H, Ribas-Carbó M, Galmés J. 2015. Effects of long-term individual and combined water and temperature stress on the growth of rice, wheat and maize: relationship with morphological and physiological acclimation. Physiol Plant 155: 149–165.

Perez-Martin A, Michelazzo C, Torres-Ruiz JM, et al. 2014. Regulation of photosynthesis and stomatal and mesophyll conductance under water stress and recovery in olive trees: correlation with gene expression of carbonic anhydrase and aquaporins. J Exp Bot 65: 3143–3156.

Perrone I, Pagliarani C, Lovisolo C, Chitarra W, Roman F, Schubert A. 2012. Recovery from water stress affects grape leaf petiole transcriptome. Planta 235(6): 1383-1396.

Plavcová L, Hacke U.G. Sperry JS. 2011. Linking irradiance-induced changes in pit membrane ultrastructure with xylem vulnerability to cavitation. Plant Cell Environ 34,501–513.

Plavcová L, Hacke UG. 2012. Phenotypic and developmental plasticity of xylem in hybrid poplar saplings subjected to experimental drought, nitrogen fertilization, and shading. J Exp Bot 63: 6481–6491.

Plavcová L, Schreiber SG, Sperry JS, Wright IJ, Zanne AE. 2016. Weak tradeoff between xylem safety and xylem-specific hydraulic efficiency across the world's woody plant species. New Phytol 209: 123–136.

Prasad PVV, Boote KJ, Allen LH. 2006. Adverse high temperature effects on pollen viability, seed-set, seed yield and harvest index of grain sorghum [*Sorghum bicolor* (L.) Moench] are more severe at elevated carbon dioxide due to higher tissue temperatures. Agric For Meteorol 139: 237–251.

Prasad PVV, Staggenborg SA, Ristic Z. 2008. Impacts of drought and/or heat stress on physiological, developmental, growth, and yield processes of crop plants. Pages 301-355 in Ahuja LR, Reddy VR, Saseendran SA, Yu Q, eds. Response of

Crops to Limited Water: Understanding and Modeling Water Stress Effects on Plant Growth Processes. Madison, WI 53711, USA.

Preston K A, Cornwell WK, Denoyer JL. 2006. Wood density and vessel traits as distinct correlates of ecological strategy in 51 California coast range angiosperms. New Phytol 170, 807–818.

Prins A, Orr DJ, Andralojc PJ, Reynolds MP, Carmo-Silva E, Parry MAJ. 2016. Rubisco catalytic properties of wild and domesticated relatives provide scope for improving wheat photosynthesis. J Exp Bot 67: 1827–1838.

Quentin AG, Pinkard EA, Ryan MG et al. 2015. Non-structural carbohydrates in woody plants compared among laboratories. Tree Physiol 35:1146–1165.

Rae AM, Ferris R, Tallis MJ, Taylor G. 2006. Elucidating genomic regions determining enhanced leaf growth and delayed senescence in elevated CO_2. Plant Cell Environ 29:1730–41.

Rameau C, Bertheloot J, Leduc N, Andrieu B, Foucher F, et al. 2015. Multiple pathways regulate shoot branching. Front Plant Sci 5:741.

Ramírez V, Xiong G, Mashiguchi K, Yamaguchi S, Pauly M. 2018. Growth- and stress-related defects associated with wall hypoacetylation are strigolactone-dependent. Plant Direct 2: e00062.

Regier N, Streb S, Cocozza C, Schaub M, Cherubini P, Zeeman SC, Frey B. 2009. Drought tolerance of two black poplar (*Populus nigra* L.) clones: contribution of carbohydrates and oxidative stress defence. Plant Cell Environ 32(12): 1724-1736.

Rennenberg H, Loreto F, Polle A, Brilli F, Fares S, Beniwal RS, Gessler A. 2006. Physiological responses of forest trees to heat and drought. Plant Biology 8: 556–571.

Rennenberg H, Wildhagen H, Ehlting B. 2010. Nitrogen nutrition of poplar trees. Plant Biology 12: 275–291.

Roden JS, Pearcy R. W. 1993. The effect of leaf flutter on the flux of CO_2 in poplar leaves. Funct Ecol. 7, 669–675.

Roelfsema MRG, Hedrich R. 2002. Studying guard cells in the intact plant: modulation of stomatal movement by apoplastic factors. New Phytol 153: 425–431.

Rosas T, Galiano L, Ogaya R, Peñuelas J, Martínez-Vilalta J. 2013. Dynamics of non-structural carbohydrates in three Mediterranean woody species following long-term experimental drought. Front Plant Sci 4: 400.

Rosner S, Heinze B, Savi T, Dalla-Salda G. 2018. Prediction of hydraulic conductivity loss from relative water loss: new insights into water storage of tree stems and branches. Physiol Plant 165: 843–854.

Rungrat T, Awlia M, Brown T, Cheng R. 2016. Using phenomic analysis of photosynthetic function for abiotic stress response gene discovery. Arabidopsis Book 14: e0185.

Ruyter-Spira C, Kohlen W, Charnikhova T, et al. 2011. Physiological effects of the synthetic strigolactone analog GR24 on root system architecture in *Arabidopsis*: another belowground role for strigolactones? Plant Physiol 155:721–734.

Růžička K, Ursache R, Hejátko J, Helariutta Y. 2015. Xylem development – from the cradle to the grave. New Phytol 207: 519–535.

Sage RF. 2002. Variation in the k_{cat} of Rubisco in C_3 and C_4 plants and some implications for photosynthetic performance at high and low temperature. J Exp Bot 53: 609–620.

Sah SK, Reddy KR, Li J. 2016. Abscisic acid and abiotic stress tolerance in crop plants. Front Plant Sci 7: 571.

Sala A, Piper F, Hoch G. 2010. Physiological mechanisms of drought induced tree mortality are far from being resolved. New Phytol 186: 274–281.

Sala A, Woodruff DR, Meinzer FC. 2012. Carbon dynamics in trees: feast or famine? Tree Physiol 32:764–775.

Salleo S, Lo Gullo MA, Trifilo' P, Nardini A. 2004. New evidence for a role of vessel-associated cells and phloem in the rapid xylem refilling of cavitated stems of *Laurus nobilis* L. Plant Cell Environ 27: 1065-1076.

Salleo S, Trifilo' P, Esposito S, Nardini A, Lo Gullo MA. 2009. Starch-to-sugar conversion in wood parenchyma of field-growing *Laurus nobilis* plants: a component of the signal pathway for embolism repair? Funct Plant Biol 36: 815-825.

Salmon J, Ward SP, Hanley SJ, Leyser O, Karp A. 2014. Functional screening of willow alleles in *Arabidopsis* combined with QTL mapping in willow (*Salix*) identifies *SxMAX4* as a coppicing response gene. Plant Bio J 12: 480–491.

Salomón R, Valbuena-Carabaña M, Teskey R, et al. 2016. Seasonal and diel variation in xylem CO_2 concentration and sap pH in sub-Mediterranean oak stems. J Exp Bot 67: 2817–2827.

Salvucci ME, Crafts-Brandner SJ. 2004. Inhibition of photosynthesis by heat stress: the activation state of Rubisco as a limiting factor in photosynthesis. Physiol Plant 120(2):179-186.

Sarwar M, Saleem MF, Ullah N. et al. 2019. Role of mineral nutrition in alleviation of heat stress in cotton plants grown in glasshouse and field conditions. Sci Rep 9: 13022.

Savi T, Bertuzzi S, Branca S, Tretiach M, Nardini A. 2015. Drought-induced xylem cavitation and hydraulic deterioration: risk factors for urban trees under climate change? New Phytol 205: 1106–1116.

Savi T, Casolo V, Luglio J, Bertuzzi S, Trifilo P, Lo Gullo MA, Nardini A. 2016. Species-specific reversal of stem xylem embolism after a prolonged drought correlates to endpoint concentration of soluble sugars. Plant Physiol Biochem 106: 198-207.

Savi T, García González A, Herrera JC, Forneck A. 2019. Gas exchange, biomass and non-structural carbohydrates dynamics in vines under combined drought and biotic stress. BMC Plant Biol 18: 19(1): 408.

Schachtman DP, Goodger JQD. 2008. Chemical root to shoot signaling under drought. Trends Plant Sci 13(6): 281-287.

Scheenen TWJ, Vergeldt FJ, Heemskerk AM, Van As H. 2007. Intact plant magnetic resonance imaging to study dynamics in long-distance sap flow and flow-conducting surface area. Plant Physiol 144(2): 1157-1165.

Scholz A, Klepsch M, Karimi Z, Jansen S. 2013. How to quantify conduits in wood? Front Plant Sci 4:56.

Schrader SM, Wise RR, Wacholtz WF, Ort DR, Sharkey TD. 2004. Thylakoid membrane responses to moderately high leaf temperature in Pima cotton. Plant Cell Environ 27: 725–735

Schumann K, Leuschner C, Schuldt B. 2019. Xylem hydraulic safety and efficiency in relation to leaf and wood traits in three temperate Acer species differing in habitat preferences. Trees 33(5): 1475–1490.

Secchi F, Zwieniecki MA. 2011. Sensing embolism in xylem vessels: the role of sucrose as a trigger for refilling. Plant Cell Environ 34(3): 514-524.

Secchi F, Zwieniecki MA. 2012. Analysis of xylem sap from functional (nonembolized) and nonfunctional (embolized) vessels of *Populus nigra*: chemistry of refilling. Plant Physiol 160(2): 955–964.

Secchi F, Zwieniecki MA. 2016. Accumulation of sugars in the xylem apoplast observed under water stress conditions is controlled by xylem pH. Plant Cell Environ 39, 2350–2360.

Secchi F. Pagliarani C. Zwieniecki MA. 2017. The functional role of xylem parenchyma cells and aquaporins during recovery from severe water stress. Plant Cell Environ 40: 858–871.

Sedaghat M, Tahmasebi-Sarvestani Z, Emam Y, Mokhtassi-Bidgoli Ali. 2017. Physiological and antioxidant responses of winter wheat cultivars to strigolactone and salicylic acid in drought. Plant Physiol Biochem 119: 59-69.

Seto Y, Sado A, Asami K, Hanada A, Umehara M, Akiyama K, et al. 2014. Carlactone is an endogenous biosynthetic precursor for strigolactones, Proc. Natl Acad Sci 111: 1640-1645.

Sevanto S, Dickman LT. 2015. Where does the carbon go? Plant carbon allocation under climate change. Tree Physiology 35,581–584.

Sevanto S. 2014. Phloem transport and drought. J Exp Bot 65:1751–1759

Shah N, Paulsen G. 2003. Interaction of drought and high temperature on photosynthesis and grain-filling of wheat. Plant Soil 257 219–226.

Sharkey TD. 2005. Effects of moderate heat stress on photosynthesis: importance of thylakoid reactions, rubisco deactivation, reactive oxygen species, and thermotolerance provided by isoprene. Plant Cell Environ 28: 269–277.

Sharp RG, Davies WJ. 2009. Variability among species in the apoplastic pH signalling response to drying soils. J Exp Bot 60: 4363–4370.

Shinozaki K, Yamaguchi-Shinozaki K. 2007. Gene network involved in drought stress response and tolerance. J Exp Bot 58: 221-227.

Siciliano I, Carneiro GA, Spadaro D, Garibaldi A, Gullino ML. 2015. Jasmonic acid, abscisic acid, and salicylic acid are involved in the phytoalexin responses of rice to *Fusarium fujikuroi*, a high gibberellin producer pathogen. J Agric Food Chem 63(37): 8134-8142.

Smith M. 2011. An ecological perspective on extreme climatic events: a synthetic definition and framework to guide future research. J Ecol 99: 656–663.

Sobeih WY, Dodd IC, Bacon MA, Grierson D, Davies WJ. 2004. Long-distance signals regulating stomatal conductance and leaf growth in tomato (*Lycopersicon esculentum*) plants subjected to partial root-zone drying. J Exp Bot 55: 2353–2363.

Song Y, Chen Q, Ci D, Shao X, Zhang D. 2014. Effects of high temperature on photosynthesis and related gene expression in poplar. BMC Plant Biol 14: 111.

Sorefan K, Booker J, Haurogne K, et al. 2003. *MAX4* and *RMS1* are orthologous dioxygenase-like genes that regulate shoot branching in *Arabidopsis* and pea. Genes Develp 17:1469–1474.

Sorrentino G, Haworth M, Wahbi S, Mahmood T, Zuomin S, Centritto M. 2016. Abscisic acid induces rapid reductions in mesophyll conductance to carbon dioxide. PLoS One 11: e0148554.

Sperry JS, Adler FR, Campbell GS, Comstock JP. 1998. Limitation of plant water use by rhizosphere and xylem conductance: results from a model. Plant Cell Environ 21(4): 347-359.

Sperry JS, Hacke UG, Pittermann J. 2006. Size and function in conifer tracheids and angiosperm vessels. Am J Bot 93: 1490–1500.

Sperry JS, Hacke UG, Wheeler JK. 2005. Comparative analysis of end wall resistivity in xylem conduits. Plant Cell Environ 28: 456-465.

Sperry JS, Hacke UG. 2004. Analysis of circular bordered pit function. I. Angiosperm vessels with homogenous pit membranes. Am J Bot 91: 369– 385.

Sperry JS, Tyree MT. 1990. Water-stress-induced xylem embolism in three species of conifers. Plant Cell Environ 13, 427–436.

Spicer R. 2014. Symplasmic networks in secondary vascular tissues: parenchyma distribution and activity supporting long-distance transport. J Exp Bot 65(7): 1829-1848.

Stiller V, Sperry JS. 2002. Cavitation fatigue and its reversal in sunflower (*Helianthus annuus* L.). J Exp Bot 53(371): 1155-1161.

Stirnberg P, van de Sande K, Leyser HMO. 2002. *MAX1* and *MAX2* control shoot lateral branching in Arabidopsis. Development 129: 1131-1141.

Szymańska R, Ślesak I, Orzechowska A, Kruk J. 2017. Physiological and biochemical responses to high light and temperature stress in plants. Environ Exper Bot 139: 165-177.

Takeda T, Suwa Y, Suzuki M, Kitano H, Ueguchi-Tanaka M, et al. 2003. The *OsTB1* gene negatively regulates lateral branching in rice. Plant J 33: 513–520.

Tao F, Zhang Z. 2013. Climate change, wheat productivity and water use in the North China Plain: a new super-ensemble-based probabilistic projection. Agric For Meteorol 170 146–165.

Taylor G. 2002. *Populus*: Arabidopdid for forestry. Do we need a model tree? Ann Bot 90: 681-689.

Teskey R, Timothy W, Bauweraerts I, Ameye M, McGuire MA, Steppe K. 2015. Responses of tree species to heat waves and extreme heat events. Plant Cell Environ 38: 1699–1712.

Teskey R, Wertn T, Bauweraerts I, Ameye M, Mcguire, MA. Steppe K. 2015. Responses of tree species to heat waves and extreme heat events. Plant Cell Environ 38: 1699–1712.

Tomasella M, Haberle KH, Nardini A, Hesse B, Machlet A, Matyssek R. 2017. Post-drought hydraulic recovery is accompanied by non-structural carbohydrate depletion in the stem wood of Norway spruce saplings. Sci Rep 7.

Tombesi S, Nardini A, Frioni T, Soccolini M, Zadra C, Farinelli D, Poni S. Palliotti A. 2015. Stomatal closure is induced by hydraulic signals and maintained by ABA in drought-stressed grapevine. Sci Rep 5: 12449.

Torres-Ruiz JM, Cochard H, Choat B, et al. 2017. Xylem resistance to embolism: presenting a simple diagnostic test for the open vessel artefact. New Phytol 215: 489–499.

Trifilò P, Casolo V, Raimondo F, Petrussa E, Boscutti F, Lo Gullo MA, Nardini A. 2017. Effects of prolonged drought on stem non-structural carbohydrates content

and post-drought hydraulic recovery in *Laurus nobilis* L.: The possible link between carbon starvation and hydraulic failure. Plant Physiol Biochem 120: 232-241.

Trifilò P, Kiorapostolou N, Petruzzellis F, Vitti S, et al. 2019. Hydraulic recovery from xylem embolism in excised branches of twelve woody species: Relationships with parenchyma cells and non-structural carbohydrates. Plant Physiol Biochem 139: 513–520.

Trifilò P, Nardini A, Lo Gullo MA, Barbera PM, Savi T, Raimondo F. 2015. Diurnal changes in embolism rate in nine dry forest trees: relationships with species specific xylem vulnerability, hydraulic strategy and wood traits. Tree Physiol 35: 694–705.

Trifilò P, Raimondo F, Lo Gullo MA, Barbera PM, Salleo S, Nardini A. 2014. Relax and refill: xylem rehydration prior to hydraulic measurements favours embolism repair in stems and generates artificially low PLC values. Plant Cell Environ 37:2491–2499.

Tukey JW. 1949. Comparing individual means in the analysis of variance. Biometrics 5: 99-114.

Tuteja N. 2007. Abscisic acid and abiotic stress signaling. Plant Signal Behav 2(3): 135–138.

Tyree MT, Davis SD, Cochard H. 1994. Biophysical perspectives of xylem evolution – Is there a tradeoff of hydraulic efficiency for vulnerability to dysfunction? IAWA J 15: 335-360.

Tyree MT, Ewers FW. 1991. The hydraulic architecture of trees and other woody-plants. New Phytol 119(3): 345-360.

Tyree MT, Zimmermann MH. 2002. Xylem structure and ascent of sap. Springer Verlag, Berlin, Germany.

Umehara M, Hanada A, Yoshida S, Akiyama K, et al. 2008. Inhibition of shoot branching by new terpenoid plant hormones. Nature 455: 195–200.

Urli M, Porté AJ, Cochard H, Guengant Y, Burlett R, Delzon S. 2013. Xylem embolism threshold for catastrophic hydraulic failure in angiosperm trees. Tree Physiol 33:672–683.

Van Ha C, Leyva-Gonzalez MA, Osakabe Y, Tran UT, Nishiyama R, et al. 2014. Positive regulatory role of strigolactone in plant responses to drought and salt stress. Proc Natl Acad Sci 111: 851e856.

Vander Willigen C, Sherwin HW, Pammenter NW. 2000. Xylem hydraulic characteristics of subtropical trees from contrasting habitats grown under identical environmental conditions. New Phytol 145: 51–59.

Velikova V, Sharkey TD, Loreto F. 2012. Stabilization of thylakoid membranes in isoprene-emitting plants reduces formation of reactive oxygen species. Plant Signal Behav 7: 139–141.

Visentin I, Vitali M, Ferrero M, Zhang Y, Ruyter-Spira C, Novák O, et al. 2016. Low levels of strigolactones in roots as a component of the systemic signal of drought stress in tomato. New Phytol 212 954–963.

Vishwakarma K, Upadhyay N, Kumar N, Yadav G, Singh J, Mishra RK et al. 2017. Abscisic acid signaling and abiotic stress tolerance in plants: A review on current knowledge and future prospects. Front Plant Sci 8:161.

von Caemmerer S. 2000. Biochemical models of leaf photosynthesis. CSIRO Publishing, Collingwood, Australia.

Vu JCV, Newman YC, Jr Allen LH, Gallo-Meagher M, Zhang MQ. 2002. Photosynthetic acclimation of young sweet orange trees to elevated growth CO_2 and temperature. Plant Physiol 159: 147–157.

Wahid A, Close TJ 2007. Expression of dehydrins under heat stress and their relationship with water relations of sugarcane leaves. Biol Plantarum 51: 104-109.

Wahid A, Gelani S, Ashraf M, Foolad MR. 2007. Heat tolerance in plants: an overview. Environ Exp Bot 61: 199-223.

Wahid A. 2007. Physiological implications of metabolite biosynthesis for net assimilation and heat-stress tolerance of sugarcane (*Saccharum officinarum*) sprouts. J Plant Res 120:219-228.

Wang D, Heckathorn SA, Hamilton EW, Frantz J. 2014. Effects of CO_2 on the tolerance of photosynthesis to heat stress can be affected by photosynthetic pathway and nitrogen. Am J Bot 101(1): 34-44.

Wang D, Heckathorn SA, Mainali K, Tripathee R. 2016. Timing Effects of Heat-Stress on Plant Ecophysiological Characteristics and Growth. Front Plant Sci 7: 1629.

Ward SP, Salmon J, Hanley SJ, Karp A, Leyser O. 2013. Using Arabidopsis to study shoot branching in biomass willow. Plant Physiol 162: 800-811.

Waters MT, Gutjahr C, Bennett T, Nelson DC. 2017. Strigolactone signaling and evolution. Annu Rev Plant Biol 68: 291–322.

Weise SE, Kim KS, Stewart RP, Sharkey TD. 2005. beta-maltose is the metabolically active anomer of maltose during transitory starch degradation. Plant Physiol 137(2): 756-761.

Weston DJ, Karve AA, Gunter LE, Jawdy SS, Yang X, Allen SM, Wullschleger SD. 2011. Comparative physiology and transcriptional networks underlying the heat shock response in *Populus trichocarpa*, *Arabidopsis thaliana* and *Glycine max*. Plant Cell Environ 34: 1488-1506.

Wheeler JK, Sperry JS, Hacke UG, Hoang N. 2005. Inter-vessel pitting and cavitation in woody Rosaceae and other vesselled plants: a basis for a safety versus efficiency tradeoff in xylem transport. Plant Cell Environ 28: 800–812.

Whitney SM, Houtz RL, Alonso H. 2011. Advancing our understanding and capacity to engineer nature's CO_2-sequestering enzyme, Rubisco. Plant Physiol 155: 27–35.

Wilkinson S, Davies WJ. 1997. Xylem sap pH increase: A drought signal received at the apoplastic face of the guard cell that involves the suppression of saturable abscisic acid uptake by the epidermal symplast. Plant Physiol 113(2): 559-573.

Wilkinson S, Davies WJ. 2008. Manipulation of the apoplastic pH of intact plants mimics stomatal and growth responses to water availability and microclimatic variation. J Exp Bot 59:619–631

Würth MKR, Peláez-Riedl S, Wright SJ, Körner C. 2005. Non-structural carbohydrate pools in a tropical forest. Oecologia 143 (1): 11-24.

Xie X, Yoneyama K, Yoneyama K. 2010. The strigolactone story. Annu Rev Phytopathol 48: 93–117.

Xie X. 2016. Structural diversity of strigolactones and their distribution in the plant kingdom. J Pestic Sci 41(4): 175–180.

Yamada M, Hidaka T, Fukamachi H. 1996. Heat tolerance in leaves of tropical fruit crops as measured by chlorophyll fluorescence. Sci Hortic 67(1-2): 39-48.

Yamaguchi M, Mitsuda M, Ohtani M, Ohme-Takagi M, Kato M, Demura T. 2011. VASCULAR-RELATED NAC-DOMAIN7 directly regulates the expression of a broad range of genes for xylem vessel formation. Plant J 66: 579-590

Yamaguchi-Shinozaki K, Shinozaki K. 2006. Transcriptional regulatory networks in cellular responses and tolerance to dehydration and cold stresses. Annu Rev Plant Biol 57:781–803.

Yoneyama K, Xie X, Yoneyama K, Takeuchi Y. 2009. Strigolactones; structures and biological activities. Pest Manag Sci 65:467–470.

Yoshida S, Iwamoto K, Demura T, Fukuda H. 2009. Comprehensive analysis of the regulatory roles of auxin in early transdifferentiation into xylem cells. Plant Mol Biol 70: 457–469.

Yoshimura M, Sato A, Kuwata K, Inukai Y, Kinoshita T, Itami K, et al. 2018. Discovery of shoot branching regulator targeting strigolactone receptor DWARF14. ACS Cent Sci 4: 230–234.

Young JN, Hopkinson BM. 2017. The potential for co-evolution of CO_2-concentrating mechanisms and Rubisco in diatoms. J Exp Bot 68(14): 3751–3762.

Zhang FP, Sussmilch F, Nichols DS, Cardoso AA, Brodribb TJ, McAdam SA. 2018. Leaves, not roots or floral tissue, are the main site of rapid, external pressure-induced ABA biosynthesis in angiosperms. J Exp Bot 69: 1261–1267.

Zhang J, Jia W, Yang J, Ismail A.M. 2006. Role of ABA in integrating plant responses to drought and salt stresses. Field Crops Res 97: 111-119.

Zhang J, Schurr U, Davies W. 1987. Control of stomatal behaviour by abscisic acid which apparently originates in the roots. Environ Exp Bot 38: 1174–1181.

Zhang J. Davies WJ. 1989. Abscisic acid produced in dehydrating roots may enable the plant to measure the water status of the soil. Plant Cell Environ 12: 73-81.

Zhang R, Sharkey TD. 2009. Photosynthetic electron transport and proton flux under moderate heat stress. Photosynth Res 100(1): 29-43.

Zhang Y, van Dijk AD J, Scaffidi A, Flematti GR, Hofmann M, Charnikhova T, et al. 2014. Rice cytochrome P450 *MAX1* homologs catalyze distinct steps in strigolactone biosynthesis. Nat Chem Biol 10: 1028-1033.

Zwanenburg B, Mwakaboko AS. 2011. Strigolactone analogues and mimics derived from phthalimide, saccharine, p-tolylmalondialdehyde, benzoic and salicylic acid as scaffolds Bioorg. Med Chem 19: 7394-7400.

Zwieniecki MA, Holbrook NM. 2009. Confronting Maxwell's demon: biophysics of xylem embolism repair. Trends in Plant Sci 14(10): 530-534.

Zwieniecki MA, Melcher PJ, Feild TS, Holbrook NM. 2004. A potential role for xylem-phloem interactions in the hydraulic architecture of trees: effects of phloem girdling on xylem hydraulic conductance. Tree Physiol 24(8): 911-7.